Evaluating the Performance of an Eggshell-Bagasse Biosorption system in removing Lead and Cadmium from Aqueous Solutions

A thesis submitted in fulfilment of the academic requirements for the award of the degree of

Master of Engineering

In the Department of Chemical Engineering

By

Charlene Harripersadth

SUPERVISOR: PROF P. MUSONGE

CO – SUPERVISOR: PROF Y. ISA

February 2021

Declaration

I, Charlene Harripersadth, hereby declare that the content presented in this thesis entitled "***Evaluating the Performance of an Eggshell – Bagasse Biosorption system in removing Lead and Cadmium from Aqueous Solutions***" is a record of my own research work conducted with the intention of obtaining the Masters in Engineering in Chemical Engineering degree at the Durban University of Technology (DUT). The content of this research work has not been previously published or written by another person for the award of any other degree at DUT or at any other educational institution. Moreover, I declare that the content presented in this thesis does not violate any copyright as all the work of others has been indicated accordingly by means of in – text referencing and a comprehensive list of references has been listed at the end of this thesis.

Author: Charlene Harripersadth

Signature: ___ __ Date: __28/01/21_____

Supervisor: Prof Paul Musonge

Signature. __ _ Date: _28/01/21_____

Co – Supervisor: Prof Yusuf Isa, Makarfi

Signatur _____ Date: _04/02/21__

Dedication

This thesis is dedicated to my parents, Preth and Shireen Harripersadth, my pillars of strength, who are constantly encouraging and motivating me no matter the circumstances in which I find myself in. Without them, I would not be who I am today and I will be eternally grateful.

Acknowledgements

I would like to express my sincere and heartfelt gratitude to Prof P. Musonge and Dr Y.M. Isa for their valuable insights, words of encouragement and mentorship, but most of all, for allowing me to conduct my research work at my own pace when the need arose.

Special thanks to the NRF foundation, who have assisted in the funding of this research work.

Publications

Research Paper: Charlene Harripersadth, Paul Musonge, Yusuf Makarfi Isa, Moises Garcia Morales, Ana Sayago. "The application of eggshells and sugarcane bagasse as potential biomaterials in the removal of heavy metals from aqueous solutions". *South African Journal of Chemical Engineering* 34 (2020): 142-150.

Book Chapter: Paul Musonge, Charlene Harripersadth. "The applicability of eggshell waste as a sustainable biosorbent medium in wastewater treatment – A review" (In Progress).

Conference Presentation: Presented an abstract titled "The application of eggshells and sugarcane bagasse as potential biomaterials in the removal of Pb and Cd" at the 4th International Interdisciplinary Research and Innovation Conference (Hilton Hotel, Durban) in 2019.

Award: An honourable mention for best research work in Sustainability for research conducted at the University of Huelva (Spain) under the Erasmus Scholarship program in 2018.

Abstract

In this research investigation, the simultaneous use of 2 biomaterials, sugarcane bagasse and eggshells, were applied as biosorbents in the treatment of metal laden effluent. Under the characterisation measurements investigated, it was found that carbon, calcium and oxygen atoms which constitute carboxylic and carbonate functional groups were prominent in eggshells, whereas for bagasse, it was carbon, hydrogen and oxygen atoms constituting hydroxyl and carbonyl groups. Batch studies were conducted to investigate the effect of fundamental process variables such as particle size (75 – 250 µm), initial metal ion concentration (40 – 240 mg/L), pH (2 – 7) and contact time (0 – 120 min). With respect to the equilibrium studies, the applicability of the Langmuir isotherm implied a monolayer formation of metal ions onto the surface of both biomaterials with the maximum amounts of Pb and Cd adsorbed based on 1 g of biosorbent being 277.8 and 13.62 mg/g for eggshells and 31.45 and 19.49 mg/g for bagasse, respectively. Moreover, kinetic modelling revealed that the process was well described by the pseudo – second order model for both Pb and Cd using eggshells and bagasse.

Fixed bed studies were used to assess the dynamic adsorption behaviour of the eggshell – bagasse system using a lab – scale adsorption column of 2.3 cm in diameter and 30 cm in height. The effect of bed depth (4 – 12 cm) on 5 adsorbents (eggshells, bagasse, adsorbent A, adsorbent B and adsorbent C) in the removal of Pb were investigated. Adsorbents A, B and C were a combination of both eggshells and bagasse with adsorbent A constituting 75wt % bagasse and 25wt % eggshells, adsorbent B constituting 50wt % bagasse and 50wt % eggshells and adsorbent C constituting 25wt % bagasse and 75wt % eggshells. The column experiments highlighted an improvement in bed performance with an increase in bed depth resulting in greater mass transfer zones, breakthrough times and larger quantities of effluents treated. Two kinetic models (Thomas and Yoon–Nelson) were used to interpret the breakthrough curves where the data showed good fits to both models used. In determining the efficacy of the eggshell – bagasse biosorption system, adsorbent C was found to be most proficient in the removal of Pb with eggshells, adsorbent B, adsorbent A and bagasse following suit.

The results from this investigation strongly suggest the plausible reuse of agricultural waste materials in the treatment of contaminated effluent through the biosorption process.

Keywords: Biosorption, Eggshells, Sugarcane Bagasse, Bioremediation, Heavy metals

Table of contents

LIST OF TABLES

LIST OF FIGURES

ACRONYMS/ABREVIATIONS

SCB	Sugarcane bagasse
AMD	Acid mine drainage
SEM	Scanning electron microscopy
FTIR	Fourier Transform Infrared Spectroscopy
XRD	X – Ray Diffraction
BET	Braunner Emmett Teller
EDS	Electron Dispersive Spectroscopy
EPA	Environmental Protection Agency
WHO	World health Organisation
SANS	South African National Standards
NWIB	National Waste Information Baseline
ESM	Eggshell Membrane
RMSE	Root Mean Squared Error
MAE	Mean Absolute Error
IUPAC	International Union of Pure and Applied Chemistry
AAS	Atomic Absorption Spectrometry

1. INTRODUCTION

1.1. Introduction and Background

In recent decades, the rate of industrialisation has vastly increased, consequently resulting in the seepage of heavy metals into the environment. The contamination of waste effluent by heavy metals is a worldwide environmental challenge which is alarming due to its adverse health, aquatic and plant life effects. Heavy metals are common environmental pollutants and due to their non-degradable and bio – accumulation nature, they have drawn a lot of attention owing to their potential health and environmental risks. It is worthy to note that the presence of even trace amounts of heavy metals can be harmful and/or toxic to both flora and fauna (Volesky and Naja, 2007). The primary source of metal pollution arises from anthropogenic activities with metal laden effluent being of primary concern affecting the preservation and sustainability of the environment. Wastes that contain heavy metals are directly and/or indirectly released into the environment resulting in severe environmental pollution. As a result, tough regulatory laws that restrict the levels of heavy metals present in water and wastewater have been imposed in the past decades (Simate and Ndlovu, 2015).

Heavy metals can be defined as metallic elements that induce toxicity even at low levels of exposure (Jan et al., 2015). There are more than 60 metals which fall into this category, some of which include lead, cadmium, zinc, nickel, chromium, cobalt, copper and mercury. Of these, lead, mercury, cadmium and chromium are at the top of the toxicity list (Abdi and Kazemi, 2015). Current treatment technologies for the removal of metal ions include precipitation, oxidation/reduction, membrane filtration such as reverse osmosis and ion exchange processes amongst others (Malkoc et al., 2006a). However, there are many challenges associated with these processes. They are often ineffective, uneconomical or technically complicated when the target metal ion concentration falls below 100 mg/L. Additionally, some methods also have the disadvantages of high reagent usage, high energy requirements and toxic secondary sludge production (Abdolali et al., 2014).

In view of the many challenges experienced with current treatment processes, there is a need to source cleaner (environmentally friendly) cost – effective technologies that are technically efficient. One such technology that has gained a vast interest in recent years is the process of adsorption which has been the focus of many research studies (Vijayaraghavan and Umid

2013, Putra et al., 2014, Schwantes et al., 2016). The main attraction of the adsorption process is its cost effectiveness and good removal performance (Aksu, 2005). Commercially available adsorbents such as activated carbon and zeolites have restricted its widespread use due to their high costs (Malkoc et al., 2006a) which leaves a gap in the market for alternative low – cost and easily available adsorbents.

The search for a low cost and easily available adsorbent has led to the investigation of materials of agricultural and biological origin together with industrial by – products (Aksu, 2005). Raw and natural agricultural wastes are among some of the cheap waste materials that are used as adsorbents. There are several kinds of agricultural materials which have been researched in heavy metal removal such as kenaf fibres by Hasfalina et al. (2012), phoenix tree leaf powder by Han et al. (2009), wheat bran by Hasan et al. (2010), wheat straw (Triticum sativum) by Muhamad et al. (2010) , pongamia oil cake by Shanmugaprakash and Sivakumar (2015) and cassava peels by Simate and Ndlovu (2015) to name a few. However, this study concentrated on the use of eggshells and sugarcane bagasse as the adsorbent medium for the biosorption process.

The chemical and physical properties of eggshells and sugarcane bagasse makes it an exemplary material to be used in the biosorption of heavy metals. The functional groups present in agricultural wastes such as carbonyl, phenolic, acetamido, alcoholic, amido, amino and sulfhydryl groups have an affinity for heavy metal ions to form metal complexes or chelates (Renu et al., 2017). The removal of heavy metal ions from wastewater using agricultural wastes is based upon metal biosorption. The mechanism of biosorption includes chemisorption, complexation, surface adsorption, diffusion through pores and ion exchange.

Eggshells have been recommended for use as an adsorbent because of it's low cost, copious availability in nature, non – toxicity, high specific surface area and high potential of ion exchange for charged pollutants (Zhang et al., 2012). The composition of the shell is approximately 98.2% calcium carbonate, 0.9 % magnesium carbonate and 0.9% phosphorus (Romanoff and Romanoff, 1949). Adsorption by eggshells occurs mainly by an ion exchange reaction and it should be usable as an adsorbent of metal ions (Choi 2015). The eggshell consists predominantly of three layers, the outermost layer called the cuticle, the calcium carbonate layer, the testa, and the innermost layer, the mammillary layer. Each eggshell has been estimated to contain between 7000 and 17,000 pores (William and Owen, 1995) making

them an efficient adsorbent to use since the pores allow for an increase in the number of binding sites and surface area for the biosorptive process. Many studies have centred around the use of eggshells for metal removal including the works of several researchers (Vijayaraghavan and Umid 2013, Ahmad, 2012, Choi 2015, Park et al., 2007, Zhang et al., 2017).

Another such waste is sugarcane bagasse (SCB), a low – cost residual cane pulp known as pith which remains after sugar juice has been extracted. Bagasse is largely composed of cellulose, pentosan and lignin (Mohan and Singh, 2002). It consists of approximately 50% cellulose, 25% hemicellulose and 25% lignin (Moubarik, 2015). Bagasse adsorbs metal ions by the cation exchange phenomena due to the presence of adsorptive sites such as carboxylic, carbonyl, amine and hydroxyl groups present (Raymundo et al., 2010). Previous research works that have cited the use of bagasse for metal removal include the works of (Homagai et al., 2010, Corrales et al., 2012, Moubarik, 2015, Ríos-Parada et al., 2017, Chandel et al., 2014) etc.

Considering the above, the main objective of this research work was to investigate the efficiency of an eggshell – bagasse biosorption system in removing lead and cadmium from aqueous solutions. It is expected that the organic compounds and functional groups of bagasse together with the carbonate properties of eggshells which favour metal ion binding (Schaafsma et al., 2000) will work together to attract a varied range of pollutants.

1.2. Problem Statement

The mining of gold is a major source of heavy metal emissions into the environment (Ngole-Jeme and Fantke, 2017) and whilst the mining industry in South Africa is a key driver of the economy, it has consequently resulted in the detrimental problem of acid mine drainage (Ramla and Sheridan, 2015). Heavy metal contamination of water bodies, which are by – products of acid mine drainage (AMD), are considered as serious toxic pollutants due to their non – biodegradability and presence in the food chain. Moreover, with global warming effects contributing to the detriment of aquatic bodies and the terrestrial environment, the sustainability of both is at its precipice. Sustainability efforts are at the forefront of industrial operations and comes at the dawn of circular economy which is aimed at reducing wastes. With that said, there have been increased efforts to remediate the environmental challenge of heavy metal pollution, however, progress in this field has not been rapid enough considering the detrimental effects it has. Currently, a wide range of treatment technologies exist and the

process of adsorption has been widely used as an efficient and economically sustainable technology for metal removal (Chowdhury et al., 2013). Waste materials, in particular, have gained traction in research and development, as adsorbents for heavy metal removal (De Angelis et al., 2017). Hence, the proposed study aims to conduct adsorption studies using natural waste materials to remove metal contaminants from aqueous solutions.

1.3. Research Aims and Objectives

The aim of this investigation is to develop a viable low – cost treatment option for the removal of metal contaminants from aqueous solutions. The efficiency of an eggshell – bagasse biosorbent system for the removal of heavy metal ions was investigated. Two heavy metals, lead and cadmium, were considered in this investigation. Both metals were chosen on the basis of their presence and toxicity in most industrial effluents including acid mine drainage (AMD). The eggshell – bagasse system were prepared by varying the proportions of bagasse and eggshells to produce adsorbents with the properties of both. A quantitative experimental approach was applied in this investigation. For characterisation, different analytical techniques such as SEM (Scanning Electron Microscope), FTIR (Fourier Transform Infrared Spectroscopy), XRD (X-Ray Diffraction) and BET (Braunner EmmetT Teller) analysis were conducted.

Batch studies was performed to assess the adsorption capacity of eggshells and bagasse under the action of various operating conditions with placed focus on the effect of particle size, pH, initial metal concentration and contact time while focusing on the effect of bed depth in the fixed bed column studies. Kinetic (pseudo – first order and pseudo – second order reaction models) and isotherm modelling (Langmuir and Freundlich models) were analysed in the batch studies and the data from the breakthrough curves applied to the Thomas and Yoon-Nelson mathematical models.

The research objectives of this investigation are as follows:

- To characterise the biosorbents
- To evaluate the effect of operational parameters on the biosorptive process
- To analyse kinetic models, isotherm models, breakthrough curves and mathematical models for the process

1.4. Structure of the Thesis

The thesis has been presented over six chapters, each highlighting different aspects of this study. A brief summary of each chapter has been highlighted below.

Chapter One foregrounds the context of the study by detailing the need to find a cost-effective solution to the problem of metal pollution and acid mine drainage. An outline of the motivation and the aim and objectives of this research work were briefly discussed.

Chapter Two presents an overview of the literature pertaining to Acid Mine Drainage; its source, environmental impact and the different treatment technologies were presented. The process of biosorption was explained in greater detail with its general characteristics. Subsequently, a review of previous research involving the use of eggshells and bagasse in removing different pollutants were discussed.

Chapter Three describes the research methodology by detailing the experimental research approach that was adopted in this study. This included the preparation of the synthesised solutions and biosorbent materials together with the relevant analytical techniques used for characterisation. The different methods used to characterise the biosorbents were Scanning Electron Microscope – Energy Dispersive Spectroscopy (SEM-EDS), Fourier Transform Infrared Spectroscopy (FTIR), X – Ray Diffraction (XRD) and Brunauer–Emmett–Teller (BET) analysis.

Chapter Four presents the results from the adsorption studies using both eggshells and bagasse with tables, graphs and images which support the analytical results. Overall, this chapter provides a rigorous discussion of the effect of the different operational parameters of the system which include the pH, contact time, particle size, concentration and bed height.

Chapter Five forms the final chapter of this thesis which provides the conclusions drawn from this study. It also identifies any limitations placed on the investigation and considers future directions of work done in this field.

2. LITERATURE REVIEW

2.1. Introduction

A high degree of industrialization and urbanization has vastly enhanced the degradation of the aquatic environment through the discharge of industrial effluent and domestic wastes (Senthikumaar, 2000). One of the many challenges associated with industrial processes is the release of heavy metals and metalloids into water bodies (Mashangwa, 2017) most of which are introduced through geogenic (weathering) and anthropogenic sources. These include waste disposal, agricultural activities, vehicular traffic, petroleum refineries, paint industries, photography, and mining. Thus, the release of heavy metals brings about serious environmental pollution posing a significant threat to the health and wellbeing of human life not to mention the detrimental effects posed on our ecosystem (Wang, 2009).

South Africa is renowned for its rich mineral wealth, the exploitation of which has sustained its economic growth thereby ensuring the country's position in the global market (Humphries, 2016). Consequently, the activities of the mining sector have led to serious environmental challenges especially concerning acid mine drainage (AMD) and heavy metal contamination. AMD is recognized as one of the more serious environmental problems in the mining industry (Akcil, 2006) and is a major source of environmental pollution experienced worldwide due to current or past mining activities. Its generation, release, mobility and attenuation involve complex processes governed by a combination of physical, chemical, and biological factors (Simate and Ndlovu, 2015). The problem of AMD has resulted in a decline in water quality in the economic heartland of South Africa (Humphries, 2016) and if not remedied, it will result in long-term impairment to waterways and biodiversity (Akcil, 2006).

Several treatment technologies geared towards the treatment of AMD have been explored, most of which present either economic, environmental or technical challenges. Hence, the nature and severity of this problem has probed research in this field with the intention of sourcing a viable low – cost, eco – friendly solution. Thus, this literature review will concentrate on research in the field of AMD placing focus on the adsorption process and its applicability in removing heavy metals from aqueous effluents. It will serve to inform the reader of new

insights to existing information in order to understand the problem of acid mine drainage in its vast context.

2.2. Heavy Metals

Heavy metals are defined as dense metallic elements which are known to adversely affect living organisms and the environment even at low metal ion concentrations (Jaishankar et al., 2014). They possess high electrical conductivity, malleability and luster and voluntarily lose their electrons to form cations. Natural and anthropogenic sources are the common sources of these pollutants with metal contamination being mainly due to the discharge of sewage, mining activities and industrial effluents (Lakherwal, 2014). Other known sources include soil erosion, natural weathering and urban runoff. Due to their non-degradable nature, they can bio-accumulate causing a great deal of health issues and environmental risks.

Heavy metals present in waste effluent includes arsenic, cadmium, chromium, copper, lead, nickel and zinc to name a few. Of these, mercury, lead, cadmium and arsenic pose the greatest environmental health risk due to their extensive use, toxicity and widespread distribution (Tchounwou, 2014). The aforementioned metals are dangerous as cations (from soluble compounds) and as organometallic forms (bonded to organic molecules). The toxic effect of these metals, even though they have no biological role in the human body, remain present in some form which is harmful to the functioning of the body.

Lead and cadmium accumulate in the body through the food chain and is known to exhibit a chronic nature. Chronic metal exposure has been implicated in several degenerative diseases and may increase the risk of some cancers (Lakherwal, 2014). Due to the nature and effect of lead and cadmium exposure, the above-mentioned metal ions were chosen to be investigated in this study.

2.2.1. Lead in the environment, toxicity and uses

Lead is a heavy, soft, grey- blue metal which has widespread applications (Singh, 2005). It is used in the production of batteries, cosmetics, metal products such as ammunition and solder, to name a few. The widespread use of lead has resulted in extensive environmental pollution across the world. Lead industries, mining and smelting are the main sources of contamination in the environment (Gerhardsson et al., 2002) although vehicle emissions, piping fixtures and

solder contribute to the minority. Mining, manufacturing and the burning of fossil fuels have resulted in the accumulation of lead-based compounds in the air, water, soil and the environment (Jaishankar et al., 2014). The leaching of the cationic form of lead from landfills are the biggest contributing factor of contamination. Lead is extremely toxic which disturbs several plant physiological processes and unlike other metals such as zinc, iron, copper and manganese, it does not play a role in any biological functions. In its elemental form, it is not an environmental hazard unless it dissolves into its cationic form Pb (II). It decomposes on contact with air forming a complex mixture of compounds, depending on the conditions present. The cationic form of lead usually enters the human body through the ingestion of contaminated water and food.

Symptoms of lead toxicity include those mainly related to the central nervous system and gastrointestinal tract. Lead poisoning can occur from drinking water and according to the Environmental protection agency (EPA) , lead is considered a carcinogen. Exposure can be acute or chronic with acute exposure resulting in a loss of appetite, headaches, hypertension, abdominal pain, renal dysfunction, fatigue, sleeplessness, arthritis, hallucinations and vertigo. Acute exposure however, mainly occurs in the place of work and in some manufacturing industries which make use of lead. Chronic exposure results in mental retardation, birth defects, psychosis, autism, allergies, dyslexia, weight loss, hyperactivity, paralysis, muscular weakness, brain damage, kidney damage and in some cases, are known to cause death (Martin and Griswold, 2009).

The toxicity of lead in living cells occurs mainly through an ionic mechanism or that of oxidative stress. The ionic mechanism occurs mainly due to the ability of lead ions to replace other bivalent cations like Ca (II), Mg (II) and Fe (II) and monovalent cations like Na (I), which disturbs the biological metabolism of the cell leading to significant changes in biological processes such as cell adhesion, intra and inter cellular signaling, protein folding, maturation, apoptosis, ionic transportation, enzyme regulation, and the release of neurotransmitters (Flora et al., 2012).

2.2.2. Cadmium in the environment, toxicity and uses

Cadmium is a soft bluish white metal known to produce highly toxic compounds (Singh, 2005). It is present primarily in the ores of zinc, copper and lead, the extraction and processing of

which releases large quantities of it into the atmosphere, hydrosphere and soil thereby contaminating the soils, the aquatic environment, fauna and flora (Sarkar et al., 2013). Common applications include alkaline batteries, platings, coatings, pigments and as a plastic stabilizer. Human exposure is generally through inhalation and ingestion resulting in either acute and chronic intoxications (Chakraborty et al., 2013). Cadmium distributed in the environment will remain in soils and sediments for several decades. Cadmium and its compounds are classified as Group 1 carcinogens for humans by the International Agency for Research on Cancer (Henson and Chedrese, 2004). It is a highly water-soluble heavy metal in comparison to other metals with a high bioavailability where long-term exposure can result in morphopathological changes in the kidneys.

Studies on humans and animals have revealed that osteoporosis (skeletal damage) is a critical effect of cadmium exposure along with disturbances in calcium metabolism, formation of renal stones and hypercalciuria. When ingested in higher concentrations, it can lead to stomach irritation which results in vomiting and on very long exposure, it can become deposited in the kidney and finally lead to kidney disease, fragile bones and lung damage (Bernard, 2008). Premature birth and reduced birth weights are the issues that arise if cadmium exposure is high during human pregnancy (Henson and Chedrese, 2004) . The exact mechanism of cadmium toxicity is not clearly understood but its effect on cells are well known (Jaishankar et al., 2014).

The world health organization (WHO) drinking water standards for cadmium and lead are 0.005 mg/L and 0.01 mg/L respectively of which all countries are obliged to comply with. In South Africa, the standards set out by the (SANS241-1:2015) guideline is $\leq 3\ \frac{\mu g}{L}$ for cadmium and $\leq 10\ \frac{\mu g}{L}$ for lead.

2.3. Background, Sources and Constituents of Acid Mine Drainage

Coal and gold mining operations are amongst the two major contributors afflicted by acid production in South Africa (McCarthy, 2011). The areas that are most afflicted include the Witwatersrand Gold fields, Mpumalanga, KwaZulu-Natal Coal fields and the O'Kiep Copper District. However, the Western, Central and Eastern basins in the Witwatersrand are identified as priority areas which require immediate attention (Ramontja et al., 2011). The case of acid

production arising from the Western mining basin near Krugersdorp on the West Rand have become prominent in recent years (Cobbing, 2008).

The Western gold mining basin emphasized severe impacts of acid production when the last mine to shut down in this basin ceased pumping in 2002 (Ramontja et al., 2011). The volume of AMD decants uncontrolled at a flow-rate of 10-60 ML/day (Maree et al., 2013). Basic treatment of this water currently permits the release of 12 ML/day into the Crocodile (West) and Marico drainage system. However, the existing pumping and treatment capacity is inadequate to effectively manage the impact of AMD with the excess volume flowing untreated into the receiving aquatic environment. This water has a pH of 2.8 and contains iron(II), free acid amongst other metals (Maree et al., 2013). Similar situations exist in the Central Basin near Boksburg and in the Eastern Basin near Springs where the quality of this water is as acidic and contaminated as that decanting in the Western Basin. In the Eastern basin, the pumping rate is set at approximately 75 – 108 ML/day (Ramontja et al., 2011).

The gold mining Witwatersrand conglomerates consist of quartz pebbles, typically 1–3 cm in diameter, set in a matrix of quartz sand. The matrix typically contains around 3% pyrite (about 1.6% S), with minor quantities of a wide variety of other sulphide and oxide minerals, in addition to gold (Naicker et al., 2003) . Table 1 below depicts the major constituents typically present in gold mine tailings.

Table 1. Major Constituents of Gold Mine Tailings (Malatse and Ndlovu, 2015)

Component	Composition (%)	Component	Composition (%)
$\mathbf{Na_2O}$	0.613	Fe_2O_3	4.51
MgO	1.79	Co_2O_3	0.0063
$\mathbf{Al_2O_3}$	10.2	NiO	0.0177
$\mathbf{SiO_2}$	77.7	CuO	0.007
$\mathbf{P_2O_3}$	0.085	ZnO	0.008
$\mathbf{SO_3}$	0.905	As_2O_3	0.01
$\mathbf{K_2O}$	1.19	Pb_2O	0.0041
CaO	1.93	SrO	0.0151
$\mathbf{T_iO_2}$	0.469	ZrO_2	0.0312
$\mathbf{C_{r_2}O_3}$	0.45	U_3O_8	0.0064
MnO	0.0549		

Typically, acid mine drainage is produced when rainwater falls over tailing dumps that contain sulphide ores especially pyrite to form sulphuric acid which percolates through the dump, dissolving heavy metals (including uranium) in transit and emerges from the base of the dump to join the local groundwater as a pollution plume ((McCarthy, 2011, Kefeni et al., 2017, Wong et al., 2014). This acidic water may then dissolve other minerals and metals, which can lead to high concentrations of pollutants such as lead, zinc, aluminium or cadmium with high salinity levels (Cobbing, 2008). A study conducted by (Naicker et al., 2003) revealed that the ground water within the mining district was heavily contaminated and acidified as a result of the oxidation of pyrite (FeS_2) contained within the mine tailing dumps.

The acidic reactions produced can be offset by the neutralising capacity contained within many of the surrounding rocks (Becker et al., 2015) however, gold and coal acid production often exceeds the neutralisation capacities capable by these dolomitic rocks. The overall impact of AMD depends on local conditions which varies widely depending on the geomorphology, climate and the extent and distribution of the AMD generating deposits (McCarthy, 2011) and before treatment options can be proposed, a comprehensive understanding of the chemistry behind acid mine drainage is needed.

Table 2. Sulphides responsible for acid generation with Pyrite and Marcasite being the predominant acid producers (Simate and Ndlovu, 2015)

Metal Sulphide	Chemical Formula
Pyrite	F_eS_2
Marcasite	F_eS_2
Pyrrhotite	$F_{e_{1-x}}S_x$
Chalcocite	Cu_2S^x
Covelite	CuS
Chalcopyrite	CuF_eS_2
Arsenopyrite	F_eAsS_2
Molybdenite	MoS_2
Galena	PbS
Millerite	NiS
Sphalerite	ZnS

2.4. Chemistry of Acid Mine Drainage

The formation of AMD depends on the type and amount of sulphide mineral oxidised as well as the gangue material present. The most common pathway starts with the mineral pyrite although there are other reactive sulphur containing minerals that have the ability to produce AMD (Table 2). The generalised reaction pathway (based on pyrite acid production) can be represented by the following set of reactions:

The first reaction is the oxidation of iron sulphide into dissolved iron, sulphate and hydrogen:

$$F_eS_2 + \frac{7}{2}\ O_2 + \ H_2O \ \rightarrow \ {F_e}^{2+} + 2{SO_4}^{2-} + 2H^+ \quad (1)$$

Under normal conditions, when pyrite mineral is exposed to air and water, equation 1 proceeds at a very slow rate however, after mining activities have commenced, the ore is extensively fragmented thereby increasing the surface area dramatically such that more pyrite is exposed at any given time. The dissolved iron, sulphate and hydrogen represents an increase in acidity of the water with lower pH levels.

Ferrous iron is thereafter oxidised to ferric iron according to the following reaction:

$$ {F_e}^{2+} + \frac{1}{4}\ O_2 + \ H^+ \ \rightarrow \ {F_e}^{3+} + \frac{1}{2}H_2O \quad (2)$$

At pH values between 2.3 and 3.5, ferric iron precipitates as $F_e(OH)_3$ and jarosite, leaving little ${F_e}^{3+}$ in solution while simultaneously lowering the pH to produce reaction 3:

$$ {F_e}^{3+} + 3H_2O \ \rightarrow \ F_e(OH)_3 + \ 3H^+ \quad (3)$$

The iron hydroxide produced from reaction 3 is in a solid form. Any ${F_e}^{3+}$ from equation 2 that does not precipitate from solution through equation 3 may be used to oxidise additional pyrite according to the following reaction:

$$F_eS_2 + 14\ {F_e}^{3+} + 8\ H_2O \ \rightarrow \ 15\ {F_e}^{2+} + \ 2{SO_4}^{2-} + \ 16H^+ \quad (4)$$

Based on the above reactions, acid generation that produced iron will eventually precipitate as $F_e(OH)_3$ which is represented as a combination of equations to produce the following final equation:

$$F_eS_2 + \frac{15}{4}\ O_2 + \frac{7}{2}\ H_2O\ \rightarrow\ F_e(OH)_3 + \ 2SO_4{}^{2-} + \ 4H^+ \qquad (5)$$

2.5. Existing Treatment Technologies

Several treatment technologies for the elimination of heavy metals are currently in use which are divided into biological, chemical and physical processes with the physical and chemical processes being the prominent ones used in industry. Chemical precipitation, ion exchange, reverse osmosis and adsorption are often the chemical and physical methods used for heavy metal elimination (Volesky and Naja, 2007, Luptakova et al., 2012, Gaikwad et al., 2010, Buzzi et al., 2011).

The use of a specific treatment technology depends on the type of effluent treated, the contaminant of interest and the conditions that prevail. Presented below are the conventional technologies that are used for the elimination of pollutants, heavy metals in particular.

2.5.1. Chemical Precipitation

Chemical precipitation involves adding chemical reagents to cause solids to precipitate from the solution (Lakherwal, 2014). Several coagulants such as alum, lime, iron salts and organic polymers are added to precipitate the contaminants out of solution. The precipitated solids formed by this reaction are removed from solution by settling out which is followed by filtration. The major challenge associated with using this process is the cost of the precipitating agent used (Lakherwal, 2014).

A study by Harper and Kingham (1992) achieved a 99% removal of arsenic using a combination of hydrated lime and ferric chloride chemicals where their findings highlighted that a combination of methods inclusive of precipitation, filtration and carbon absorption were necessary to treat high volumes of water (~605000L) demonstrating that a combination of treatment options are generally required to achieve effective removal efficiencies for large

volumes of water. As reported by Freitas et al. (2013), potassium permanganate was used to precipitate manganese from acid mine drainage effluent. A 99% removal capacity was achievable at pH 7 however additional by-products of the reaction, birnessite, hausmannite and manganite were found to be present which consequently incurred additional sludge disposal costs. In the work of Matlock et al. (2002), a potassium salt of a ligand was applied to remove lead from wastewaters containing concentrations from 2-300 ppm at pH 1.5. A 99.4 % removal efficiency was accomplished from an average initial concentration of 3.61 ppm within 15 min using an equimolar dosage of 1,3-benzenediamidoethanethiol dianion ligand.

2.5.2. Ion exchange

Ion exchange uses synthetic polymers known as resins to treat waste effluent. Insoluble resins with loosely held ions exchange with other ions in solution without physical alteration to the ion exchange material. The exchangers are acids or bases with insoluble salts which enable them to exchange positively or negatively charged ions with the polystyrene resins. Some of the advantages of using ion exchangers are its low operational costs, low energy requirements, cheap costs of regenerant chemicals and when well maintained, resin beds can last for many years before replacement is needed (Alchin and Wansbrough, 2017). There are however, limitations, which cannot be overlooked such as the precipitation of salts which fouls the resin beds and bacterial contamination of the resin beads.

Cadmium removal using a sulphonate based cation resin with insoluble amber beads was investigated in a study conducted by Bai and Bartkiewicz (2009). They reported a sorption capacity of 3.0 meq/g Cd within a pH range of 3 – 7 highlighting that small volumes of concentrated solutions were the preferred choice. In elaborating on ion exchange processes, findings from a study conducted by Ahmed et al. (1998) emphasized that the extent of metal removal is independent of the nature of anion used when a solid Na-Y zeolite was used to remove Pb and Cd ions. Ahmed et al. (1998) argued that an increase in concentration lowered the affinity of the zeolite for the inlet metal ions where Pb was preferred to the initial Na ion over the range of concentrations tested. In addition, Pb removal was found to be much greater than that of Cd under identical experimental conditions where the Na-Y exchange efficiency was shown to increase in the order Ni(I) < Cu(II) <Cd(I) < Pb(I). Contrasting to this view, cations of Cd and Te from an acid leaching solution of CdTe was found to be highly dependent on dosage and affinity of the sulfonate groups to the cations in a study optimizing CdTe to

prepare sulfonated magnetic microspheres as adsorbents via an aqueous suspension polymerization of styrene-divinylbenzene and a sulfonation reaction (Zhang et al., 2014).

The removal of Pb ions were investigated by Aydin et al. (2011) who used ashes of Sirnak burned coal waste and Chirkst et al. (2010) who used iron-manganese concretions (IMCs). Results from Aydin and co-workers revealed a spontaneous and exothermic reaction at 293–333 K with pseudo-2nd order kinetics and the work of Chirkst focused on the rate limiting step of the process. Chirkst concluded that diffusion is a function of temperature and the grain size of Fe–Mn concretions. A low activation energy of 14.64 kJ/mol was yielded in this study which verified outer diffusion to be the rate-determining stage.

Another important aspect in water treatment processes is mathematical modelling which was the main focus in a study by Cardoso et al. (2016) who investigated microporous stannosilicate in the removal of Cd ions. The system was modelled using the mass action law combined with activity coefficient models for the solution (Ideal, Debye–Hückel and Pitzer equations) and for the solid (Wilson equation) with absolute average relative deviations (AARDs) between 6.56% and 6.75%. It was concluded that the system embodied strong intraparticle nonidealities, namely solid activity coefficients between 0.2602 and 0.7180 for Cd (II). Kinetics revealed that the best fit kinetic models were achieved using the Maxwell–Stefan (MS) and Nernst–Plank (NP) models in comparison to the pseudo-first and second order models which are commonly adopted models in literature as demonstrated by a study by Wong and co-corkers (Wong et al., 2014).

2.5.3. Reverse Osmosis

In reverse osmosis, an external pressure is applied to drive the effluent through a semi-permeable membrane. High removal efficiencies are often attainable however the major challenge associated with this process is the unsuitable nature of the membrane to treat effluent containing low concentrations of metal ions. Membrane fouling is also a contributing factor in addition to being an energy intensive process where the applied pressure is required to exceed the osmotic pressure in order to obtain an adequate flowrate (Lakherwal, 2014).

The applicability of using Fe-derived drinking water treatment solids (DWST) for the selective removal of B, Cu, Cr, Pb and Se from brine were investigate in a study by Lin et al. (2014). DWST was found to be very effective in removing Cu and Pb which was attributed to the

formation of strong inner sphere complexes between the metal cations and Fe/Al oxide surface sites in the DWTs and the attractive electrostatic interactions with the negatively charged DWST surface. In contrast, the sorption of B and Se yielded lower results due to Se being a weakly bonded anion and B a nonionic acid. Sorption was found to be affected by the speciation of ions and electrostatic interactions with DWTS highlighting the specificity of removal in reverse osmosis processes. Higher influent pH increased boron and copper sorption but was found to inhibit the removal of chromium. Additionally, temperature, solid moisture content, and loading rate did not have significant impact on sorption to the DWTS.

Qdais and Moussa (2004), on the other hand, focused on the effect of concentration on the removal of Cu and Cd ions using reverse osmosis and ultrafiltration. A 98 % removal of Cu and 99% removal of Cd was achieved using reverse osmosis with a more than 90 % removal achievable using nanofiltration. In the case of wastewater containing more than one heavy metal, the reverse osmosis membrane achieved a 99.4% removal reducing wastewater with a concentration of 500 ppm to around 3 ppm, while the average removal efficiency of the nanofiltration membrane was 97% demonstrating the applicability of these membranes to treat metal laden water with high initial ion concentrations.

2.5.4. Adsorption

Adsorption is traditionally defined as the accumulation of a gas or liquid on the surface of an adsorbent to form a molecular or atomic film of adsorbate (Lakherwal, 2014). It can be applied to natural, physical, biological or chemical systems and is widely used in industrial applications. A wide range of commercial adsorbents are used but are relatively expensive, one such adsorbent being activated carbon. Activated carbon is commonly used in the water treatment industry but despite its effectiveness, the high cost of activated carbon has restricted its more widespread use (Malkoc et al., 2006b). Other types of adsorbents include clay minerals, biomaterials and zeolites (Stafiej and Pyrzynska, 2007, Celis et al., 2000). Of great importance are biosorbents which are an attractive alternative to conventional adsorbents since they can be locally sourced in large quantities. The main attraction of biosorption include its cost effectiveness and good removal performance (Aksu and Gönen, 2004a). Several works have been cited using a range of biosorbents proving that biosorption is an effective alternative

to the treatment of waste effluents (Hasfalina et al., 2012, Hasan et al., 2010, Shanmugaprakash and Sivakumar, 2015, Naddafi et al., 2007, Vendruscolo et al., 2017).

2.5.5. Biosorption

The concept of biosorption refers to a physiochemical process which transpires naturally in particular biomaterials that allow it to passively concentrate and bind pollutants onto its cellular structure (Mashangwa, 2017). The major advantage of using this technology is the effectiveness of bio-sorbent in reducing the concentration of pollutants to very low levels. Generally, biosorption processes can significantly reduce capital costs, operational costs and total treatment costs when compared with the conventional systems (Abdolali et al., 2014). Biosorbents attract and bind heavy metals by complex processes that comprise of ion exchange, surface precipitation, surface adsorption, metal detoxification and transformation (Martín-Lara et al., 2016). However, the selection of the biomass used is a critical step of biosorption since most biological materials have specific affinities towards metal ions. Generally, the goal for biosorption is large scale applicability, so the main factors to be taken into account during selection are cost and availability (Figueroa-Torres et al., 2016).

Table 3. Comparison of different technologies for removing heavy metals from wastewater (Nguyen et al., 2013)

Methods	Disadvantages	Advantages
Chemical Precipitation	Large quantity of sludge produced	Simple operation, inexpensive, capable of removing most metals
Ion exchange	High cost, less number of metal ions removed	High regeneration of metals, metal selective process
Reverse Osmosis	High operational costs due to membrane fouling	Small space requirement, low pressure, high separation selectivity
Adsorption using activated carbon	Cost of activated carbon, no regeneration, performance depends upon adsorbent	Most metals can be removed, high efficiency (>99%)
Biosorption	Early saturation, limited potential for biological process improvement, no potential for biologically altering the metal valence state	Low cost, high efficiency, minimization of sludge, regeneration of biosorbents, no additional nutrient requirement, metal recovery

2.6 Challenges of Waste disposal in South Africa

According to the National Waste Information Baseline (NWIB), South Africa generated approximately 108 million tonnes of waste in 2011, consisting of 59 million tonnes of general waste, 48 million tonnes of unclassified waste and 1 million tonnes of hazardous waste. The waste industry in South Africa currently consists mainly of collection and landfilling, with a limited amount (10%) being recycling. Consequently, alternative waste treatment is now being driven by restrictions on materials going to landfill sites due to pressures on landfill airspace, among other factors (Waste Economy: Market Intelligence Report).

By diverting even 20% of industrial waste away from landfill sites, the waste sector could potentially grow by R17 billion/year. Accordingly, the South African government has mandated waste management as a priority (Waste Economy: Market Intelligence Report). Furthermore, the National Environmental Management: Waste Act (No. 59 of 2008) (NEM:WA) and the National Waste Management Strategy (NWMS, 2011) has mandated municipalities to implement alternative waste management plans to divert waste from landfills to minimise environmental degradation. In this regard, the reuse of agricultural wastes such as sugarcane bagasse and eggshells will serve a twofold solution, the first being a promising solution to divert wastes to be sent to landfills and the second being a cost-effective remediation strategy to remove heavy metals from waste effluents.

2.6. Eggshell as a Biosorbent

In South Africa, the total egg production in 2014 amounted to 20.8 million cases of which egg production on an industrial level leads to a considerable quantity of shell residue, which is considered as a waste (Oliveira et al., 2013, SAPA, 2015). Many landfill sites are unwilling to accept eggshell waste due to the protein component of the membrane which attracts vermin (Choi 2015). Additionally, the costs associated with eggshell disposal (mainly on landfill sites) are significant and are expected to continue increasing as landfill taxes increase (Carvalho et al., 2011). Thus, several research studies have been conducted on eggshell waste to source alternative uses to solve this issue (Oliveira et al., 2013, King'ori, 2011, Carvalho et al., 2011). Possible applications range from uses such as fertilizer and animal feed to the adsorption of heavy metals, paper treatment, catalysts for biodiesel production, production of hydrolyzed

protein and bone and dental implants (Oliveira et al., 2013). As a countermeasure, eggshells can be utilized for various purposes to minimize their effect on environmental pollution.

A highly promising application for the reuse of eggshells is as an adsorbent due to its low cost, copious availability in nature, non-toxicity, high specific surface area, and high potential of ion exchange for charged pollutants (Zhang et al., 2012). Sorption by eggshells occurs mainly by an exchange reaction and it should be usable as a biosorbent of metal ions (Choi 2015). Currently, eggshells have few industrial applications despite being a plentiful waste and several potential applications are being investigated due to its calcium carbonate structure (Flores-Cano et al., 2013).

2.7.1. Structure of Eggshells

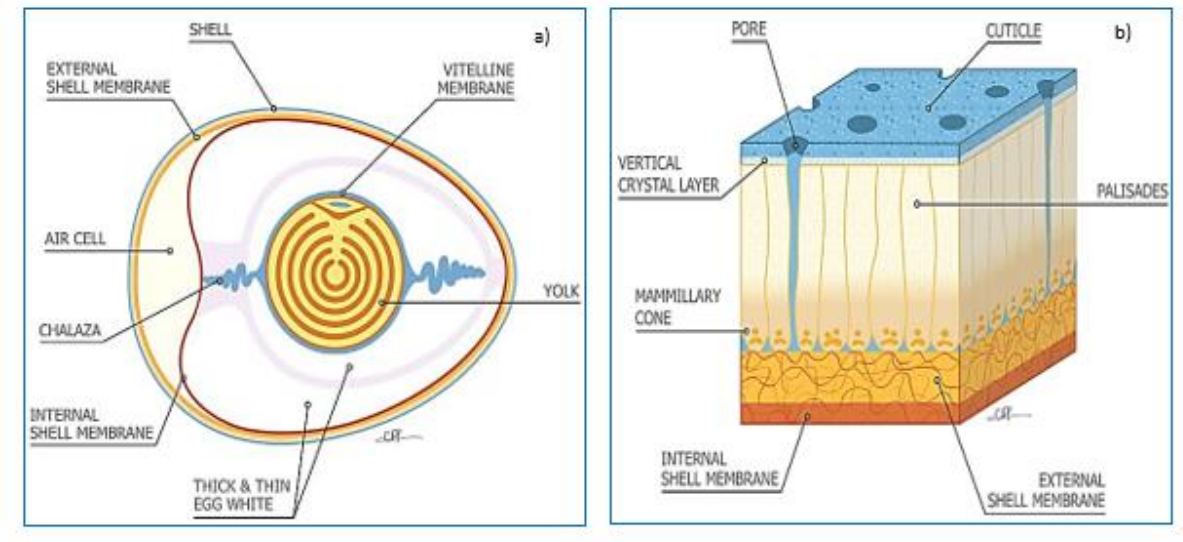

Figure 1. (a) Longitudinal section to depict the interior contents of a chicken egg and (b) Cross-sectional view (Hincke et al., 2012)

The eggshell, which is the by-product represents approximately 11% of the total weight (approximately 60 g) of the egg (Carvalho et al., 2011). It is comprised of a calcified shell and shell membrane layer including inner and outer membranes (Nakano et al., 2003). There are three layers, the outermost layer called the cuticle, the calcium carbonate layer called the testa, and the innermost layer called the mammillary layer. The cuticle and mammillary layers both form a matrix composed of protein fibers bonded to calcite (calcium carbonate) crystal. The two layers are also constructed such that there are numerous circular openings (pores), which

allow the transpiration of water and gaseous exchange, throughout the shell. Each eggshell has been estimated to contain between 7000 and 17,000 pores (Carvalho et al., 2011) making it an excellent choice to be used as an adsorbent.

The outer surface of the shell is covered with a mucin protein, which acts as a soluble plug for the pores in the shell (Tsai et al., 2006) with the organic matter of the shell and shell membrane containing proteins as major constituents with small amounts of carbohydrates and lipids (Nakano et al., 2003).

2.7.2. Eggshell Membrane (ESM)

The membrane layer of the eggshell is an amorphous natural biomaterial with an intricate lattice of stable and water insoluble fibers (Mittal et al., 2016). There are two membranes which lie directly beneath the shell called the inner and outer shell membrane. The outer membrane remains adhered to the mammillary layer of the shell, while the inner membrane surrounds the liquid of the egg. The two membranes separate at the larger end of the egg and create a space between them called the 'Air Cell'. The membranes are composed of protein fiber arranged to form a semi-permeable membrane with a total thickness of around 100 μm (Tsai et al., 2006). The membrane surface bears positively charged sites produced by basic side chains of amino acids. It has a very high surface area with functional groups such as hydroxyl (−OH), thiol (−SH), carboxyl (−COOH), amino (−NH2) and amide (−CONH2) to name a few (Mittal et al., 2016).

2.7.3. Chemical Composition of the Eggshell & Eggshell Membrane

The mineralized shell constitutes about 96% calcium carbonate with the remaining components comprising of the organic matrix (2%), magnesium, phosphorus and a variety of trace elements (Mittal et al., 2016, Hincke et al., 2012). The membrane constitutes nearly 60% protein of which 35 % is collagen, 10% glucosamine, 9% chondroitin and 5 % hyaluronic acid together with other inorganic components like Ca, Mg, Si, Zn, etc. in minor quantities. The density of the shell is approximately 2.53 g/cm^3, which is significantly larger than that of the membrane which is 1.358 g/cm^3 (Mittal et al., 2016).

2.7.4. Biosorptive Removal of Heavy Metals using Eggshells

In the last decade, the use of poultry waste in wastewater treatment processes have received much attention from researchers all over the world (Mittal et al., 2016). The removal of heavy metals from waste effluent is a matter of great interest due to the water scarcity and declining quality of water in South Africa. Numerous metals such as lead, copper, chromium, cadmium, lead, arsenic etc are known to be significantly toxic and in recent years their effective removal using eggshell biomass as adsorbents have been achieved (Putra et al., 2014, Eletta et al., 2016, Senthilkumar, 2015, Park et al., 2007, Chojnacka, 2005, Flores-Cano et al., 2013).

Operational variables such as concentration, dosage and pH greatly affect the efficacy of biomaterials and it is important to investigate these variables to achieve the optimal conditions which will give the highest percentage removal. In this regard, a study conducted by Putra et al. (2014) revealed optimal conditions at a pH of 6.0, 0.1 g biomass with 90 min equilibrium time in the removal of Cu, Pb and Zn ions. Mezenner and Bensmaili (2009), however, reported optimal conditions at a biomass dosage of 10g/L, pH 7, 60 min contact time with an initial concentration of 2.8 mg/L for the removal of phosphate. In addition, in a study by Yeddou and Bensmaili (2007), the optimum conditions were found to be 2.5 g/L biomass dosage, pH 6, 40 min of contact time of a 10 mg/L concentrated solution at a temperature of 20°C for the removal of Fe(II) ions.

It is generally agreed upon that optimal conditions depend on the type of biomass used, the adsorbate being removed as well as environmental conditions that prevail as can be demonstrated by a study conducted by Bhatt (2015) who varied the contact time, agitation speed and pH to investigate the removal efficiency of Cu and Pb ions. The optimized conditions concluded from this experiment was obtained at a pH of 7, 100 rev/min with a contact time of 90 minutes. In this regard, process parameters in an investigation by Mashangwa (2017) revealed optimal conditions being attainable at pH 7, biomass dose of 7 g with a contact time of 360 min (for the removal of 100 ppm metal ions) in the removal of Zn, Pb, Cu and Ni ions from synthetic solutions and several metals from three acid mine drainage (AMD) samples. Under these conditions, a 97% removal for Pb, 95% for Cu, 94% for Ni, and 80% for Zn was achievable signifying the applicability of eggshells as a biosorbent. It is also of note that many other metals, inclusive of Al, Fe, K, Ni, and Zn, exhibited removal capacities greater than 75 % in AMD sample 1. Additionally, K had a 98.78% adsorption, while Mg, Sr, and Zn had 72.33, 68.75, and 53.07% capacities respectively in sample 2. In sample 3, As, Cr, Cu, Fe,

antimony, and tellurium ions were greater than 75%. Particle size is another variable which affects the removal capacity as highlighted by a study investigating the removal of divalent Pb cations by Vijayaraghavan and Umid (2013) who used eggshells as an additive to precipitation. On reducing the particle size from 750 to 100 microns, a significant increase in removal efficiency from 30.7 to 99.6% was achieved with 35 min being sufficient to achieve equilibrium.

Characterisation studies form a vital component in understanding the interaction between a biosorbent and adsorbate in the adsorption process. Putra et al. (2014) used the techniques of Scanning Electron Microscope (SEM), Energy Dispersive X-ray Spectroscopy (EDS) and Fourier Transform Infrared Spectrometer (FTIR) to characterise the biomass which revealed interactions with metal ions resulting in the formation of discrete aggregates on the biosorbent surface. Ion exchange proceeded through the electrostatic attraction between the metal ion and carbonate group whilst the complexation mechanism involved electron pair sharing between electron donor atoms (O and N). Results from this study proposed that carbonate, carbonyl, hydroxyl and amine groups were the main adsorption sites in eggshells. In a study involving the sorption mechanism of Cd(II), Flores-Cano et al. (2013) attributed the main mechanisms to the calcareous layer of the eggshell, but also slightly on the membrane layer. It was demonstrated that the sorption process was not reversible with the main mechanisms of removal being attributed to precipitation and ion exchange. The precipitation of $(Cd,Ca)CO_3$ on the surface of the eggshell was corroborated by SEM and XRD analysis where the biosorbent was characterized by several techniques which confirmed the calcite phase of the eggshell due to its $CaCO_3$ structure. In elaborating on cadmium removal, research conducted by Balaz and co-workers revealed a significant increase in adsorption upon milling with the main driving force for adsorption proven to be the presence of the aragonite phase as a consequence of phase transformation from the calcite phase which occurred during milling. Cadmium was found to be adsorbed in a non-reversible way, as documented by XRD and EDX measurements (Baláž et al., 2015). Ok et al. (2011) investigated the effectiveness of eggshells on the immobilization of Cd and Pb using techniques such as SEM and XRD to characterize the eggshell biomass.

2.7.5. Biosorptive Removal of Dyes using Eggshells

Apart from heavy metals, dyes and pigments also pose an environmental threat as they are emitted into wastewaters from various industries such as dye manufacturing, textile finishing, food, cosmetics, paper and carpet industries (Slimani et al., 2014). The adsorption characteristics of basic yellow 28 dye onto calcined eggshells was investigated in batch studies which revealed a maximum biosorption capacity of 28.87 mg/g (Slimani et al., 2014). Results obtained inferred multilayer adsorption from the Freundlich model which was in agreement with studies conducted by other researchers in the removal of brilliant green dye, methylene blue, congo red dye and reactive red 123 dye (Kobiraj et al., 2012, Abdel-Khalek et al., 2017a, Ehrampoush et al., 2011). Contrasting to these views, a study by Zulfikar and Setiyanto (2013) involving the adsorption of congo red (CR) using untreated powdered eggshells, revealed the Langmuir model as the best fit model, as did Elkady et al. (2011) who used immobilized eggshells with a polymer mixture of alginate and polyvinyl alcohol applied as a biocomposite adsorbent in the removal of C.I. Remazol Reactive Red 198 dye.

In investigating optimal conditions for dye removal, many studies have been conducted. An adsorption capacity of 1.26 mg/g was achieved in the removal of reactive red 123 dye by Ehrampoush et al. (2011) with Kobiraj and co-workers able to achieve capacities of 44.7 mg/g, 34.23 mg/g and 30.23 mg/g at 303 K,313 K and 323 K respectively in the removal of brilliant green dye (Kobiraj et al., 2012). Zulfikar and Setiyanto (2013) studied the adsorption of Congo red (CR) achieving a maximum capacity of 95.25 mg/g at a contact time of 20 minutes, adsorbent dosage of 20 g, initial concentration of 20 mg/L and pH 2. In elaborating on this, the maximum capacity of methylene blue and congo red was 94.9 mg/g and 49.5 mg/g for a concentration of 1000 mg/L at room temperature in a study by Abdel-Khalek et al. (2017b) who investigated the feasibility of using the whole eggshell matrix (eggshell and membrane) to remove methylene blue and Congo red. Mohamad (2017) on the other hand, focused on malachite green removal, achieving a 92.39% removal efficiency with optimal conditions of 70 mg/L, dosage of 1.99 g and contact time of 16.25 minutes using eggshell biochar.

Belay (2015) used thermally treated eggshells to remove methyl orange and was able to achieve a 98.8% removal efficiency with conditions of 12.5mg/L, 2g adsorbent with a contact time of 20 minutes. Batch studies conducted by Elkady et al. (2011) using immobilized eggshell with a polymer mixture of alginate and polyvinyl alcohol applied as a biocomposite adsorbent to remove C.I. Remazol Reactive Red 198 dye revealed a maximum dye removal capacity of 46.9

mg/g at the optimum pH of 1.0 at a temperature of 22 °C. An adsorption capacity of 1.26 mg/g was achieved when chicken eggshells were used to remove Reactive red 123 dye (Ehrampoush et al., 2011). The work of Podstawczyk et al. (2014) focused on the removal mechanism of malachite green dye where it was found that physical adsorption, alkaline fading phenomenon and microprecipitation were the main mechanisms. Elaborating on this, Kobiraj and co-workers found that adsorption followed both surface and intra-particle diffusion mechanisms in a study using hen eggshell powder to remove brilliant green dye (Kobiraj et al., 2012).

2.8. Bagasse as a Biosorbent

The South African sugar industry is ranked in the top 15 out of approximately 120 sugar producing countries worldwide. On average, 22 million tons of sugar cane are produced each season from 14 mill supply areas, extending from Northern Pondoland in the Eastern Cape to the Mpumalanga Lowveld in South Africa (SASA). Of the 22 million tonnes production capacity, around 3.3 million tonnes of dry bagasse is produced as a by-product of the sugar manufacturing processes (Mwasiswebe, 2005).

Presently, around 6 to 7% of the bagasse that is produced is used in the production of animal feed, paper and furfural products, 2% as pith in the production of animal feed, 4 to 5% as refined fibre while the net use of bagasse for furfural production is negligible (Economists, 2013). The primary use for bagasse is for steam generation to meet energy requirements however owing to improved steam economy and boiler efficiencies, there is still a surplus of bagasse (Mwasiswebe, 2005) in many factories.

The disposal of bagasse has become a problem in sugar factories all over the world where some factories have resorted to landfills and incineration. Landfills, however, pose a potential hazard due to the risk of spontaneous combustion as a result of microbial activity in the dumps (Mwasiswebe, 2005). Traditionally, bagasse was left on site, burned or allowed to rot. The renewed interest to utilize bagasse as a potential biosorbent comes in the wake of the negative effects due to metal contamination of industrial effluents into the environment. The use of bagasse as a biosorbent is one such alternative that offers huge opportunities to overcome these problems. Thus, several research studies have been conducted on waste sugarcane bagasse (Homagai et al., 2010, Chandel et al., 2014, Raymundo et al., 2010, Leão et al., 2017, Chao et al., 2014).

2.8.1. Structure of Bagasse

Sugarcane bagasse (Saccharum officinarum L.) is the fibrous material left over after crushing and juice extracting (Ullah et al., 2013) and is one of the most abundant lignocellulosic agro-industrial residues (Sarker et al., 2017). It is composed of several useful components, including cellulose, hemicelluloses, lignin, ash, and a small amount of extractives.

There are several types of cellulose in the cell wall of lignocellulosic materials. Cellulose which comprises typically between 30 – 50% by composition, is a linear polymer of b–D–glucopyranose sugar units whose average chain has a degree of polymerization of around 9000–10,000 units (Abdolali et al., 2014). A large portion of cellulose is highly oriented and crystalline with no accessibility to water and other solvents, while the rest of the material is composed of less oriented chains which have association with hemicellulose (20–40%) and lignin (15–25%) (Abdolali et al., 2014). Lignin molecules, on the other hand, are highly branched without a crystalline structure, and are composed of nine carbon units with small amounts of water, ash, cyclic hydrocarbons, organic and inorganic materials and a large number of lipophilic and hydrophilic constituents (Cagnon et al., 2009).

Biomass produced from sugarcane bagasse are composed of macromolecules containing humic and fulvic substances, lignin, cellulose, hemicelluloses, and proteins, which have several functional groups that act as adsorptive sites, including –OH, –COOH, –NH2, –CONH2, –SH2, and –OCH3 (Rezende et al., 2011). Strong attractive forces of the pollutant to the active sites are due to its numerous and varied functional groups which makes bagasse a good biosorbent (Okoro and Okoro, 2011). These sites enable the biosorbent to attract and bind pollutants, either by replacing them with hydrogen ions (ion exchange), adsorption, or by the donation of electron pairs (complexation) (Rocha et al., 2015).

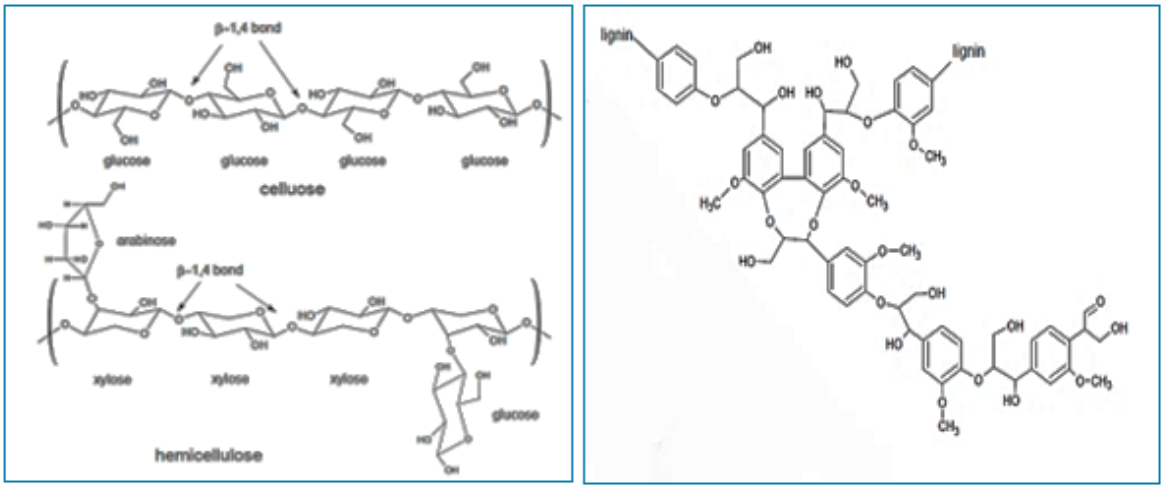

Figure 2. Structure of Sugarcane Bagasse (Mthembu, 2015 and Walford, 2008)

2.8.2. Biosorptive Removal of Heavy Metals using Bagasse

The effect of pH, concentration, contact time and temperature were factors highlighted in a study by Moubarik (2015), who investigated the removal of Cd(II) using sugar cane bagasse. Optimum conditions were achieved at a temperature of 298 K, pH 7, 30 min equilibrium time with a concentration of 30 mg/L. Conversely, optimum conditions of 500 mg/L concentration, 3 hours contact time at a pH of 4 was required for cadmium removal in the work of (Swathanthra, 2014). In another study by Ibrahim et al. (2006), 150 rpm speed, 90 min contact time at a pH of 5 – 7 was required to achieve optimised conditions for Cd removal.

Ullah et al. (2013) investigated the removal of Cr(III) and Cr(VI) ions using native and immobilized bagasse with a maximum uptake of 80.6% and 41.5% for Cr(VI) and Cr(III) ions onto the immobilized biomass and up to 73% for the Cr(III) ion at optimized conditions. Rapid uptake was observed within the first 20-30 min, conclusive of surface adsorption which was in agreement with findings reported by other studies as well (Yu et al., 2013, Liu et al., 2015, Khoramzadeh et al., 2013, Krishnan and Anirudhan, 2003). Another important finding demonstrated in this study was the dependence of the ionic form on the uptake capacity. The capacity of the Cr(VI) ion was found to be higher at pH 2 while for the Cr(III) ion sorption, it increased up to pH 5 which was corroborated by a study conducted by Vinodhini and Das (2009) who concluded an optimal pH of 2 in the removal of the Cr(VI) ion.

According to Alomá et al. (2012), information about the surface chemistry characterization of a biomass, for example the alteration of functional groups, can be used as evidence in proposing biosorption mechanisms. Moubarik (2015) characterized sugarcane bagasse by means of FTIR, BET, SEM and zeta potential analysis which is also the preferred choice by several other researchers ((Pillai et al., 2013, Sounthararajah et al., 2015, Rubcumintara, 2015). The use of FTIR highlights the functional groups present on a biomass surface which is responsible for adsorption. Results from a study by Chao et al. (2014) revealed carboxylic acid groups, which function as exchangeable cation and complexation sites as the mechanism of adsorption in heavy metal removal with the primary groups being attributed to OH and COOH. The COOH group provided a complexation site, whereas both OH and COOH groups generated exchangeable cation sites. As noted by Martín-Lara et al. (2010), carboxyl and amine groups were the sites responsible for adsorption in the removal of Pb(II) ions using native and modified bagasse.

2.8.3. Biosorptive Removal of Dyes using Bagasse

A study conducted by Madhav et al. (2013) focused on the effect of operational parameters on the removal of Acid Orange 7 (AO7) dye from textile wastewater. The effect of pH, biosorbent dose, concentration, agitation speed and temperature were investigated. From this study, the optimum conditions were found at a dosage of 8 g, concentration of 4 mg/100mL, pH of 2.5 at 30°C. Kinetics showed that the process followed the Langmuir isotherm more proficiently than the Freundlich isotherm as did other works in the removal of methyl red (Azhar et al., 2005), direct yellow 12 (Said et al., 2013), orange olimax TGL (Fontana et al., 2016) and methylene blue (Filhoa et al., 2007). In contrast to these views, the work of Said et al. (2013) investigated the removal of reactive yellow 2 and reactive blue 4 where the equilibrium adsorption data best fitted the Freundlich isotherm for reactive yellow 2 and the Langmiur isotherm for reactive blue 4 dye respectively.

Wong et al. (2009) demonstrated the effectiveness of using quartenized bagasse in removing basic and reactive dyes from aqueous solution. The results showed that sorption was strongly affected by pH, with the optimum pH being in the range of 6 – 8. The removal of basic blue 3 was favourable at higher temperatures, indicating that the sorption process was endothermic. On the other hand, sorption of reactive orange 16 was more favourable at a lower temperature.

2.9. Factors Affecting Biosorption

2.9.1. Effect of pH

Solution pH is a fundamental parameter that affects the speciation of metal ions in solution through hydrolysis, complexation, and redox reactions (Das, 2010). Among all other variables, pH is most critical since it not only influences the speciation of metal ions but also the charge on the sorption site of a biomass (Gao and Wang, 2007). Thus, it is vital to consider the ionic state of a functional group in the biomass together with the metal solution chemistry at different pH values. With a change in pH, the behaviour of a functional group will change accordingly.

Adsorption due to complexation is pH dependent which occurs at a specific pH (Farooq et al., 2010) and when the pH of a solution changes, the complex formation will be affected resulting in a change in biosorption efficiency of the biomass. In low pH environments, metal ions are generally positively charged and are attracted by negatively charged biomass. As the pH of a solution is increased, the amount of hydroxide ions increases.

The effect of pH on the removal of Cd and Cu was investigated by Muhamad et al. (2010), using wheat straw (Triticum sativum). Maximum removal was achieved within a pH range of 3 – 7 with Cu being removed at a higher rate. The author attributed the hindrance of adsorption to the high concentration of H^+ ions in solution at low pH values. However, as the pH was raised between 4 – 6.5, they noted the competition between Cu and Cd to be more predominant due to the lower concentration of H^+ ions.

The maximum uptake of Zn was observed at pH 5, concentration of 100 mg/L, temperature of 303K and biosorbent dose of 4g/L using defatted pongamia oil cake (Shanmugaprakash and Sivakumar, 2015). The results highlighted that negatively charged functional groups are protonated in acidic conditions resulting in decreased efficiencies. As a result, the deprotonation of functional groups produced an increase in the attraction sites towards the negatively charged ions which increased the removal efficiency. Several other works have corroborated this finding (Areco et al., 2012, Hawari and Mulligan, 2006).

In another study, the effect of pH was examined by Han et al. (2006) in the removal of Cu and Pb using chaff within a range of 3 – 5. At low pH, they observed that the biomass was surrounded by hydronium ions decreasing the Cu and Pb interaction with binding sites by greater repulsive forces. At a pH of 2, a lower biosorption capacity was achieved which

indicated that the mechanism of biosorption was not only ion-exchange. With an increase in pH, the overall surface charge of the biosorbent became negative which increased the adsorptive capacity, which was supported by a study conducted by Areco et al. (2012). Conversely, when the pH increased beyond 6.5, the precipitation of insoluble Cu and Pb hydroxide occurred on the adsorbent surface which demonstrated that metal removal beyond this pH was due to precipitation only. Studies by Farooq et al. (2010) reported the effect of precipitation at different pH values within the range of 5.5 to 12.5 which is an important factor to consider when dealing with solution pH.

In general, metal ions are precipitated out in the alkaline pH range and do not contribute towards biosorption which inherently highlights the upper limit of pH to be studied. Lead is present as Pb^{2+} as the dominant species at pH values < 5.5, as $Pb(OH)_4{}^{2-}$ at pH values > 12.5 and as $Pb(OH)_2$ at 5.5 < pH < 12.5 (Farooq et al., 2010). Similarly, cadmium is present as free Cd^{2+} species along the acid pH range. At pH values > 7.5, it begins to precipitate as $Cd(OH)_2$ and therefore is not able to participate in biosorption (Basualto Flores et al., 2006). Thus, pH directly influences the mechanism and uptake of metals by the biosorbent used. Generally, when the pH of a solution exceeds 8, metal ions are precipitated out. It therefore seemed apt that the work conducted in this study be performed within a range of 2 – 7.

2.9.2. Effect of Concentration

The effect of concentration affects the sorption capacity of a biosorbent with a higher concentration resulting in higher solute uptake. At low solute concentrations, the ratio of moles of solute to available surface area is low and the resultant fraction sorbed becomes independent of the initial metal concentration (Das, 2010). At higher concentrations, the sites available for adsorption are fewer compared to the number of moles of solute present, hence the removal of solute strongly depends on the initial solute concentration.

Malakondaiah et al. (2010) proposed that a lower biosorption capacity is obtained with an increase in metal ion concentration due to insufficient surface area to accommodate higher concentrations of metal ions available in solution. Singha and Das (2012) corroborated this observation in their study using 6 biosorbents, namely, rice straw, rice bran, rice husk, coconut shell, neem leaves and hyacinth roots in the removal of Pb where the percentage removal decreased with an increase in initial lead concentration. The sorption capacity was found to

increase in the range of 0.4 – 21.0 mg/g when the initial concentration of Pb(II) ions increased from 5 to 300 mg/L.

At lower concentrations, metal ions present in solution interact with the binding sites and thus the percentage biosorption is higher than those at higher initial metal ion concentrations. At higher concentrations, lower biosorption yield is due to the saturation of biosorption sites. As a result, diluting effluent containing high metal ion concentrations can increase the purification yield (Malakondaiah et al., 2010). In a study conducted by Hamissaa et al. (2010), the removal of Pb and Cd was found to be 3.5 – 12 mg/g and 4 – 37 mg/g within a range of 20-160 mg/L and 20-300 mg/L using Agave Americana fibres. The author proposed that the rapid increase in metal sorption (first 15 min) was due to a large number of available sites with no less than 80% of metals being removed. However, owing to a reduction in the number of available sites, the metal ions took more time to access the least accessible sites, thus the sorption decelerated. Studies conducted by other researchers obtained similar results (Dong and Lin, 2017, Jin et al., 2018).

Malakondaiah et al. (2010) used hen egg shell to remove Cu from a concentration range of 20-100 mg/L with an increase in metal uptake observed at increased initial metal ion concentrations. In contrast, the biosorption capacity was found to decrease from 89.25% – 74.84%. It was proposed that metal uptake increased due to the increase in driving force, that is the concentration gradient. In the studies of Pillai et al. (2013) the biosorption capacity of xanthated nano banana cellulose was investigated in the removal of Cd where the influence of initial cadmium concentration was used to determine the biosorption efficiency of the biomass. From a range of 50 – 300 mg/L, the percentage removal decreased from 97.5-85.8 % with increasing initial concentration which was due to the limitation of vacant binding sites thus decreasing removal yield.

Jin et al. (2018) reported the increase in biosorption capacity from 24.3 to 85.8 mg/g with a decreased biosorption rate of 97.4% to 57.2% with increasing Cd (II) concentration in the range of 25 – 150 mg/L. In this study, immobilized Pleurotus Ostreatus spent substrate (POSS) was used to remove Cd (II) ions. The author discovered that at lower concentrations, the ratio of metal ions to available sites was low which resulted in a lower sorption capacity and a higher sorption rate. Results from a study conducted by Cruz-Olivares et al. (2013) who used the residue of allspice (Pimenta dioica L. Merrill) to investigate the removal of Pb agreed with the above findings.

In fixed bed studies, high inlet concentrations result in high concentration gradients where stronger driving forces are obtained producing increased biosorption capacities. It was proposed by Morosanu et al. (2017) that in a specified amount of sorbent, an increase of the quantity of metal ions entails a greater driving force to transport the ions from the aqueous phase to the surface of the sorbent where the interaction between the metal ions and active sites increase. In the above study, the concentration of Pb solutions varied between 5 – 250 mg/L using rapeseed biomass to study the correlation between the initial amount of metal ions in aqueous phase and the metal-binding capacity of the biomass. Pb uptake was found to depend on the initial concentration and increased with an increase of metal ions available. Work by Dong and Lin (2017) supported this theory when Beer lees was used to remove Pb and Zn ions tested from 15 – 60 mg/L and 7.5 – 30 mg/L to produce adsorption capacities of 22.10 mg/g – 26mg/g and 3.5 – 3.71 mg/g respectively.

The concentration of solute in the adsorbate is an important parameter, which determines both the utilization and feasibility of a biosorbent in a biosorption process. Jin et al. (2018) suggests experiments to be carried out at the maximum possible initial solute concentration to attain the highest saturation potential of a biosorbent. In this research study, concentrations of up to 100 mg/L will be used to assess the saturation potential of the eggshell – bagasse biosorption system.

2.9.3. Effect of Adsorbent Mass

The biosorbent mass strongly influences the extent of adsorption in a biosorption process. An increase in the biomass concentration increases the amount of solute adsorbed due to the increased number of binding sites. On the other hand, the quantity of biosorbed solute per unit weight of biosorbent decreases with increasing biosorbent dosage due to complex interactions (Das, 2010). Sometimes, at high sorbent loads, the available solute is insufficient to completely cover the available exchangeable sites on the sorbent surface resulting in slow uptake. As suggested by Barka et al. (2013), a further increase in biomass concentration above a certain dosage does not lead to a significant improvement in biosorption yield which was attributed to partial aggregation of the biomass, consequently resulting in a decrease in effective specific surface area for biosorption.

Kulkarni et al. (2014) investigated the effect of biomass concentration on the sorption of Cd and Ni by dead biomass of Bacillus laterosporus. Results from this study showed an increase in removal efficiency with increase in biomass concentration at the conditions of 50 mg/L, pH 7, temperature of 28 °C and a contact time of 2 h respectively. Within a range of 2 g/L – 40 g/L biomass, the percentage sorption increased from 15.34% to 58.05% for Ni and 62.57% to 83.02% for Cd respectively. In this regard, it was noted that 58% adsorption of Ni was achieved when the biomass dosage was 40 g/L however an 83% removal of Cd (II) was achieved at the same condition which suggested that the biosorbent had a higher affinity toward Cd (II) than Ni (II). Similar results were obtained by Vimala and Das (2011) who investigated the removal of Pb and Cd using 3 biosorbents, namely, oyster mushroom (Pleurotus platypus), button mushroom (Agaricus bisporus) and milky mushroom (Calocybe indica). A maximum removal efficiency of 93.76% of Cd was achieved with 0.4 g of composite chitosan biosorbent CCB when tested in the temperature range of 298 – 318 K, pH 6, 100 ml of sorbate and adsorbent dose in the range of 0.05 – 0.5 g (Madala et al., 2017).

2.10. Batch Studies

Batch adsorption experiments are used to determine the adsorption capacity of a biosorbent.

The adsorption uptake and percentage removal of adsorbate from an aqueous solution (mg of adsorbate/g of adsorbent) is calculated using the following equations:

Amount Adsorbed: $$q = \frac{C_o - C_t}{W} V \quad (6)$$

Percentage Removal: $$q = \frac{100\,(C_o - C_t)}{C_o} \quad (7)$$

Where q is the amount of metal ion adsorbed per gram of adsorbent (mg/g), C_o (mg/L) is the initial metal ion concentration, C_t (mg/L) is the metal ion concentration at time t, W (g) is the mass of the adsorbent and V (L) is the volume of the solution.

2.10.1. Equilibrium Modelling

Adsorption isotherms reveal the specific relation between the concentration of the adsorbate and its adsorption degree onto the adsorbent surface at a constant temperature, under equilibrium conditions. To analyse the equilibrium adsorption data, two commonly employed models, the Langmuir and the Freundlich isotherm models have been presented.

The Langmuir isotherm is based on the assumptions that the maximum adsorption capacity corresponds to a saturated monolayer of adsorbate molecules on the surface of the biomass, the energy of adsorption is constant and that there is no transmigration of adsorbate molecules in the plane of the surface (Kobiraj et al., 2012). The Langmuir isotherm in its original form as well as its linearised form can be expressed by equations 8 and 9 as follows:

$$q_e = \frac{q_m C_e b}{(1 + bC_e)} \tag{8}$$

$$\frac{1}{q_e} = \frac{1}{q_m} + \frac{1}{bq_m C_e} \tag{9}$$

Where C_e is the equilibrium concentration of metal ion $\left(\frac{mg}{L}\right)$, q_e is the amount of metal ion adsorbed per unit weight of adsorbent material at equilibrium $\left(\frac{mg}{g}\right)$, b is the Langmuir constant $\left(\frac{L}{mg}\right)$ and q_m is the maximum adsorption capacity $\left(\frac{mg}{g}\right)$.

The Freundlich empirical model considers mono – layer coverage of the solute onto the adsorbent where it assumes that the adsorbent has a heterogenous surface such that binding sites are not identical (Ahmad, 2012). This model is applicable for only single component adsorption which is represented by equation 10 and in its linearised form, equation 11 below:

$$q_e = K_f {C_e}^{1/n} \tag{10}$$

$$Log\ q_e = Log\ K_f + \frac{1}{n} Log\ C_e \tag{11}$$

Where $C_e$is the equilibrium concentration of the metal ion $\left(\frac{mg}{L}\right)$, q_e the amount of metal ion adsorbed per unit weight of adsorbed material $\left(\frac{mg}{g}\right)$, K_f $\left(\frac{mg}{g}\right)\left(\frac{L}{mg}\right)_{\frac{1}{n}}$ a parameter relating the biosorption capacity and $\frac{1}{n}$ is an empirical parameter relating the biosorption intensity.

2.10.2. Kinetic Modelling

The rate of metal sorption is an important factor as it provides valuable insights into the reaction pathways and the mechanism of biosorption (Iqbal et al., 2009). Since biosorption is a metabolism independent process, it is expected to be a very fast reaction. The two most common models used in describing the reaction kinetics of heavy metals include the pseudo – first order, and pseudo – second order models. The pseudo – first order kinetic model was proposed by Lagergren (Lagergren, 1898). The general form of the model can be expressed as equation 12 and in its linearised form, equation 13:

$$\frac{dq_t}{dt} = k_1 (q_e - q_t) \quad (12)$$

$$\ln(q_e - q_t) = \ln q_e - k_1 t \quad (13)$$

in which k_1 is the rate constant (min^{-1}), q_t is the amount of metal ion sorbed at time t (mg/g) and q_e is the value at equilibrium (mg/g).

The pseudo-second-order kinetic model proposed by Ho and McKay (Ho and McKay, 1999) assumes that adsorption follows second order chemisorption. The general form and linearised form can be written as follows:

$$\frac{dq_t}{dt} = k_2 (q_e - q_t)^2 \quad (14)$$

$$\frac{t}{q_t} = \frac{1}{k_2 {q_e}^2} + \frac{t}{q_e} \quad (15)$$

in which k_2 is the pseudo-second-order rate constant (g/mg min), q_t is the amount of metal ions sorbed at time t (mg/g) and q_e is the value at equilibrium (mg/g).

2.11. Fixed Bed Column Studies

Breakthrough curves are primarily associated with fixed bed column operation. Practically, column operations are used over batch since more efficient use of the adsorbent can be attained due to the continuous contact of the adsorbent with fresh solution of initial solute concentration. Thus, the concentration of solution in contact with a given layer of sorbent remains approximately constant resulting in maximum loading of the sorbent. To determine the efficiency of a column, a breakthrough curve is used which is essentially obtained by plotting the column effluent concentration against the volume treated or the time required for treatment. From a breakthrough curve, it is possible to calculate the breakthrough capacity, exhaustion capacity and the degree of column use of a fixed bed column.

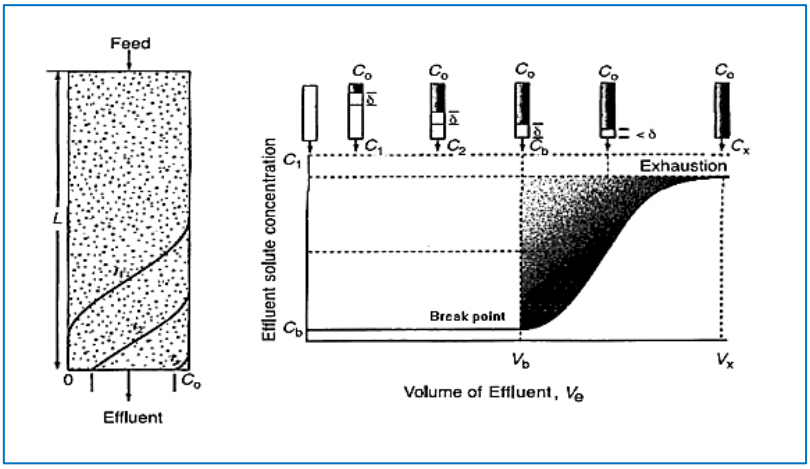

Figure 3. Representation of a typical breakthrough curve (Calero et al., 2009)

When fluid begins to flow through the column, the mass transfer zone varies from 0% of the inlet concentration (corresponding to the solute – free sorbent) to 100% of the inlet concentration (corresponding to the total saturation). From a practical point of view, the saturation time, t_s, is established when the concentration in the effluent is higher than 90–95% of the inlet concentration. The service or breakthrough time, t_b, is established when the metal concentration in the effluent reaches a determined value, generally related to the permitted disposal limit for the metal in concern, which makes it possible to determine the volume of effluent treated.

The volume of effluent is calculated as follows:

$$V_{eff} = Q\ t_{total} \tag{16}$$

Where t_{total} is the total flow time in min , and Q is the volumetric flowrate which circulates through the column in $\left(\frac{mL}{min}\right)$.

The performance of an adsorption column for a given adsorbent is directly related to the number of bed volumes processed before the breakthrough point is reached (Masukume et al., 2014). The number of bed volumes treated before breakthrough can occur is given by the following equation:

$$Number\ of\ bed\ volumes\ (BV) = \frac{Volume\ of\ water\ treated\ at\ breakthrough\ point\ (L)}{Volume\ of\ adsorbent\ bed\ (L)} \qquad (17)$$

The rate at which the adsorbent gets exhausted during adsorption is used to determine when the adsorbent needs replacement or needs to be regenerated. The AER of an adsorbent is determined by equation 18:

$$AER = \frac{mass\ of\ adsorbent\ (g)}{Volume\ of\ water\ treated\ (L)} \qquad (18)$$

The area under the breakthrough curve represents the maximum column capacity, q_{total}, in mg, for a given feed concentration and flowrate which is determined by integrating the following equation:

$$q_{total} = \frac{Q}{1000} \int_{t=0}^{t=t_{total}} C_{ad}\, dt \qquad (19)$$

Where $C_{ad} = C_i - C_e$ is the adsorbed metal concentration in mg/L, t_{total} is the total flow time in min, Q is the flowrate ($\frac{mL}{min}$) and A is the area under the breakthrough curve (cm^2).

The total amount of adsorbate sent to the column is expressed by equation 20 below:

$$m_t = \frac{C_o Q t_{total}}{1000} \qquad (20)$$

Where C_o is the initial concentration in $\frac{mg}{L}$, Q is the flowrate in $\frac{mL}{min}$ and t_{total} is the total time in min.

The total removal percentage of adsorbate is found from the ratio of total adsorbed quantity of adsorbate M_{total} to the total amount of adsorbate sent to the column m_{total}, as given by equation 21:

$$\%\, Removal = \frac{M_{total}}{m_{total}} \times 100 \tag{21}$$

Where M_{total} is the total adsorbed quantity of adsorbate in g and m_{total} is the total amount of adsorbate sent to the column in g.

2.11.1. Mathematical Modelling

The process of biosorption is a complex process which is governed by many operating variables. Mathematical models provide a way to establish process parameters without a column being in operation.

2.11.1.1. The Thomas Model

In the Thomas model, performance is governed by the thomas rate constant and the outlet concentration. The Thomas model is based on two assumptions (Luo et al., 2011b). The first assumption assumes Langmuir kinetics of adsorption-desorption with no axial dispersion whilst the second one assumes that the rate driving force obeys 2nd order reversible reaction kinetics (Thomas, 1944). In this model, the rate constant is used to calculate the maximum solid phase concentration of the solute (q_o) which is represented by the following equation:

$$\frac{C_t}{C_o} = \frac{1}{1 + \exp\left(\frac{k_{TH}}{Q}\left(q_o X - C_o V_{eff}\right)\right)} \tag{22}$$

Where k_{TH} is the thomas rate constant($\frac{ml}{mg.min}$) , q_o is the equilibrium adsorbate uptake $\frac{mg}{g}$ and m is the adsorbate quantity.

The linearized form of the model is given as:

$$\ln\left[\left(\frac{C_o}{C_t}\right)-1\right]=\left(\frac{k_{TH}q_o m}{Q}\right)-\left(\frac{k_{TH}q_o V_{eff}}{Q}\right) \quad (23)$$

The k_{TH} and q_o values are calculated from slope and intercepts of linear plots of $\ln\left[\left(\frac{C_o}{C_t}\right)-1\right]$ against t using values from the column experiments (Acheampong et al., 2013).

2.11.1.2. The Yoon – Nelson Model

The Yoon and Nelson model is derived based on the assumption that the rate of decrease in the probability of adsorption for each adsorbate molecule is proportional to the probability of adsorbate breakthrough on the adsorbent (Yoon and Nelson, 1984). The linearized model for a single component system is expressed as follows:

$$\ln\frac{C_t}{C_o-C_t}=k_{YN}t-k_{YN}\tau \quad (24)$$

Where k_{YN} is the rate constant $\left(\frac{L}{min}\right)$ and τ is the time required for 50% of adsorbate breakthrough to occur. The values of k_{YN} and τ are estimated from slope and intercepts of the linear graph between $\ln\frac{C_t}{C_o-C_t}$ versus t at different operational conditions (Acheampong et al., 2013).

2.12. Basis of Research

Separation technologies for the extraction of pollutants from waste effluent depend heavily on expensive chemicals for the treatment of industrial effluent, not to mention secondary constraints such as secondary sludge production. Moreover, due to the technical applicability and stringent environmental regulations imposed in recent decades, the use of locally available biomass aligns perfectly in driving sustainability efforts. With industrial practices continually changing, the value of resources is of utmost importance which is where bioremediation fits this purpose in that it uses agricultural waste materials for the treatment process. Hence, this research work is aimed at investigating the use of low-cost biosorbents to remove heavy metals from aqueous solutions.

3. METHODOLOGY

This chapter details the materials and methods used in this research study. The research methodology employed in this study is experimental in nature. The preparation of the biosorbents will first be detailed followed by the different analytical techniques (XRD, FTIR, BET and SEM-EDS) used for characterization. Subsequently, the methodology used in the main study, that is the experimental work and analyses, will be given.

3.1. Materials

- Biomaterials: Eggshells and Sugarcane Bagasse
- Solvent: Deionized water
- Adsorbates: Cd (II) ions obtained from cadmium nitrate tetrahydrate , $Cd(NO_3)_2.4H_2O$ and Pb (II) ions from lead nitrate, $Pb(NO_3)_2$ salts
- Other chemicals used: $0.1\,M\ H_2SO_4,\ 0.1M\ NaOH,\ 1N\ HNO_3$

3.2. Biosorbent Preparation

For this research study, the waste agricultural materials, sugarcane bagasse and eggshells were prepared to be used as adsorbents. Based on this, the following adsorbents were produced.

Table 4. Weight percentages used for the adsorbents

	Bagasse	Adsorbent A	Adsorbent B	Adsorbent C	Eggshells
Bagasse	100%	75%	50%	25%	-
Eggshells	-	25%	50%	75%	100%

3.2.1. Preparation of Sugarcane Bagasse

Waste sugarcane bagasse was sourced from Illovo Sugar, South Africa. After collection, it was washed with deionized water several times to remove the sand and dirt particles present. Following the methodology of Wong et al. (2009), bagasse was boiled in hot water for 1 hour. It was then allowed to air dry followed by drying in an oven at 105°C until constant weight. After drying, the biomass was crushed using a coffee grinder to achieve the desired size of biosorbent material. It was crushed in 30 second intervals and sieved to achieve the desired particle sizes within the range of 75 – 250 µm.

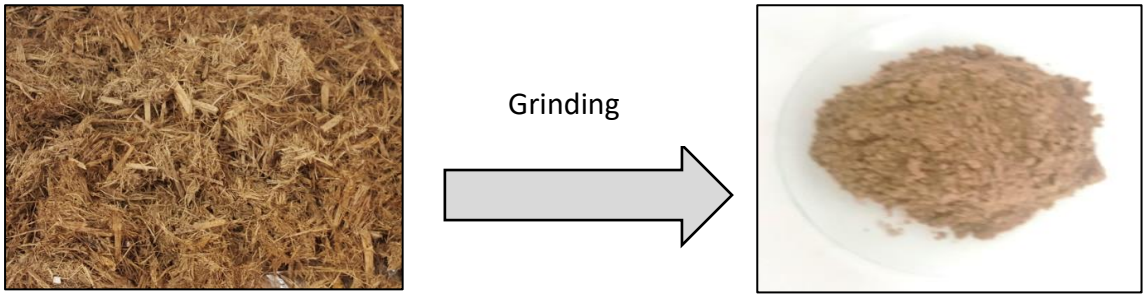

Figure 4. Transformation Process of Sugarcane Bagasse

3.2.2. Preparation of Eggshells

Discarded chicken eggshells were collected from local restaurants in Durban, South Africa. The shells were washed several times with deionized water to remove any debris and dirt particles. Following the drying method of Mao (2017), the biomass material was dried in an oven at 105 ºC until constant weight. The dried eggshells were then crushed using a coffee grinder to achieve the desired particle size of biosorbent material. It was crushed in 30 second intervals and sieved to achieve the desired particle sizes within the range of 75 – 250 µm.

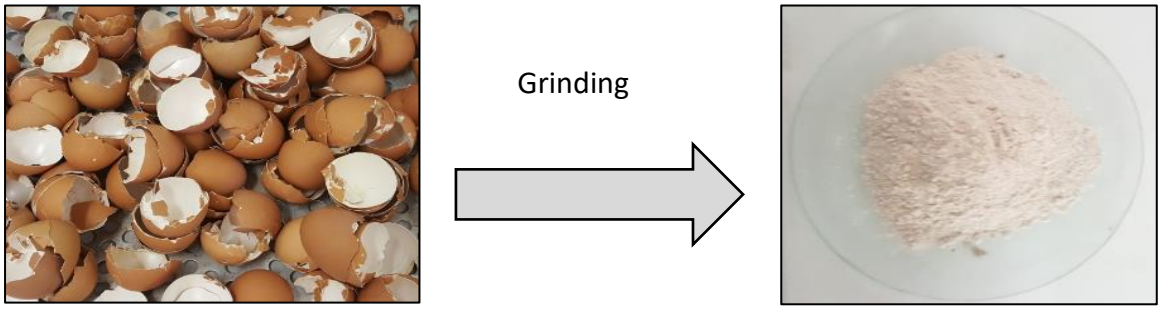

Figure 5. Transformation Process of Eggshells

3.2.3. Preparation of adsorbents A – C

For adsorbents A – C, this involved using 2 biosorbent materials (eggshells and bagasse) in varied proportions where density played a fundamental role in determining the masses that were used.

The density was determined as follows:

A fixed volume of adsorbent was added to a volumetric cylinder on a dry basis which was tapped several times to minimise the entrapment of air. The mass was recorded where the density was calculated using the following equation:

$$\rho = \frac{m}{V} \tag{25}$$

For the adsorbents, the mass of each adsorbent was calculated using equations 26 – 30.

$$m_{bag} = \rho_B V \tag{26}$$

$$m_{ad\ A} = \rho_B . 0.75\ V + \rho_E . 0.25\ V \tag{27}$$

$$m_{ad\ B} = \rho_B . 0.5\ V \ + \rho_E . 0.5\ V \tag{28}$$

$$m_{ad\ C} = \rho_B . 0.25\ V + \rho_E . 0.75\ V \tag{29}$$

$$m_{egg} = \rho_E V \tag{30}$$

For adsorbent A, 75% of bagasse was mixed with 25 % of eggshells on a dry weight basis. To ensure homogeneity, the 2 component biosorbent material was mixed together with a paddle stirrer for a fixed duration and thereafter stored in an air tight container for use. Adsorbents B and C were prepared in the same manner with adsorbent B using 50 % of bagasse and 50 % of eggshells with adsorbent C using 25 % of bagasse and 75 % of eggshells.

Following the preparation of the adsorbents, XRD, SEM-EDS, BET and FTIR analysis were conducted to characterize the surface of the biomaterials.

3.3. Characterisation Studies

3.3.1. Energy Dispersive X-Ray Spectroscopy (EDS)

A FEI Nova Nano SEM 230 Energy Dispersive Spectrophotometer system was used to determine the elemental composition of the biomass. An Everhart – Thornley detector (ETD) and through the lens (TLD) detector was used with a high-resolution immersion lens. A EDS detector (Oxford X-Max equipped with INCA software Landing E 5.00KeV), HFW of 5.97 – 298, Spot of 3.5 and WD of 4.9 – 7.4 was used.

3.3.2. Fourier Transform Infrared Spectroscopy (FTIR)

The functional groups present on the surface of the biomass was qualitatively detected by Fourier Transform Infrared (FTIR) spectroscopy using a spectrum spectrophotometer. This is important in elucidating the mechanisms responsible in the biosorption process. The spectrum was obtained in a frequency band range from 4000 to 400 cm^{-1}.

3.3.3. X-Ray Diffraction (XRD)

A Phillips PW 3830/40 Generator with a PW 3710 mpd control X-ray diffraction system using the Xpert data collector software was used to identify the crystalline materials and mineralogical composition of the biomass. The measurements were done continuously on a J-J scan in locked coupled mode and the tube was Cu-Ka radiation (lKa_1=1.5406Å). The measurement range was 4° to 69.997° with an increment (D2J: 0.034°).

3.3.4. Scanning Electron Microscopy Energy Dispersive X-Ray Spectroscopy (SEM - EDS)

A FEI Nova Nano SEM 230 Scanning Electron Microscope was used to characterise the surface morphology of the biomass surface. An ETD and TLD detector was used with a high-

resolution immersion lens. A EDS detector (Oxford X-Max equipped with INCA software Landing E 5.00KeV), HFW of 5.97 – 298, Spot of 3.5 and WD of 4.9 – 7.4 was used.

3.3.5. Surface area, pore volume and pore size (BET)

The surface area, pore volume and pore size distribution of the adsorbents were obtained by measuring the nitrogen adsorption–desorption isotherms using a surface area and porosity analyzer (Micromeritics TriStar 3000). Brunnaer–Emmett–Teller surface area (BET m^2/g) and total pore volume (Vt, cm^3/g at STP) were thus obtained by the Nitrogen adsorption data according to BET theory. The pore size distribution was calculated based on differential pore volume of Barrett–Joyner–Halenda (BJH) adsorption–desorption isotherm data.

3.4. Experimental Methodology

3.4.1. Adsorbate Solution Preparation

Synthetic stock solutions of Pb (II) and Cd (II) ions of 1000 mg/L concentration were prepared by dissolving appropriate amounts of lead nitrate $Pb(NO_3)_2$ and cadmium nitrate tetrahydrate $Cd(NO_3)_2.4H_2O$ salts in 1L deionised water. The stock solutions were subsequently diluted to the required concentrations using deionized water. All chemicals used in the experiments, 0.1 $M\ NaOH$ and 0.1 $M\ H_2SO_4$ (for pH adjustment) and $1N\ HNO_3$ which was used to clean the glassware, were of analytical reagent grade obtained from the Sigma Aldrich chemical company and was used without further purification.

3.4.2. Batch Studies

Before column experiments can be performed, it is important to get a baseline for certain parameters that affect the process of adsorption. The effect of particle size, pH, initial concentration and contact time were the variables of interest in the batch studies. Additionally, kinetic and equilibrium modelling were investigated to determine the mechanisms responsible for adsorption.

For each batch test, a $100\ \frac{mg}{L}$ concentrated adsorbate solution was prepared by diluting the stock solution with the addition of an appropriate amount of deionized water. For each experiment, $1.0\ g$ of adsorbent was mixed with $100\ mL$ of metal solution in a $1\ L$ glass beaker which was agitated at $150\ rpm$ for a duration of $120\ min$ to ensure equilibrium was reached. The pH of the aqueous solutions was maintained at 5.5 with $0.1\ M\ H_2SO_4$or $0.1\ M\ NaOH$ respectively. All experiments were conducted at room temperature. After each experiment, the glassware used was cleaned with deionised water followed by $1N\ HNO_3$. The effect of contact time (0 – 120 min), pH (2 – 7), concentration (40 – 240 mg/L), and particle size (75 – 250 µm) were investigated. The supernatant solution was filtered using $0.45\ \mu m$ syringe filters where a Varian Spectra AA 50B atomic absorption spectrophotometer (Spain) was used to determine the concentration of the samples.

A calibration curve of Pb and Cd was plotted by measuring the absorbance at 283.3 nm for Pb and 228.8 nm for Cd at varying concentrations. Absorbance values with a standard deviation greater than 1% were discarded and an average value was taken from the duplicate results.

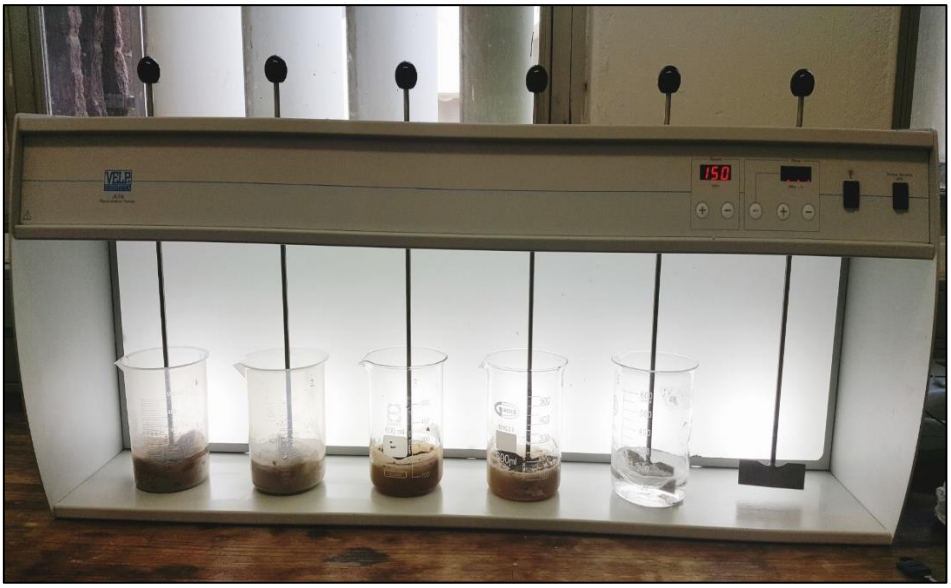

Figure 6. Jar Test equipment used for the batch tests

3.4.2.1. Metal Concentration Determination

A Varian Spectra AA 50B atomic absorption spectrophotometer (Product of Spain) was used to analyse the metal concentrations of the samples. A blank and a set of standards up to 240 mg/L (40, 80, 120, 160, 200 and 240 mg/L) were prepared for each individual metal to be tested. The absorbance for each solution was recorded and a standard calibration curve was plotted. The amount of metal ion in each sample was computed using the standard calibration curve as described above (Mashangwa, 2017).

Figure 7. Varian Spectra AA 50B atomic absorption spectrophotometer

The adsorption uptake and percentage removal of metal ions from the aqueous solution (mg of adsorbate/g of adsorbent) was calculated using the following equations:

Amount Adsorbed: $$q_e = \frac{C_o - C_t}{W} V \quad (31)$$

Percentage Removal: $$q = \frac{100\,(C_o - C_t)}{C_o} \quad (32)$$

Where q is the amount of metal ion adsorbed per gram of adsorbent ($\frac{mg}{g}$) , C_o (mg/L) is the initial metal ion concentration, C_t (mg/L) is the metal ion concentration at time t, W (g) is the mass of the adsorbent used and V (L) is the volume of the solution.

3.5. Fixed bed column studies

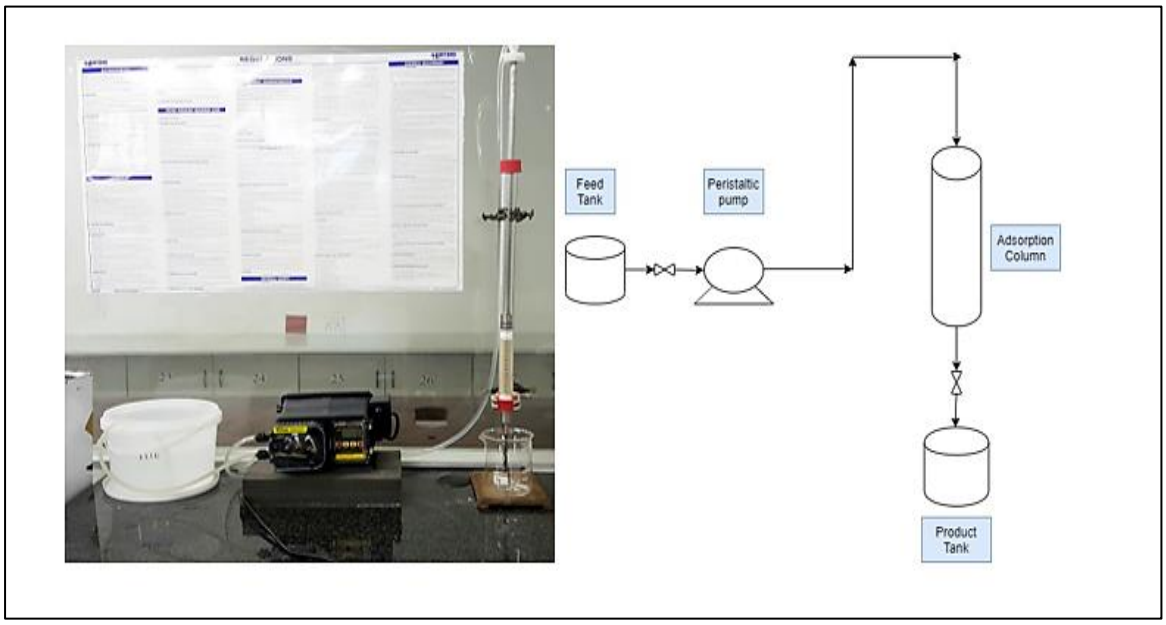

Figure 8. Visual representation of the lab – scale fixed bed column set-up

The experimental arrangement for the lab-scale fixed bed setup is shown in Fig.8 which consists of an adsorption column of borosilicate glass of 2.3 cm in diameter and 30 cm in height. Fixed bed studies using 5 adsorbents (bagasse, adsorbent A, adsorbent B, adsorbent C and Eggshells) in the removal of Pb was investigated. The column was packed with a desired amount of adsorbent between two supporting layers of glass wool (1 cm) with a 1 cm layer of glass beads (5 cm in size) at the top and bottom of the column to provide a uniform flow. All experiments were performed in a down-flow configuration using a Flexflow A – 100 NV peristaltic pump at room temperature (298 K). For each fixed bed experiment, deionised water was allowed to pass through the adsorbent bed until complete wetting of the adsorbent particles were achieved. The outlet stream (product) was collected at predefined intervals (30 min for the first 5 hrs, and thereafter at 2hr intervals) which were analysed using an AAS spectrophotomer. The effect of bed depth on the breakthrough curves was investigated at 4, 8 and 12 cm bed depth at a constant flowrate of 4 mL/min, initial Pb concentration of 100 mg/L and at pH 5.5. The pH value used for this part of the study was based on the batch studies conducted previously. All experiments were carried out in duplicate and the average values were used for further calculations.

The validity of the two breakthrough models used in this study (Yoon Nelson and Thomas models) were assessed by means of two widely used error metrics, the Root Mean Squared Error (RMSE) and the Mean Absolute Error (MAE), which evaluates the goodness of fit between the actual and predicted breakthrough curves. Generally, the lower the RMSE and MAE values are, the better the fit between the model and the experimental data are(Chai and Draxler, 2014).

The error functions were determined according to equations 33 and 34 respectively:

$$RMSE = \sqrt{\frac{1}{n}\sum_{i=1}^{n}\left(\frac{C_t}{C_o} - \frac{\widehat{C_t}}{C_o}\right)_i^2} \tag{33}$$

$$MAE = \frac{1}{n}\sum_{i=1}^{n}\left|\frac{C_t}{C_o} - \frac{\widehat{C_t}}{C_o}\right|_i \tag{34}$$

Where n is the number of experimental measurements and $\frac{C_t}{C_o}$ and $\frac{\widehat{C_t}}{C_o}$ are the actual and predicted concentrations, respectively.

4. RESULTS AND DISCUSSION

4.1. Physical Parameters

The density was determined as 1.2 g/cm^3 for eggshells and 0.23 g/cm^3 for bagasse. The densities were used to determine the mass of adsorbent used in the fixed bed studies.

4.2. Biosorbent Characterisation

4.2.1. Energy Dispersive Spectroscopy (EDS) Analysis

A FEI Nova Nano SEM 230 Scanning Electron Microscope with an Energy Dispersive Spectrophotometer system was used to quantify the elemental composition of the biomaterials. Additionally, it was used to ascertain whether the biomaterials were contaminated with heavy metals.

- Preliminary Screening Tests

Eggshells consist of 2 layers which comprises the shell of the egg and the membrane layer. Preliminary screening tests using energy dispersive spectroscopy (EDS) was performed on the shell only and the matrix (shell + membrane) to ascertain the composition of this biomaterial.

Table 5. Preliminary EDS Results of the Shell and Shell Matrix of Eggshells

Elemental atoms (%)	Eggshell Matrix	Shell Only
Oxygen	44.52	36.99
Carbon	23.96	26.28
Calcium	31.52	21.88
Nitrogen	-	12.26
Phosphorous	-	1.83
Magnesium	-	0.76

Based on table 5, the main elements that constitute the shell of the egg and the eggshell matrix (shell and membrane) consist largely of carbon, oxygen and calcium atoms. Notably, a comparably higher calcium content was present in the matrix with the absence of nitrogen. The shell of the egg bears functional groups such as amino (−NH2) and amide (−CONH2) which constitute the element nitrogen as seen above (Tsai et al., 2006, Mittal et al., 2016). Moreover, eggshells are an alkaline biomaterial due to its high calcium carbonate content of which, calcium is a major constituent (Quina et al., 2017).

In a study by Tsai et al. (2006), the characteristics of the shell and the membrane was individually characterised where it was found that the properties of both were very similar. With this in mind and seeing as the application of this biomaterial on a large-scale process will require an additional separation process for the membrane removal, it was decided that the eggshell matrix (that is the shell with the membrane attached) be used in this study. Furthermore, considering their results, a significant difference in adsorptive capability of the shell to that of the membrane is not expected as the surface properties of both are similar. Henceforth, in this thesis, the use of the word "eggshells" will be used in the context of representing the matrix, that is the shell with the membrane attached to it.

- EDS Analysis of Eggshells and Bagasse

Table 6. Elemental weight composition of eggshells and bagasse

Biosorbent	C	O	Ca	Total
Bagasse	53,29	46,71	----	100
Eggshells	23,96	44,52	31,52	100

From table 6, there were no heavy metals detected in the above analysis of both biomaterials. The composition that constitutes sugarcane bagasse comprises mainly of carbon and oxygen atoms with close to the same weight ratio. Cellulose is the main constituent in bagasse which is composed of oxygen, hydrogen and carbon atoms (Abdolali et al., 2014). However, in the above analysis, no hydrogen was detected. However, it is worthy to note that the use of

analytical techniques involving x – rays are less sensitive to lighter atoms present in a compound, if they are located at all (Rajeswari et al., 2020). Hence, in organic structures such as cellulose, $C_6H_{12}O_6$, the hydrogen atom positions are relatively inaccurate which is demonstrated by the lack of hydrogen present despite cellulose constituting hydrogen atoms. It is therefore recommended that an elemental analyser be used in conjunction with the above analysis to elucidate the above findings.

In eggshells, the above analysis was found to consist mainly of calcium, oxygen and carbon atoms with a higher calcium and oxygen content. Since eggshells are composed mainly of calcium carbonate, $CaCO_3$, this was expected.

4.2.2. Surface area, pore volume and pore size

The surface area, pore volume and pore size were obtained by measuring the nitrogen adsorption–desorption isotherms using a surface area and porosity analyzer (Micromeritics TriStar 3000). Brunnaer–Emmett–Teller surface area (BET, m^2/g) and total pore volume (Vt, cm^3/g at STP) were thus obtained by the Nitrogen adsorption data according to BET theory.

Table 7. Surface Area, Pore Volume and Pore Size of the adsorbents

Property	Bagasse	Adsorbent A	Adsorbent B	Adsorbent C	Eggshells
Surface Area (m^2/g)	1.104	0.399	0.477	0.739	1.711
Pore volume (cm^3/g)	0.00618	0.0117	0.0917	1.193	0.0163
Pore size (nm)	8.170	116.890	32.100	26.780	14.240

The surface area of eggshells was found to be 1.711 m^2/g with a pore volume of 0.0163 cm^3/g and a pore size of 14.270 nm. Bagasse, on the other hand, was found to yield lower values with a surface area of 1.0068 m^2/g, pore volume of 0.0023 cm^3/g and a pore size of 8.170 nm. As the content of bagasse increased in the other adsorbents (25 wt % to 50 wt % to 75 wt %), it was found to result in lower exposed surface areas (0.74 m^2/g to 0.48 m^2/g to 0.4 m^2/g). On the contrary, the pore sizes were found to be larger with increasing bagasse content (26.78 nm to

32.1 nm to 116.89 nm) with lower pore volumes (1.1926 cm^3/g to 0.0917 cm^3/g to 0.01164 cm^3/g).

The surface area of the adsorbents in ascending order were as follows: Eggshells > Bagasse > Adsorbent C > Adsorbent B > Adsorbent A. Adsorbent A was found to have the largest pore size of 116.89 nm with bagasse having the smallest of 8.17 nm. However, with respect to pore volume, adsorbent C had the largest pore volume of 1.193 cm^3/g with bagasse having the smallest of 0.00618 cm^3/g.

A study performed by Chao and co – workers (Chao et al., 2014) postulated that since biomaterials are not chemically modified and used in its native. i.e. "natural" form, they yield low surface areas and limited pore volumes, however, are still capable of achieving high adsorptive capacities. In general, biomaterials uptake pollutants through their affinity to the biomass surface, that is through their functional groups, rather than diffusion through their pores as evidenced by the results of their study. Native biomass is expected to yield low to moderate surface areas and porosities and the use of modifications, usually chemical or thermal, are commonly applied to enhance surface properties. However, since the objective of using biosorption is to provide alternative "environmentally green" solutions, no modifications have been employed in this research study.

To classify the porosity of the adsorbents, the International Union of Pure and Applied Chemistry (IUPAC) convention was used which classifies nanoporous materials into three groups; micropore (diameter <2 nm), mesopore (2–50 nm) and macropore (>50 nm). With the exception of Adsorbent A, the above adsorbents were found to be mesoporous, confining with the conventions adopted from the IUPAC conventions.

Figure 9 below shows the adsorption – desorption isotherms of sugarcane bagasse and eggshells with very close values between adsorption and desorption at all P/Po values indicating that the isotherms are reversible. According to the institution of pure and applied chemists (IUPAC), both isotherms can be classified as a type III isotherm. In the case of a Type III isotherm, there is no identifiable monolayer formation. Further to this, as explained by (Thommes, 2015), the adsorbent – adsorbate interactions are relatively weak and the adsorbed molecules are clustered around the most favorable sites on the surface of a nonporous or macroporous solid.

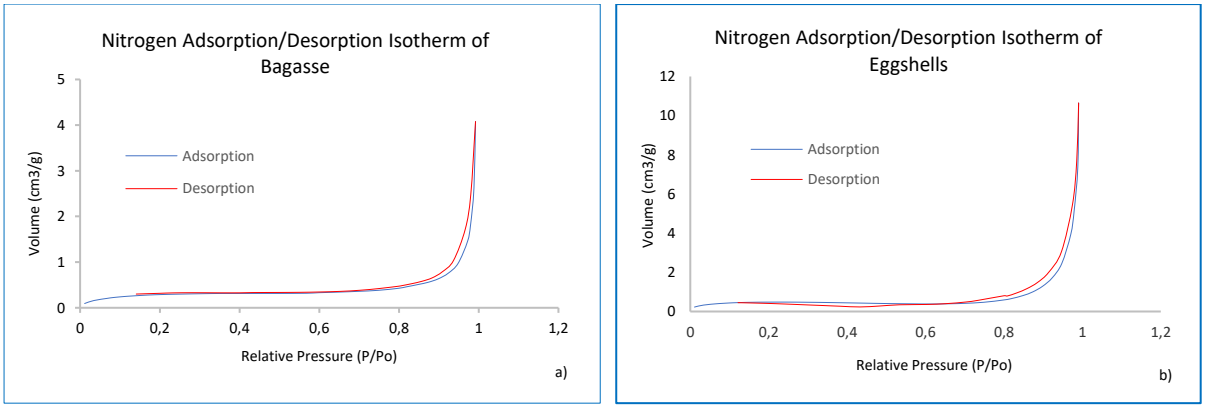

Figure 9. Nitrogen Adsorption Desorption Isotherms of Bagasse (a) and Eggshells (b)

4.2.3. Fourier Transform Infrared Spectroscopy (FTIR) Analysis

The basic chemistry of the surface of a biomass is extremely useful in exploring biosorption. Information on the active sites involved in the sequestration of heavy metals are derived using instrumental analysis such as FTIR. With the use of FTIR, a lower transmittance is an indication that there are a high population of bonds with vibrational energies capable of adsorption. The FTIR spectra obtained was measured within the range of 4000 – 400 cm^{-1} wavelengths.

4.2.3.1. FTIR spectra before adsorption

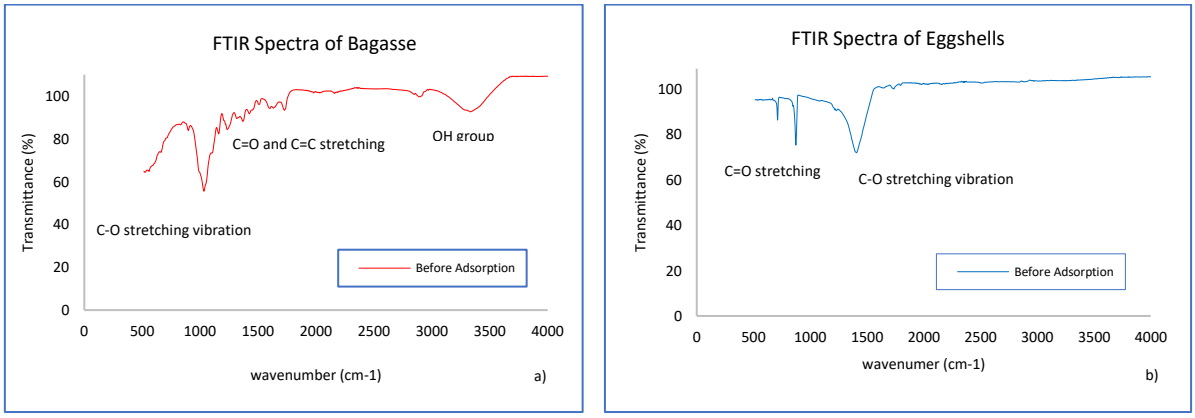

Figure 10. FTIR Spectra of bagasse (a) and eggshells (b) before adsorption

The defining peaks identified in the FTIR spectra of sugarcane bagasse occur at the wavelengths of 3345 cm^{-1}, 1736 cm^{-1}, 1364 cm^{-1}, 1217 cm^{-1}, 1035 cm^{-1} and 899 cm^{-1}. A medium broadband peak is observed at 3345 cm^{-1} which is attributed to the hydroxyl groups present in bagasse (Zhang et al., 2011b, Gurgel et al., 2008). In contrast, the sharp visible peak at 1736 cm^{-1} is representative of C=O carbonyl groups and the C=C stretching vibrations are due to the aromatic rings of lignin as reported by Zhang et al. (2011b). The bands observed within the range of 1364 cm^{-1} – 1035 cm^{-1} are due to the C–O stretching vibration of cellulose, lignin and hemicellulose as supported by Gurgel et al. (2008) and Putra et al. (2014). The minor peak observed at 899 cm^{-1} is due to the glycosidic bond in cellulose as reported by Marisa (2014). Thus, the FTIR spectra of bagasse indicates that the surface of the biomass is rich in polymeric hydroxyl groups, carbonyl groups and aromatic rings (Chao et al., 2014). Since bagasse is primarily composed of carbon and oxygen atoms, this provides the necessary ion exchange and complexation sites for biosorption to occur.

The FTIR spectra of eggshells occur predominantly at the lower end of the spectra. The weak minor absorption band at 1740 cm^{-1} is characteristic of C=O stretching of carboxylic acid. The characteristic of C=O stretching at the above wavenumber has been further discussed by Flores-Cano et al. (2013). The sharp absorption bands observed at 1405, 873 and 712 cm^{-1} are characteristic of the mineral carbonate. The absorption band centred at 1405 cm^{-1} is characteristic of the C−O bond in the carbonate due to a stretching vibration, showing a coordination bond between the oxygen atoms of the carbonate and the calcium atom. In addition, the two sharp bands at 874 and 711 cm^{-1} are due to the out-of-plane and in-plane deformation modes of carbonate, respectively. This can be further supported by Al-Ghouti and Salih (2018). This further elucidates that calcium carbonate is the main constituent in eggshells with the carbon, calcium and oxygen atoms providing the necessary ion exchange and complexation sites for biosorption to occur.

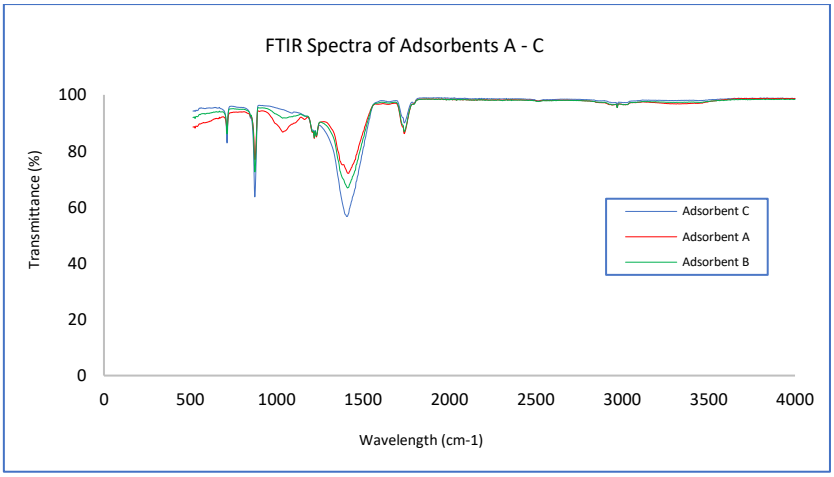

Figure 11. FTIR Spectra of Adsorbents A – C before adsorption

With adsorbents A – C, a lower transmittance can be seen with adsorbent C which indicates that there was a high population of bonds with vibrational energies capable of adsorption. In contrast, adsorbent B and A were found to have higher transmittances implying that there were fewer bonds of functional groups in those adsorbents.

It was interesting to find that the broad peaks at 3345 cm^{-1} due to the hydroxyl groups present in bagasse were completely inhibited in adsorbents A – C. This revealed that when the adsorbents were combined, both adsorbents interacted with each other altering the chemical structure and functional groups of the adsorbents. It is known that bagasse is an acidic lignocellulosic material which when combined with an alkaline biomaterial such as eggshells, it is plausible that a reaction (i.e., a modification of the structure) occurs. The weak narrow bands observed at 1217cm^{-1} due to the C – O stretching vibration of cellulose, lignin and hemicellulose are still visible but were less pronounced. Additionally, the sharp, narrow peaks observed in eggshells at 713cm^{-1}, 874 cm^{-1}, 1411 cm^{-1} and 1741 cm^{-1} were still prominent in adsorbents A – C with the peaks being more pronounced with increasing eggshell content. This was indicative that the adsorbent combinations were rich in the mineral carbonate with the C=O stretching of carboxylic acid and the stretching vibration of the C–O bond together with the in- plane and out- of plane deformation modes of carbonate respectively.

4.2.3.2. FTIR spectra after adsorption

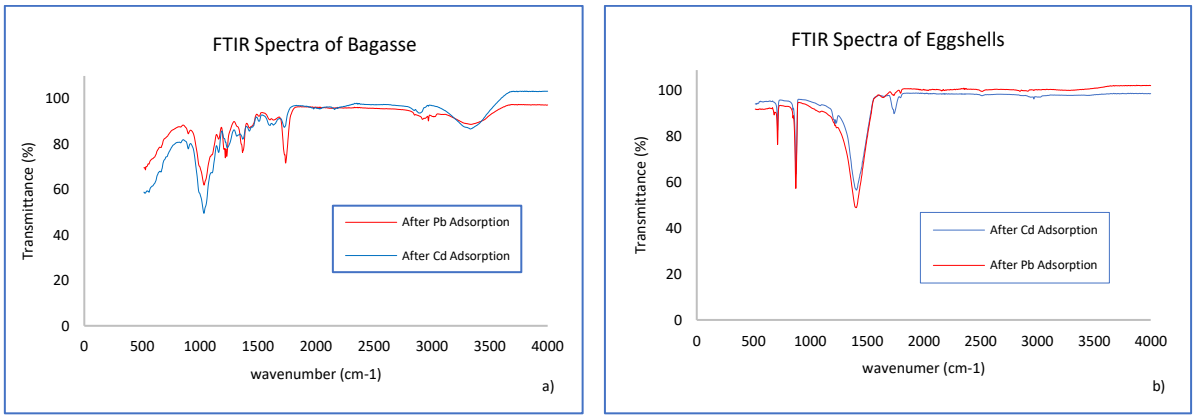

Figure 12. FTIR Spectra of bagasse (a) and eggshells (b) after adsorption

The spectra for the adsorption of Pb using bagasse was found to transmit lower values than Cd with the exception of the C–O stretching vibration of cellulose, lignin and hemicellulose at 1000 cm^{-1} indicative that the functional group present at this wavenumber (C – O) was more efficient in adsorbing Cd. Similarly, the spectra for Pb and Cd using eggshells were found to follow the same trend except at the wavenumber of 1740 cm^{-1} corresponding to the C=O stretching of carboxylic acid group in eggshells responsible for the adsorption of Cd.

In eggshells, the strong prominent bands observed at 1405 cm^{-1} are characteristic of the polar C−O bond in the mineral carbonate due to a stretching vibration which interacts more with Pb than Cd ions as seen in Fig. 12b. Carboxylic acid is a ketone which shows medium narrow bands around 1710cm^{-1} – 1745 cm^{-1} due to the highly polar C=O bonds in eggshells and shows more interaction with Cd than Pb as evidenced by the broad medium bands in the spectra of eggshells. In bagasse, the functional groups of carboxylic was prominent in Cd removal which behaves as both an alcohol and ketone with the wavelength of 3340 cm^{-1} covering the -OH stretch. The hydroxyl group was found to interact with Pb more than Cd as seen in Fig. 12 a. The polar C=O stretch in bagasse occurs more around the 1740 cm^{-1} region, again interacting with Pb a greater amount.

The spectra demonstrates the presence of negatively charged functional groups like OH^- ions in bagasse and CO_3^{2-} on the surface of eggshells (Masukume et al., 2014) which act as active adsorptive sites for the removal of Pb and Cd ions.

In general, lower transmittance values of an adsorbent suggests there will be a greater chance of deformation in that molecule/ functional group (Coates, 2000) and so will exhibit a large degree of active sites available for adsorption whereas higher transmittance values indicates that the site is more fixed and so, it is hypothesized that the site will not be as active to adsorb metal ions. However, it is impossible to determine the exact mechanism of adsorption or to support this hypothesis using FTIR alone. Moreover , the shift towards the lower end of the spectrum implies the weakening of a bond so that new bonds can occur which were evident in both bagasse and eggshells (Coates, 2000).

4.2.4. X-Ray Diffraction (XRD) analysis

X – ray diffraction was used to qualitatively analyse the crystalline phase of the biosorbents. The peak positions (2θ values) show the crystal system and qualitative phase information present in the adsorbents**.** A Phillips PW 3830/40 Generator with a PW 3710 mpd control X – ray diffraction system using the Xpert data collector software was used to interpret the XRD spectra. The diffraction patterns were collected in a 2θ range of 4° to 69.997°, with steps of 0.034° and a fixed counting time of 76.8 s/step.

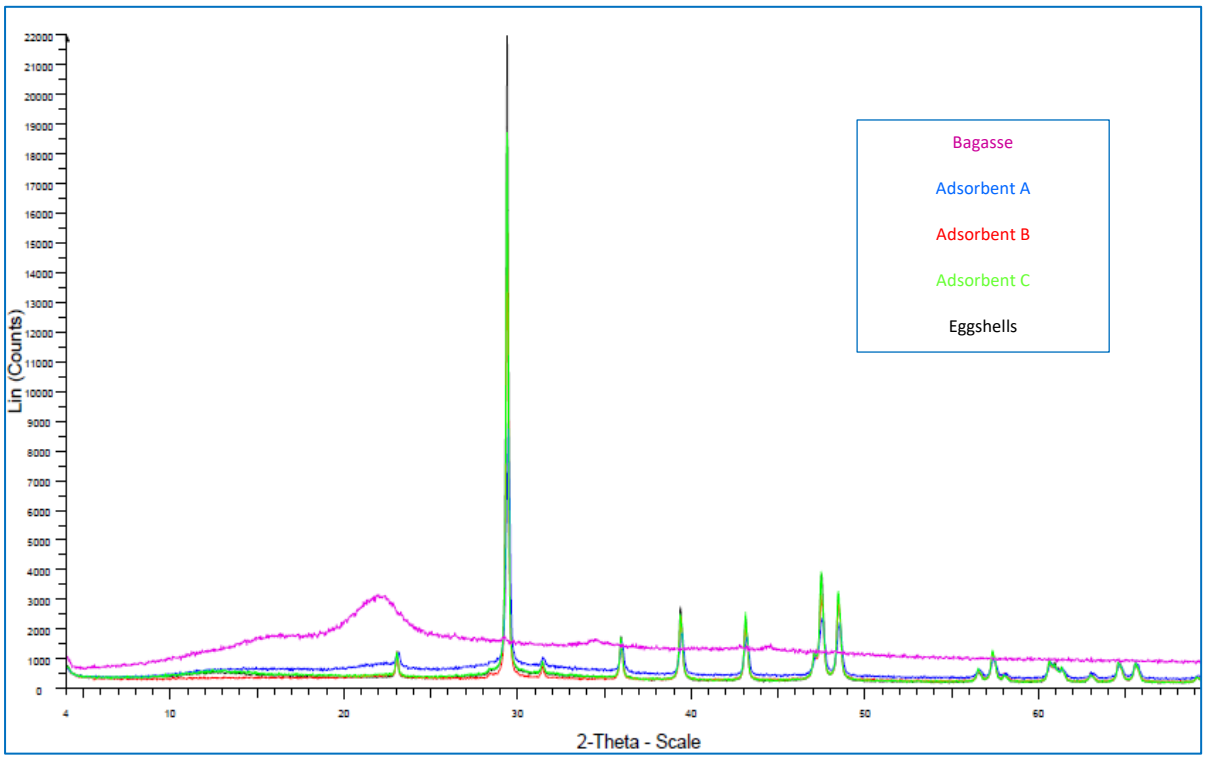

Figure 13. XRD Patterns of the adsorbents

For the diffraction pattern of bagasse, the lack of sharp diffraction peaks was characteristic of the amorphous constituents present in bagasse. This was mostly likely due to the lignin content present which is highly branched without a crystalline structure (Cagnon et al., 2009). With that said, the most noticeable peak that stands out occurred at a 2θ value of 22°. The peak formed at this angle is representative of native cellulose (Cellulose I). The work of Poletto et al. (2014) described the pronounced peak range between 21.90° and 22.20° as the crystallographic plane of cellulose who further explains that it is the intramolecular and intermolecular hydrogen bonds of the free hydroxyl groups present in the cellulose macromolecules which give rise to this ordered crystalline arrangement. Further to this, Lopičić (2016) supported the above results by assigning the 22.5° peak to the (002) plane of cellulose I. Sugarcane bagasse has both crystalline and amorphous regions with the cellulose constituent representing the crystalline region and lignin representing the amorphous one.

Cellulose I, or native cellulose can exist as two polymorphs, a monoclinic structure I_β, which is the dominant polymorph in plants or a triclinic structure I_α, which is more rare (Moon et al., 2011). Since bagasse is a lignocellulosic plant – based material, it is more likely that the monoclinic structure I_β exists. It is also worthy to note that the method of sample preparation is generally responsible for the development of texture in a sample which influences the relative intensities of the diffraction peaks and therefore influences the crystallinity of a sample. This was demonstrated by Zhang et al. (2011b) whose findings highlighted that ball milled bagasse exhibited a lower crystallinity index compared to samples that were crushed using a cutter. It can therefore be assumed that the use of simple mechanical treatments such as grinding and crushing be used to improve the ratio of crystalline to amorphous regions in a sample which alters the accessible area available for adsorption.

The sharp diffraction pattern of eggshells highlighted the highly crystalline regions of this biomaterial. Eggshells are composed mainly of calcium carbonate (Ahmad, 2012) and the experimental evidence in figure 13 has demonstrated that the crystallographic lattice of calcium carbonate found in eggshells exists in the calcite phase with the highest peak observed at a 2θ value of 29.38°. This corresponds to the reference data found for the calcite phase of calcium carbonate crystals (AMCSD) which was also supported by Ok et al. (2011). Generally, there are three possible polymorphs of calcium carbonate, namely vaterite, aragonite and calcite, listed in order of increasing thermodynamic stability. In eggshells, calcium carbonate exists predominantly in the calcite phase which typically assumes a rhombohedral structure.

With adsorbents A – C, it is evident that the sharp diffraction patterns of the biomaterials are characteristic of the crystalline constituents present in the adsorbents. The peaks that represent cellulose (2θ value of 22°) were found to be more crystalline in nature (represented as sharper diffraction patterns) as the content of eggshells increased in the adsorbents. Moreover, the peaks that were prominent in eggshells can be seen at higher intensities in adsorbents A – C highlighting that the biomaterials are rich in the mineral calcite.

4.2.5. Scanning Electron Microscopy (SEM) analysis

SEM was used to study the morphology of the adsorbents. Although, sometimes not obvious, this method of characterisation is used to visually assess the porosity of the surface (if applicable), the shape of the pores and to determine if layers are present or not. Moreover, it reveals whether the particles are in the form of aggregates or single particles.

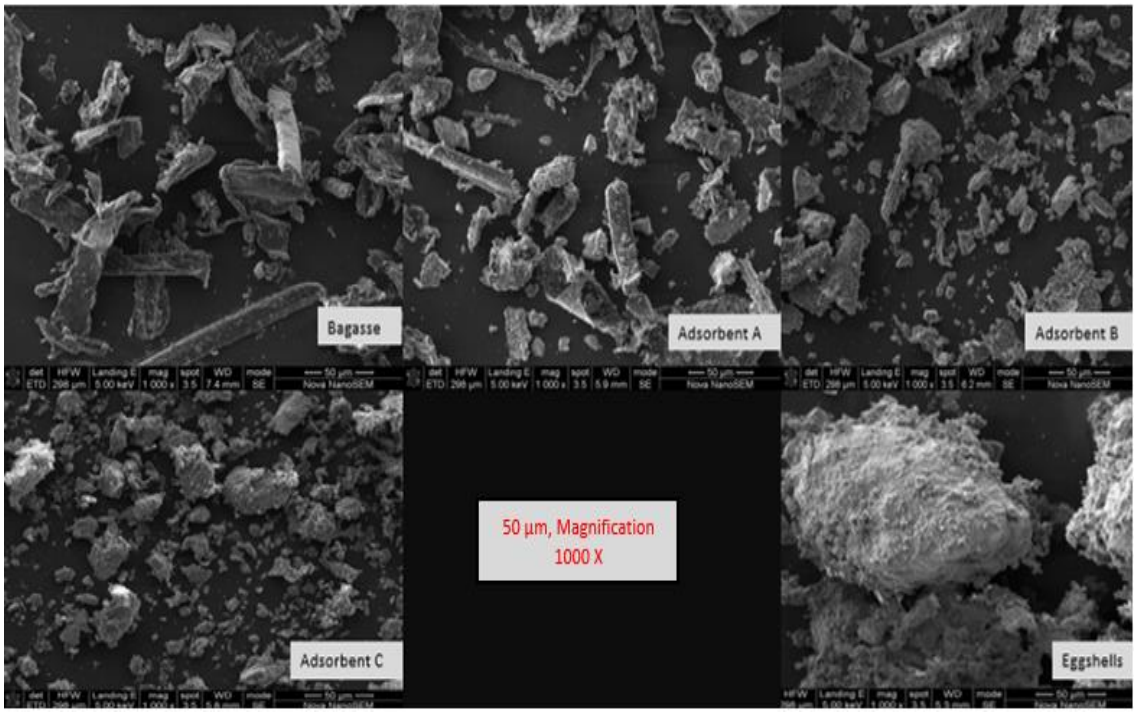

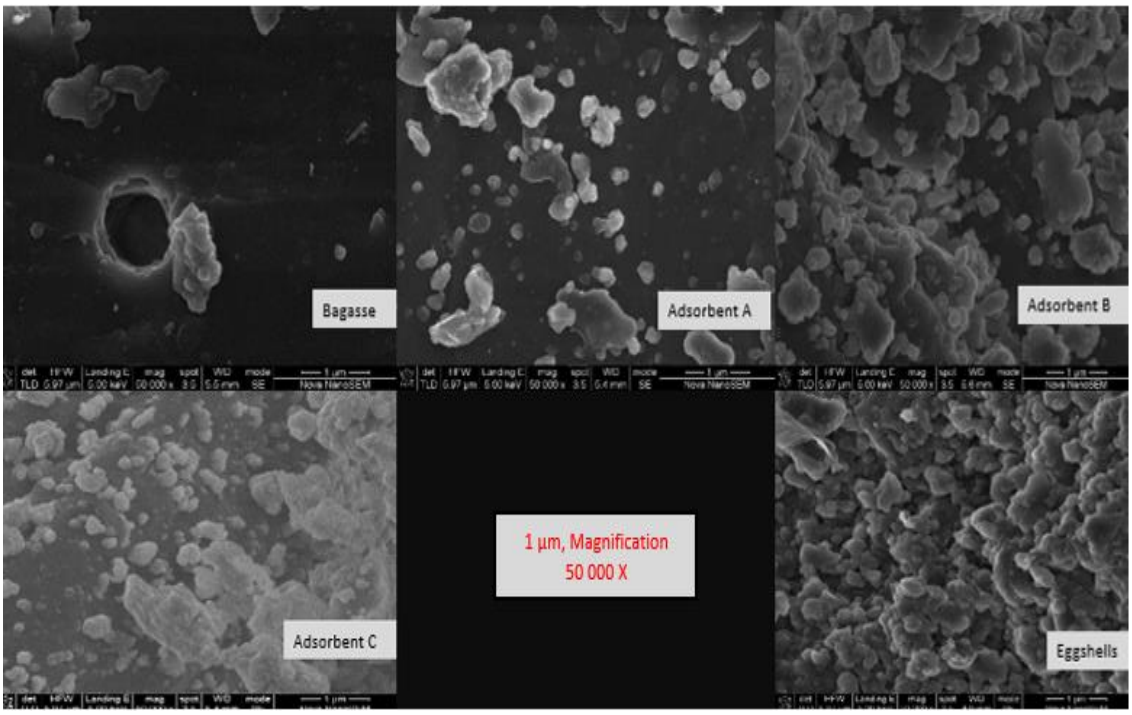

Figure 14. SEM Images of the adsorbents at 50µm (1000 X) and 1 µm (50 000 X)

The general view of bagasse depicts 1 dimensional rod like structures and particles which are randomly oriented. The work of Leão et al. (2017) characterised these particles as globular wax particles, pectins and extractives in addition to the amorphous constituents such as lignin and hemicellulose present in the biomass. The fibrous fraction of bagasse is due to the notable predominance of particles of high length to width ratio as evidenced above and supported by Driemeier et al. (2011). The surface is non – uniform and jagged with randomly oriented voids present representative of the limited pore volume.

The general view of the surface of eggshells depicts definite structures which are densely packed. The shape of the particles was mostly flake like grains with the majority being fine in size. On closer inspection (at a magnification of 50000), layered cloud like grains which form the matrix of the biomass was visible. The size of the grains differed throughout the surface. It is worthy to note that layered surfaces provide a larger surface area available for adsorption when compared to flat 1 – dimensional surfaces.

The intercept method was used to determine the average grain size of bagasse and eggshells. With this method, a random straight line is drawn though the micrograph and the number of grain boundaries intersecting the line are counted. The average grain size is found by dividing the number of intersections by the actual line length.

$$\text{Average grain size} = \frac{1}{number\ of\ intersections/actual\ line\ length} \quad (35)$$

Where the actual line length is the measured length divided by the magnification of the image.

The grain size of eggshells was found to be 0.25µm and for bagasse, 0.77 µm.

Generally, observations made on structural morphology is a subjective analytical technique and it is often difficult to interpret without the expert opinion of experienced professionals dealing with this type of analysis. In this regard, BET analysis (presented in section 4.2.2) was conducted to complement the SEM observations.

From the BET analysis, it was found that eggshells had the largest surface area and from the SEM images above, it can be seen to have a layered surface. Moreover, as the content of eggshells were increased in adsorbents A – C, the surface areas increased from the BET analysis which is visible in the SEM images consisting of layered surfaces for adsorbents B and C (magnification 50000 X).

The description from table 8 together with the images in Fig. 14 above, show that the adsorbents with greater surface areas had layered surfaces providing a larger area for adsorption to occur.

Table 8. SEM characteristics of the adsorbents

Description	Bagasse	Adsorbent A	Adsorbent B	Adsorbent C	Eggshells
Visual appearance	Cylindrical pore	Scattered granules	Agglomerates of flakes	Agglomerates of flakes	Agglomerates of flakes
Porous/ Non-porous	Non-porous	Non- porous	Non-porous	Non- porous	Non- porous
Homogenous/ Non-homogenous	Non-homogenous	Non-homogenous	Non-homogenous	Non-homogenous	Non-homogenous
Layered/ 1-Dimensional	-	1- Dimensional	Layered	Layered	Layered
Shape of pore (If visible)	Circular	Not visible	Not visible	Not visible	Not visible

4.3. Batch studies

4.3.1 Effect of particle size

The influence of particle size on Pb and Cd removal was conducted using 1 g of biosorbent for a 100 mg/L concentrated solution of 100 mL for 120 mins at pH 5.5. The particle sizes investigated were < 75 µm, 75 – 150 µm, and 150 – 250 µm. Within the range studied, no comparable difference in the sorption of Pb using eggshells were observed. The sorption capacity of eggshells remained at 99,8 – 99,9% between 75 – 250 µm. Contradictory to the above, on reducing the particle size of eggshells from the average size of < 750µm to < 100µm, the removal of Pb increased from 30.7 to 99.6% in a study conducted by Vijayaraghavan and Umid (2013). For Pb sorption using bagasse, an increase in the removal percentage was observed with decreasing particle size (94,9 – 97,1 %). The size reduction of bagasse from 250 – 150 µm to 150 – 75 µm to < 75 µm led to an increase in capacity due to the increase in surface area which was supported by Gupta et al. (2003). The work of Liu et al. (2012) reported that powder biosorbents (<150 µm) was found to exhibit much better adsorption performances than larger size particles (> 1000 µm). However, they also found that between different sized powders, no significant difference was observed.

For Cd removal (Fig 15b.), bagasse exhibited approximately the same removal percentage (73 – 75%) and for eggshells, it was found to increase (63 – 71%). It can therefore be said that when dealing with biomaterials such as sugarcane bagasse and eggshells in its native form, the contribution of the particle size reduction does not have a significant effect in comparison to other variables.

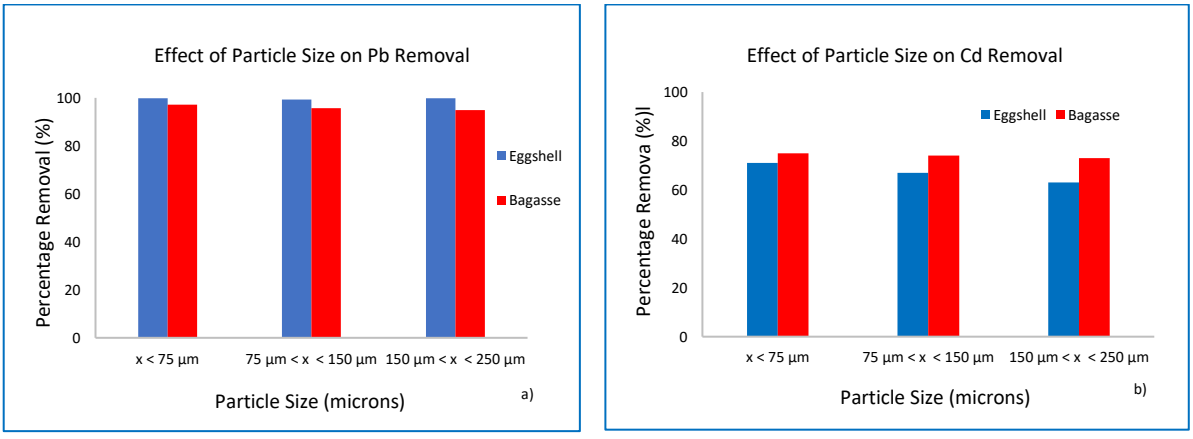

Figure 15. Effect of particle size on the biosorption of Pb and Cd

4.3.2. Effect of pH

To investigate the effect of pH on Pb and Cd removal, experiments were conducted by adjusting the pH from 2 to 7 using 1g biosorbent in a 100 mg/L concentrated solution of 100 mL with a contact time of 120 mins and < 75µm particle size. The solution pH was maintained within this range due to the precipitation of metal ions governing the adsorption process at values higher than this range.

From Fig.16a, a comparable increase in Pb removal was observed from pH 2 – 3 using eggshells, with the removal percentage increasing from 93.8% to 99.7 %. The reduced efficiency in low pH environments is due to the high concentration of H^+ ions which is in competition with Pb cations. The ionic state of the carbonyl and carboxyl groups of eggshells (as elucidated by the FTIR spectra) is negatively charged and so there is more competition between the hydronium and metal cations in acidified environments resulting in reduced removal rates. However, as the pH is increased, there is less competition for the active sites resulting in higher removal rates as evidenced in this study and supported by other researchers (Senthilkumar, 2015, Tark et al., 2016, Swathanthra, 2014). It is also noteworthy to observe that the removal of Pb using eggshells tends to be independent of the pH after pH 3. This can be explained by the fact that there may not be any Pb ions left in solution to saturate the available active sites. It is therefore advised that higher initial concentrations be investigated. With higher initial concentrations, there will be more hydroxide ions available to interact with the Pb ions.

There was a gradual increase in capacity with increasing pH in the removal of Cd using eggshells (Fig 16 b.) with the maximum uptake observed at pH 5 with a 70 % removal capacity. These results concurred with a study conducted by Tark et al. (2016). Further to this, Flores-Cano et al. (2013) revealed the surface of eggshells to be positively charged at the lower end of the pH scale, favouring the electrostatic attractions of anions and repelling cations which is in agreement with the above results.

With respect to bagasse (Fig 16.b), there was a significant spike in the removal of Cd from pH 2 – 3 (22% to 66%) with a more gradual increase (66% to 74%) from pH 3 – 4. After a pH value of 4, the removal capacity remained a steady 72 %. It is well known that the pH of a solution affects the ionic state of the functional groups of a biomaterial (Farooq et al., 2010) and so can be used to explain the Cd sorption. The adsorption of Cd at the lower end of the pH

scale is electrically unfavourable or repulsive because the surface charge is positive. However, when the pH value increases, the surface charge of the sorbent is negative and the binding of the Cd cation is thus favoured. This explains the observed increase in the removal capacity from pH 2 – 4. Justifying the results with the same theory as above, the maximum uptake of Pb ions by bagasse (Fig 16 a.) was observed at pH 7 with a 97% removal rate.

Based on the metal removal percentage of both adsorbents, the preference of the metals adsorbed onto eggshells and bagasse were found to be Pb > Cd for both biomaterials. The higher sorption affinity of Pb can be explained by its larger ionic radius (0.118 nm) when compared to Cd (0.0097 nm) allowing for better contact between Pb and the biomass surface as supported by the work of Ahmad (2012). Moreover, the pore size of eggshells (14.27 nm) is larger than that of bagasse (8.17 nm) which makes eggshells capable of attracting a larger number of adsorbate molecules in comparison to bagasse.

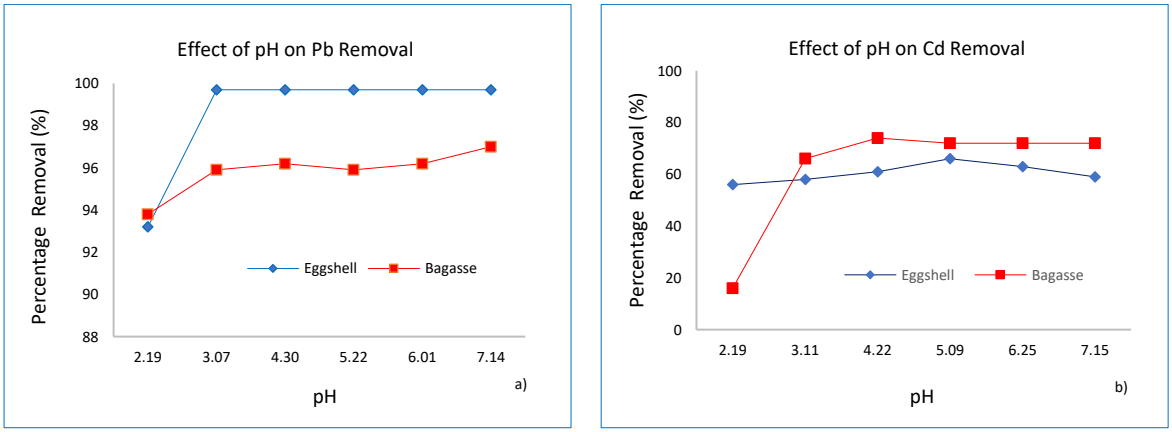

Figure 16. Effect of pH on the biosorption of Pb and Cd

4.3.3. Effect of contact time

The kinetics of adsorption governs the rate that determines the residence time between the adsorbate and adsorbent and it is a fundamental characteristic defining the efficiency of an adsorbent (Elkady et al., 2011).To investigate the effect of contact time, experiments were conducted from 0 to 60 min. The solution pH was maintained at 5.5 for all experiments. In all cases, 100 mL of metal ion solution with a concentration of 100 mg/L was used together with 1 g of biosorbent at a particle size of < 75 µm.

It was observed that the removal of Pb by eggshells and bagasse (Fig 17a) increased with increasing contact time until it reached a peak. The adsorption of Pb was rapid for the first 25 minutes of both biomaterials as a result of available binding sites on the biomass surface, while the adsorption of Cd for both eggshells and bagasse (Fig 17b) were comparably lower. The adsorption of Pb reached equilibrium within 25 minutes for eggshells and 30 minutes for bagasse where the removal percentage reached 99.2% and 96.2% respectively.

The removal rate of Cd required a longer equilibrium time of 60 minutes for both eggshells and bagasse with a removal rate of 71 and 73 % respectively. The rate of adsorption is higher initially due to surface adsorption on the adsorbent as explained by Tark et al. (2016) where the subsequent slow phase occurs due to the diffusion of metal ions onto the inner part of the biomass surface. At equilibrium, the capacity of the adsorbent gets exhausted and the net rate of uptake is zero (Vinodhini and Das, 2009).

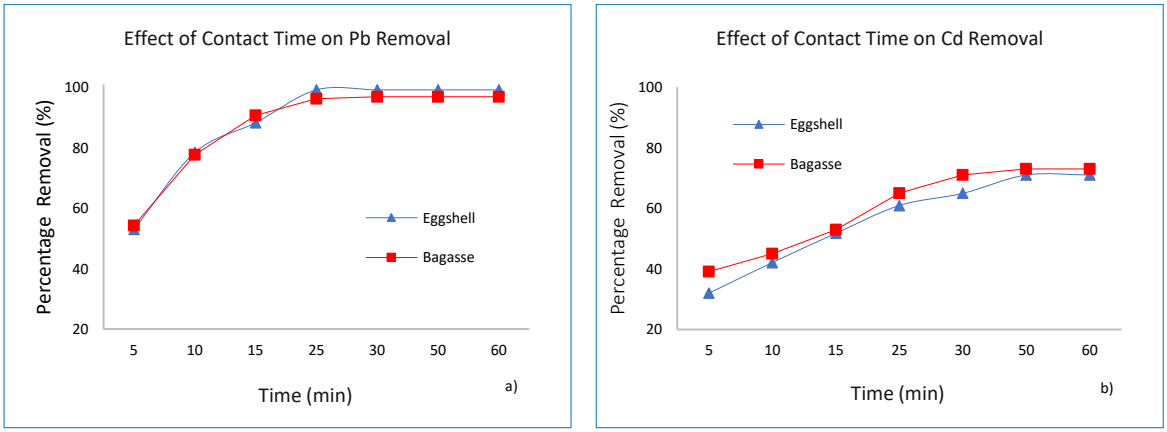

Figure 17. Effect of contact time on the biosorption of Pb and Cd

4.3.4. Effect of concentration

The concentration of metal ions was varied from 40 – 240 mg/L for this aspect of the study using 1g of biomass at pH 5.5 for 120 min. The particle size used was 75 µm. From Fig. 18a, the initial Pb concentration had a considerable effect on the adsorption capacity using bagasse. Pb removal decreased gradually from 80 % to 74.4% with increasing Pb concentration from 40 mg/L to 240 mg/L. The adsorption removal percentage decreases as the initial concentration of the pollutant ions increase, indicating the saturation of the available active sites (Tao et al., 2015). A similar trend of Pb adsorption has also been reported previously as a function of initial metal concentration by Elanza (2014). On the other hand, Pb removal using eggshells was found to be independent of the initial concentration within the range studied. A constant

removal rate of 99,55 % was achieved irrespective of the initial metal ion concentration. It is recommended that higher concentrations be investigated to determine the saturation capacity of the adsorbent.

As shown in Fig. 18b, the initial Cd concentration had a significant effect on the adsorption removal rate using eggshells. Cd removal decreased considerably from 75 % to 53% with increasing Cd concentration from 40 mg/L to 160 mg/L and decreased further to 42% with a further increase in the concentration of Cd to 240 mg/L. At lower metal concentrations, the ratio of number of moles of metal cation in solution to the available surface area is low and hence binding is independent of initial concentration. However, at higher concentrations, the available sites for binding are fewer and hence metal removal is more dependent on the initial concentration. A similar trend was observed for Cd removal using bagasse (82,25 % to 66,7 %) within the range of 40-240 mg/L.

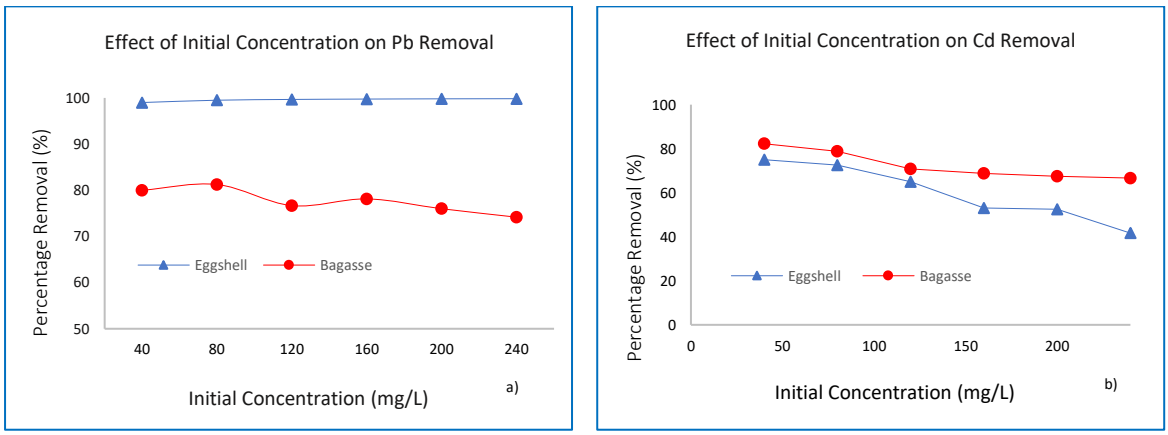

Figure 18. Effect of Initial concentration on the biosorption of Pb and Cd

4.3.5. Isotherm Modelling

The initial metal concentration of Cd was varied from 40 to 240 mg/L using 1g of biosorbent with 100 mL of aqueous solution at a pH of 5.5, < 75 µm particle size. However, for Pb, the dosage was varied from 400 to 2400 mg/L with a volume of 100 mL due to a constant removal rate of Pb being attained when the concentration was varied from 40 – 240 mg/L.

Table 9. Isotherm Modelling Parameters for Pb and Cd

Biosorbent	Metal Ion	Langmuir Isotherm Parameters			Freundlich Isotherm Parameters		
		$Q\left(\frac{mg}{g}\right)$	$b\left(\frac{L}{mg}\right)$	R^2	$K_f\left(\frac{mg}{g}\right)$	n	R^2
Eggshell	Pb	277,78	0,02	0,952	1,38	1,02	0,936
	Cd	13,62	0,029	0,9868	10,36	2,21	0,9121
Bagasse	Pb	31,45	0,017	0,9967	196,08	1,60	0,9953
	Cd	19,49	0,029	0,996	10,40	1,34	0,9805

In this study, the experimental results were fitted using two isotherm models (Langmuir and Freundlich) where the best fit isotherm model was selected based on the linear regression correlation coefficient (R^2). The Langmuir constants b and q_{max} were calculated from Fig. 19a and b and their values are listed in Table 9. It was found that the data obtained from this study exhibit deviations from linearity for the Freundlich isotherm, however for the Langmuir isotherm, the regression coefficients indicate that the data was well correlated implying the applicability of this isotherm. The maximum monolayer adsorption capacity of Pb and Cd removal using eggshells were found to be 277.78 and 13.62 mg/g respectively. For bagasse, the maximum capacity was 31.45 mg/g for Pb and 19,49 mg/g for Cd. Based on the Langmuir isotherm assumptions, it can be said that once Pb and Cd ions occupies a site, no further sorption can take place at that site. Moreover, the value of the constant b for eggshells shows a greater affinity of the binding sites and chemical interaction between the adsorbent and adsorbate.

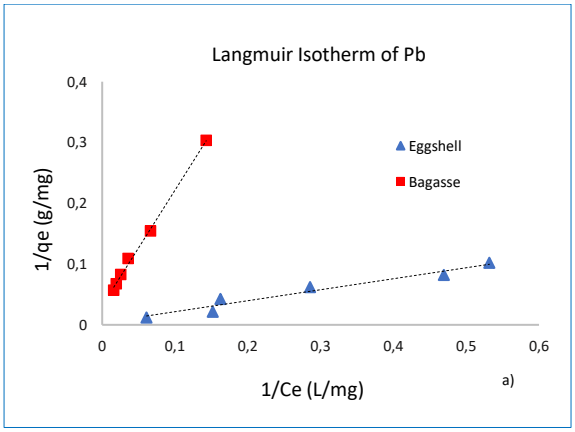

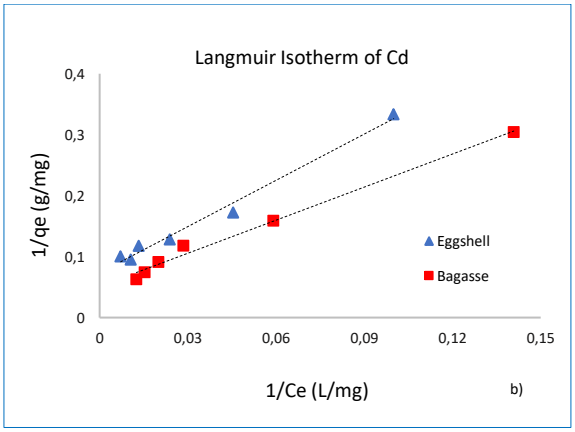

Figure 19. Langmuir Isotherm of Pb and Cd using Eggshells and Bagasse

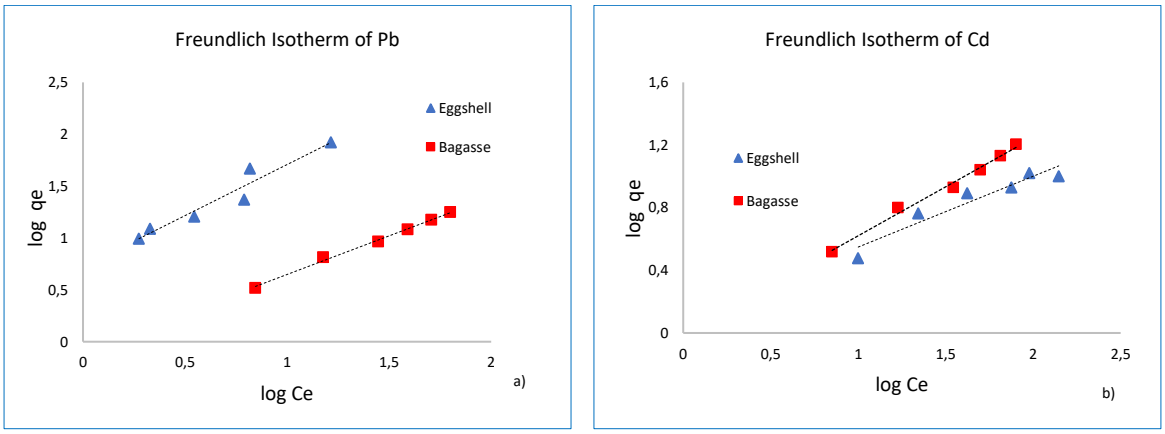

Figure 20. Freundlich Isotherm of Pb (a) and Cd (b) using Eggshells and Bagasse

4.3.6. Kinetic Modelling

The contact time was varied from 0 – 60 min for the kinetic batch experiments. For each experiment, 1.0 g of each sorbent (eggshells and bagasse) was mixed with 100 mg/L of 100 mL of metal solution at 150 rpm and <75 µm particle size at selected time intervals within the above range.

Table 10. Kinetic Modelling Parameters for Pb and Cd

Biosorbent	Metal Ion	$Q_{exp}\left(\frac{mg}{g}\right)$	Pseudo First-Order Reaction Kinetics			Pseudo Second-Order Reaction Kinetics		
			$k_1(min^{-1})$	$q_{e,calc}\left(\frac{mg}{g}\right)$	R^2	$k_2\left(\frac{g}{mg.min}\right)$	$q_{e,calc}\left(\frac{mg}{g}\right)$	R^2
Eggshell	Pb (II)	9,92	0,078	4,928	0,7791	0,028	10,638	0,9265
	Cd (II)	7,1	0,073	5,53	0,9925	0,018	8,292	0,9938
Bagasse	Pb (II)	9,69	0,21	13,68	0,9475	0,034	10,29	0,9969
	Cd (II)	7,3	0,107	7,68	0,9925	0,014	8,749	0,9214

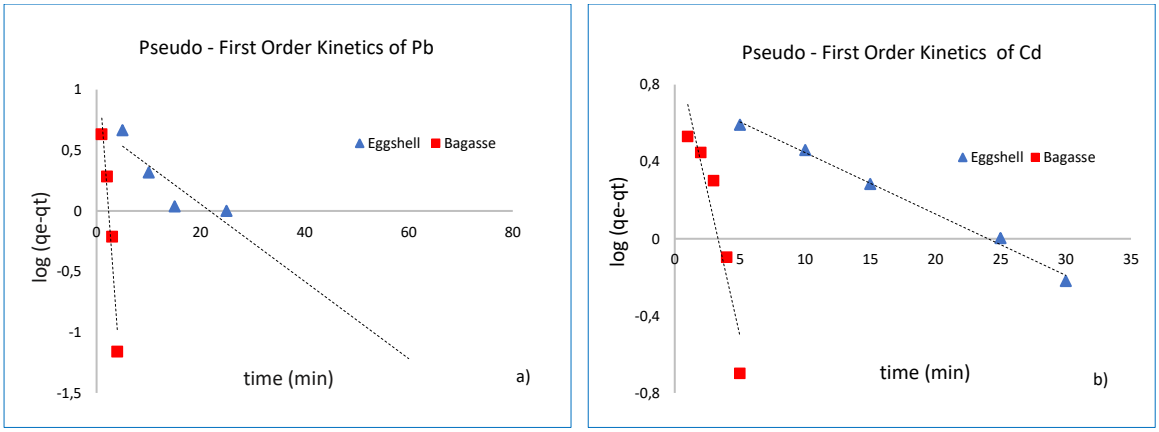

Figure 21. Pseudo-first Order Kinetics of Pb (a) and Cd (b) using Eggshells and Bagasse

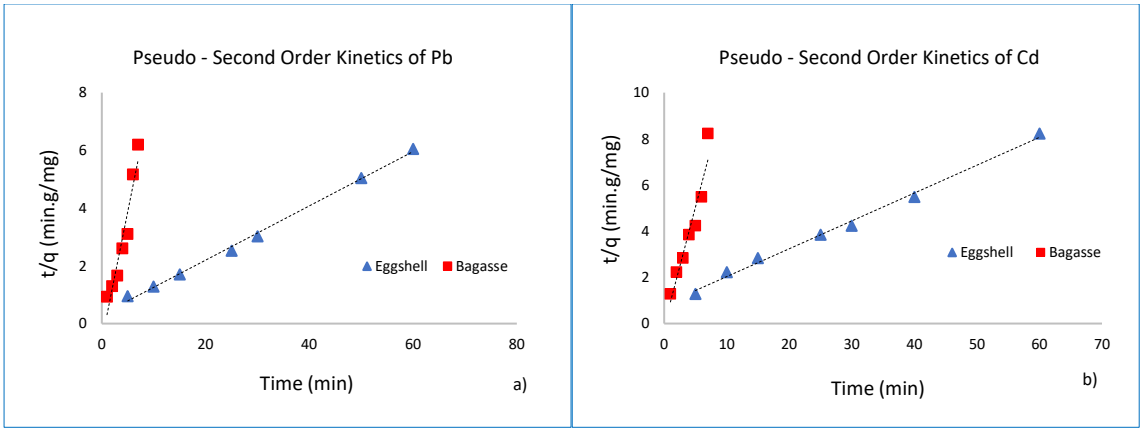

Figure 22. Pseudo-second Order Kinetics of Pb (a) and Cd (b) using Eggshells and Bagasse

In order to determine the potential rate – controlling step, the pseudo – first order and pseudo – second order models were applied to fit the experimental data in this study. From table 10, the linear correlation coefficients (R^2) provide a better fit to the pseudo – second order than the pseudo – first order kinetic model. Moreover, the pseudo – first order model predicts lower values of the equilibrium capacities ($q_{e,cal}$) than the experimental values ($q_{,exp}$). However, the equilibrium capacities obtained with the pseudo – second order model are slightly more reasonable when comparing the predicted results with the experimental data providing a better fit.

The rate constant for Pb (0.028 and 0.034 g/mg.min) were found to be higher in comparison to Cd (0.018 and 0.014 g/mg.min) using eggshells and bagasse, respectively, which suggests that the adsorption of Pb takes place at a faster rate. It is hypothesized that since Pb has a higher electronegativity (1.8) than cadmium (1.7), it has a higher chance of attracting electrons thereby

being adsorbed at a faster rate. Furthermore, electron sharing requires chemical bonding and it can therefore be said to imply a mechanism of chemisorption. To further support this, the mechanism of chemisorption has been reported by several other studies as well (Elkady et al., 2011, Banat et al., 2004, Chairata, 2005).

4.3.7. Mechanism of Metal Uptake

Several factors were found to affect the adsorption of Pb and Cd by eggshells and bagasse and as a result, the actual mechanism of metal adsorption differs for each adsorbent used. It is likely that various mechanisms operate simultaneously which will be explained below.

4.3.7.1. Proposed mechanisms in eggshells

- Ion exchange mechanism

The first mechanism proposed in eggshells is the ion exchange mechanism. From the batch studies conducted in this study, the experimental data for eggshells followed the Langmuir isotherm for Pb and Cd implying that the metal ions exchange cations with the calcium ion Ca(II) of calcite ($CaCO_3$) present in eggshells which was verified by the FTIR spectra (after adsorption).

- Complexation mechanism

The FTIR analysis in this study highlighted the carbonyl and carboxyl groups present in eggshells which are responsible for the complexation mechanism with Pb and Cd respectively. The polar C−O bond in the mineral carbonate due to a stretching vibration interacts with the metal cations. Additionally, carboxylic acid is a ketone with highly polar C=O bonds in eggshells which forms possible complexes with Cd and Pb.

The surface charge of eggshells is attributed to the surface complexes formed by the hydrolysis and hydration of the calcite surface. The main calcite surface complexes are $\equiv CaOH_2^+$ and

$\equiv CaCO_3^-$, which originates through the protonation and deprotonation of the following hydration sites as follows:

Protonation $\equiv CaOH + H^+ \rightarrow \equiv CaOH_2^+$ (36)

Deprotonation $CaCO_3H \rightarrow CaCO_3^- + H^+$ (37)

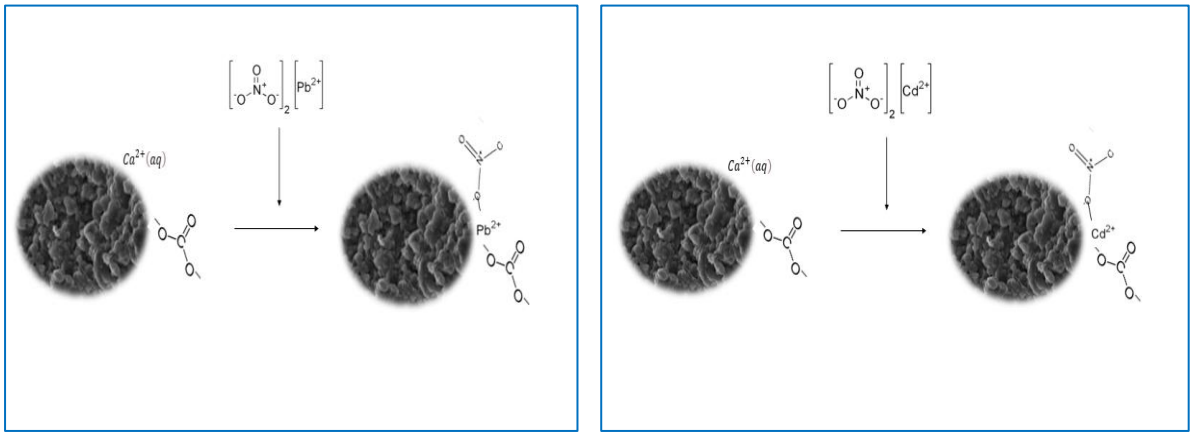

Figure 23. Possible interactions between Pb and Cd and the surface of eggshells

4.3.7.2. Proposed mechanisms in bagasse

The use of FTIR highlighted the functional groups present on the surface of bagasse which was responsible for adsorption. The results revealed that free hydroxyl groups, carbonyl and aromatic rings functioned as exchangeable cation and complexation sites. These groups exchanged their hydrogen ions for the metal cation (Pb/Cd) or gave an electron pair to form complexes with the metal cations as explained by Kumar et al. (2011). However, this was also dependent on the number of active sites, the accessibility of the sites, the chemical state of the sites and the affinity between the sites and the target metal ions (Park et al., 2010). As explained by Martín-Lara et al. (2010), the COOH group provided the complexation site, whereas both OH and COOH groups generates exchangeable cation sites.

In this regard, it should also be noted that it is not clear which component of bagasse (hemicellulose, cellulose or lignin) was responsible for the ion exchange and complexation mechanisms and further adsorption methodologies should be adopted to isolate these components individually to determine which constituent of bagasse is responsible for the above – mentioned mechanisms.

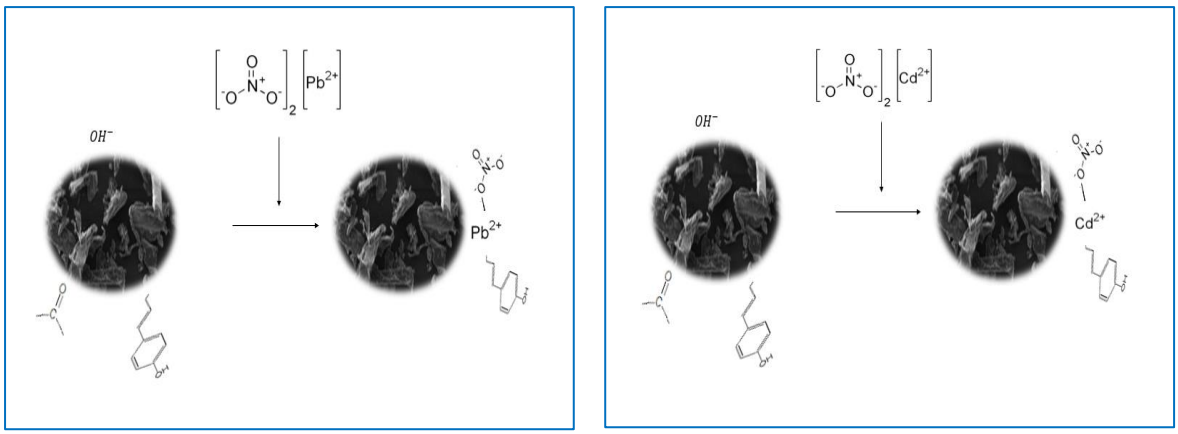

Figure 24. Possible interactions between Pb and Cd and the surface of bagasse

4.3.8. Comparative Performance of various adsorbents

For the batch tests, a 100 mg/L concentrated adsorbate solution was prepared by diluting the stock solution with the addition of an appropriate amount of deionized water. For each experiment, 1.0 g of adsorbent was mixed with 100 mL of metal solution of < 75 µm particle size for a duration of 120 minutes to ensure equilibrium was reached. The pH was maintained at 5.5 for all experiments.

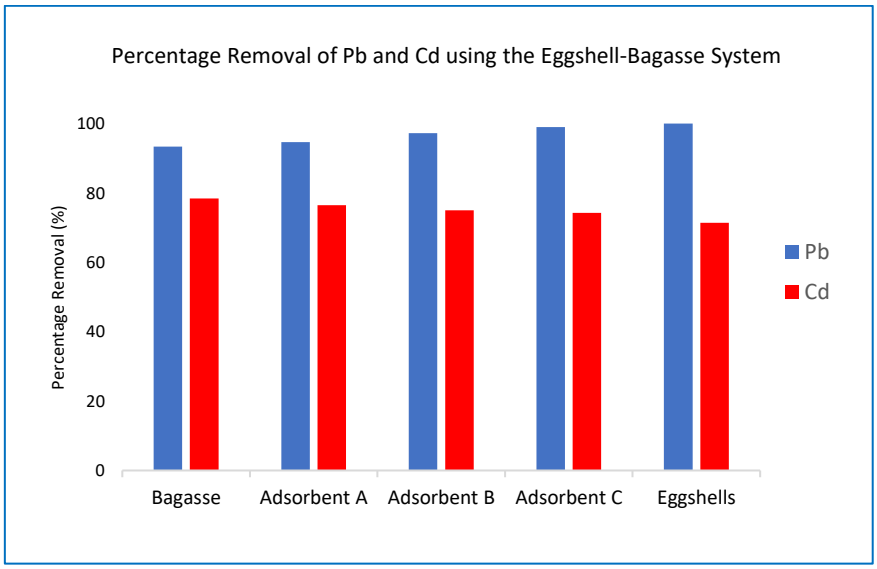

Figure 25. Batch Study comparison of Pb and Cd removal

From the batch study comparison tests, all adsorbents performed better in the removal of Pb than Cd removal. The percentage removal for Pb was in the range of 93 – 99 % with Cd removal remaining within the range of 70 – 75%. The FTIR spectra after adsorption (section 4.2.3.2)

can be used to elucidate these findings concluding that both biomaterials are more proficient in the removal of Pb than Cd ions. The order of efficiency for Pb removal were as follows: Eggshells > Adsorbent C > Adsorbent B> Adsorbent A> Bagasse. For Cd removal, Bagasse> Adsorbent A> Adsorbent B > Adsorbent A> Eggshells.

Moreover, based on the findings in section 4.3.3 (effect of concentration), and with a view to its practical application in packed bed columns, it can be said that eggshells are highly proficient in treating effluent with both high and low concentrations of Pb whereas both biomaterials would have much shorter operation times when treating effluent contaminated with Cd ions towards the higher end of the concentration range. For this reason, it was decided that the removal of Pb, and not Cd, be investigated in the fixed bed column studies.

4.4. Breakthrough curve analysis

Fixed bed experiments were conducted to investigate the effect of bed depth (4 cm, 8 cm and 12 cm) on the performance of 5 adsorbents (Eggshells, Bagasse, Adsorbent A, Adsorbent B and Adsorbent C) at a constant flowrate of 4 mL/min with an initial Pb concentration of 100 mg/L at pH 5.5. Breakthrough curves were plotted as shown in Figs. 26 – 30 and the results of the data presented in table 11.

For this study, the breakthrough point was chosen as 0.01 mg/L which is the allowable discharge limits for Pb in drinking water (WHO). From the batch studies conducted earlier in this study, the equilibrium data was found to follow the Langmuir isotherm thereby producing typical S shaped breakthrough curves (Geankoplis, 2003) in the fixed bed experiments as seen in Figs 26 – 30. After the breakthrough time of the adsorbents were reached, the concentration was found to rapidly rise to the exhaustion point (95% of the initial concentration). The effect of varying the bed height allowed for a constant mass transfer zone of the curves making it possible to scale – up for industrial use at a later stage in development.

- **Fixed bed studies using bagasse**

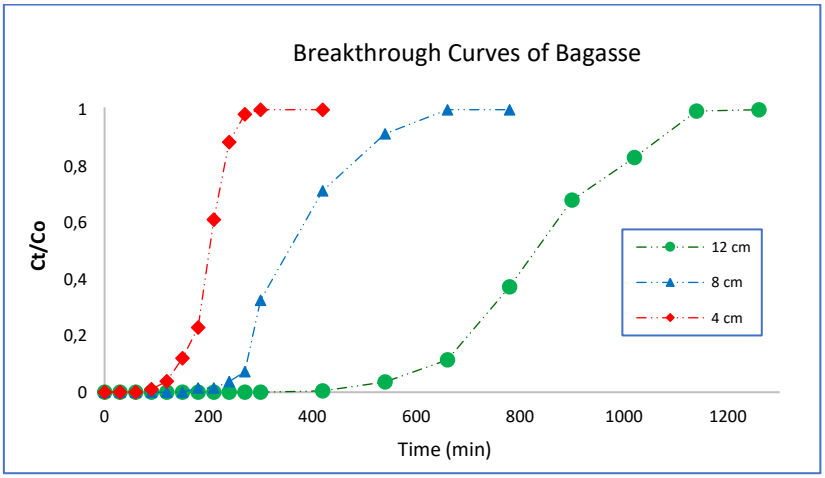

Figure 26. Breakthrough curves of bagasse

Pb removal using bagasse was found to be 47.86% for a bed depth of 4 cm with 55.77 % removal for 8cm and 65.87% for a depth of 12 cm. The breakthrough times for 4 cm, 8 cm and 12 cm bed height were 60 min, 150 min and 300 min corresponding to the exhaustion times of 201 min, 435 min, and 830 min respectively. The volume of effluent treated at breakpoint was 240 mL, 600 mL and 1200 mL with exhaustion rates of 4.75, 4.39 and 3.45. The bed volumes processed before the bed required replacement or regeneration was 14, 18 and 24 bed volumes with the length of bed used calculated as 2.81 cm making use of 70.25% of the bed for a depth of 4 cm, 5.24 cm using 70% of the bed and 7.66 cm corresponding to 63.83% of the bed.

- **Fixed bed studies using adsorbent A**

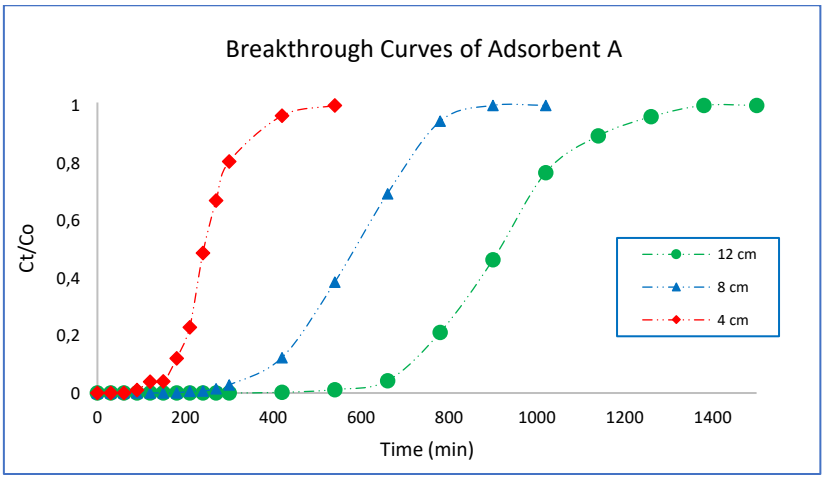

Figure 27. Breakthrough curves of Adsorbent A

Pb removal using Adsorbent A was found to be 44.81 % for a bed depth of 4 cm with 65.30 % removal for 8 cm and 66.30 % for a depth of 12 cm. The breakthrough times for 4 cm, 8 cm and 12 cm bed height were 60 min, 150 min and 300 min corresponding to exhaustion times of 242 min, 585 min, and 915 min respectively. The volume of effluent treated at breakpoint was 240 mL, 600 mL and 1200 mL with exhaustion rates of 8.12, 6.70 and 6.44. The bed volumes processed before the bed required replacement or regeneration was 14, 17 and 23 bed volumes with the length of bed used calculated as 3.00 cm making use of 75% of the bed for a depth of 4 cm, 5.95 cm using 74.38% of the bed and 8.07 cm corresponding to 67.25% of the bed.

- ## Fixed bed studies using adsorbent B

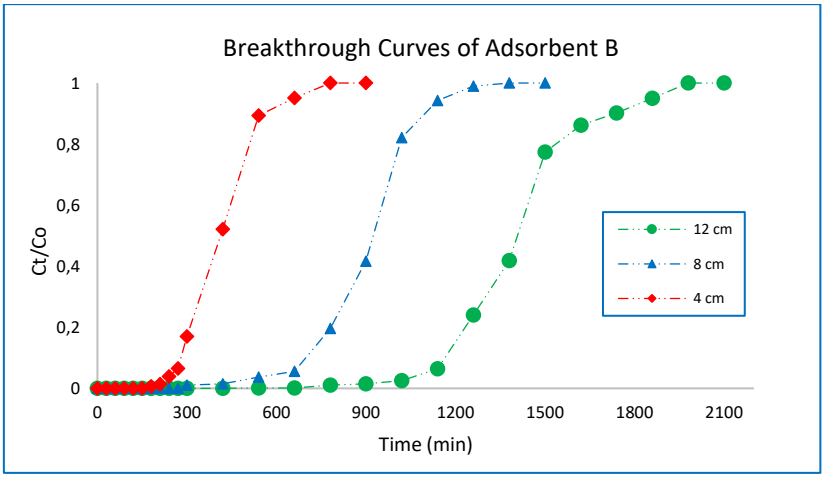

Figure 28. Breakthrough curves of Adsorbent B

Pb removal using Adsorbent B was found to be 61.15 % for a bed depth of 4 cm with 67.03 % removal for 8 cm and 71.11 % for a depth of 12 cm. The breakthrough times for 4 cm, 8 cm and 12 cm bed height were 120 min, 270 min and 520 min corresponding to exhaustion times of 242 min, 585 min, and 915 min respectively. The volume of effluent treated at breakpoint were 477 mL, 925 mL and 1408 mL with exhaustion rates of 6.22, 6.42 and 6.32. The bed volumes processed before the bed required replacement or regeneration was 27, 31 and 41 bed volumes with the length of bed used calculated as 2.99 cm making use of 74.75% of the bed for a depth of 4 cm, 5.67 cm using 70.88% of the bed and 7.40 cm corresponding to 61.67% of the bed.

- **Fixed bed studies using adsorbent C**

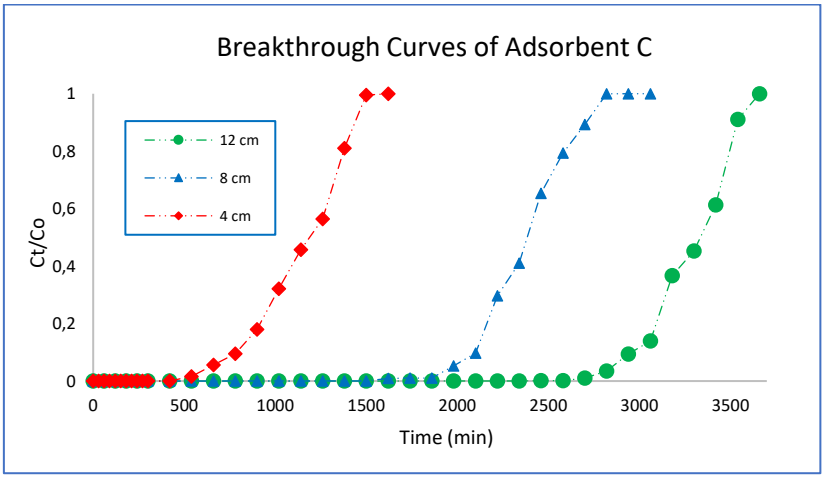

Figure 29. Breakthrough curves of Adsorbent C

Pb removal using Adsorbent C was found to be 77.33 % for a bed depth of 4 cm with 77.94 % removal for 8 cm and 91.15 % for a depth of 12 cm. The breakthrough times for 4 cm, 8 cm and 12 cm bed height were 420 min, 1140 min and 2460 min corresponding to exhaustion times of 783 min, 1690 min, and 3154 min respectively. The volume of effluent treated at breakpoint was 1680 mL, 4560 mL and 6960 mL with exhaustion rates of 3.35, 3.34 and 3.58. The bed volumes processed before the bed required replacement or regeneration was 95, 121 and 131 bed volumes with the length of bed used calculated as 2.59 cm making use of 64.75% of the bed for a depth of 4 cm, 4.18 cm using 47.75% of the bed and 5.74 cm corresponding to 52.16% of the bed.

- **Fixed bed studies using eggshells**

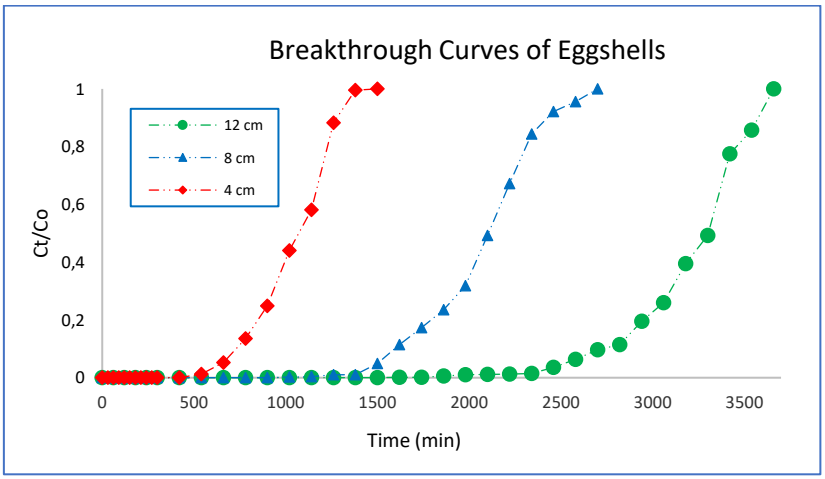

Figure 30. Breakthrough curves of eggshells

Pb removal using Eggshells were found to be 71.40 % for a bed depth of 4 cm with 77.96 % removal for 8cm and 90.25 % for a depth of 12 cm. The breakthrough times for 4 cm, 8 cm and 12 cm bed height were 420 min, 780 min and 1860 min corresponding to exhaustion times of 882 min, 1677 min, and 2781 min respectively. The volume of effluent treated at breakpoint was 1680 mL, 4560 mL and 6960 mL with exhaustion rates of 4.65, 4.74 and 4.53. The bed volumes processed before the bed required replacement or regeneration was 94, 88 and 103 bed volumes with the length of bed used calculated as 2.43 cm making use of 60.75% of the bed for a depth of 4 cm, 5.04 cm using 63.00% of the bed and 6.99 cm corresponding to 58.25 % of the bed.

4.4.1. Breakthrough Curve Parameters

Table 11. Summary of technical parameters for Pb removal in a fixed bed column.

$Adsorbent$	$Bed\ depth\ (cm)$	$t_b(min)$	$t_e(min)$	$MTZ(cm)$	$\%\ Removal$	$V_b(mL)$	BV	AER
$Bagasse$	4	60	201	2.81	47.86	240	14	4.75
	8	150	435	5.24	55.77	600	18	4.39
	12	300	830	7.66	65.87	1200	24	3.45
$Adsorbent\ A$	4	60	242	3.00	44.81	240	14	8.12
	8	150	585	5.95	65.30	600	17	6.70
	12	300	915	8.07	66.30	1200	23	6.44
$Adsorbent\ B$	4	120	477	2.99	61.15	480	27	6.22
	8	270	925	5.67	67.03	1020	31	6.42
	12	520	1408	7.40	71.11	2160	41	6.32
$Adsorbent\ C$	4	420	783	2.59	77.33	1680	95	3.35
	8	1140	1690	4.18	77.94	4560	121	3.34
	12	2460	3154	5.74	91.15	6960	131	3.58
$Eggshells$	4	420	882	2.43	71.40	1680	94	4.65
	8	780	1677	5.04	77.96	3120	88	4.74
	12	1860	2781	6.99	90.25	5520	103	4.53

4.4.1.1. Bed volumes

The performance of breakthrough curves is governed by the number of bed volumes processed before the bed is deemed ineffective. Generally, it is preferred to have a large number of bed volumes for a particular adsorbent since this means regeneration is not needed as often. From the results of this study, it was found that by increasing the bed length, the adsorbent could process more water before requiring regeneration or needing to be discarded.

Adsorbent C was found to have the largest bed volumes thereby being able to be used for a longer period of time before requiring regeneration. By increasing the length from 4 to 8 cm, the adsorbent was able to be used 20 % longer (from 95 to 121 bed volumes). However, the effect of moving from 8 to 12 cm was not as significant with a 10 % increase in usage (121 to 131 bed volumes). The performance of the remaining adsorbents were as follows: Eggshells > Adsorbent B > Adsorbent A > Bagasse.

4.4.1.2. Adsorption exhaustion rate

The adsorption exhaustion rate is another performance indicator used in fixed bed operations where low AER values implies good performance of a bed (Masukume et al., 2014). As can be seen from table 11, as the bed depth of the adsorbents were increased, the adsorption exhaustion rate decreased for the adsorbents concerned. For a depth of 4 cm, 8 cm and 12 cm, adsorbent C was found to be most proficient with the lowest recorded AER values of 3.35, 3.34 and 3.58 respectively.

4.4.1.3. Effect of bed height

From the results, a consensus was found where an increase in dosage (bed depth) increased the removal percentage, the mass transfer zone, volume of effluent treated to breakpoint, breakthrough time, exhaustion time and adsorption capacity for all adsorbents concerned. The work of (Du et al., 2018) explained that with increased dosage, there is a larger quantity of adsorbent particles that are present in the column, therefore there are more available sites for the adsorbate to be adsorbed, in addition to longer contact times for adsorbate – adsorbent interaction to take place. The results of this study were in accordance with their findings as

well as several other researchers (Masukume et al., 2014, De Angelis et al., 2017, Chowdhury et al., 2013). Moreover, longer beds have longer diffusion paths thus allowing the adsorbate more time to penetrate the adsorbent particles in the column allowing for a longer distance for the mass transfer zone to reach the exit resulting in extended breakthrough times (Malkoc et al., 2006a, Chowdhury et al., 2013). Having said that, according to (Luo et al., 2011a), at lower bed depths, the axial dispersion phenomena dominates in the mass transfer zone and reduces the diffusion of adsorbate ions.

It is worthy to note that the majority of adsorption of the solute takes place in the mass transfer zone where it is preferred to have a sharp mass transfer zone so that efficient use of the adsorbent occurs (Geankoplis, 2003). The order of efficiency of the adsorbents were as follows: Adsorbent C > Eggshells > Adsorbent B > Adsorbent A > Bagasse. In general, as the content of eggshells in the adsorbents increased, the removal efficiency of Pb increased.

Notably, for a bed height of 4 cm, adsorbent C and eggshells were most efficient reaching removal rates of 77.33% and 71.40% making use of 2.81 cm and 2.43 cm of the mass transfer zone respectively. In addition, when tripled to a height of 12 cm, both adsorbents experienced a shift of 20% higher removal rates reaching 91.15% and 90.25 % removal of Pb corresponding to mass transfer zones of 5.74 cm and 6.99 cm respectively. However, on increasing the bed height from 4 to 8 cm, it did not impact the removal rates significantly.

It is hypothesized that when an acidic lignocellulosic biomaterial such as bagasse is combined with an alkaline dolomitic one such as eggshells, it interacts with each other producing a “new” adsorbent with the properties of both materials. This was seen by the results of the FTIR spectra and XRD results of adsorbents A – C. Of notable interest, when eggshells and bagasse were combined to produce adsorbents A – C, it was found to inhibit some of the cellulosic components in the biomass (hydroxyl groups, OH) to produce adsorbents with a higher carboxyl group contents (COOH) as the mass of eggshells were increased (25%, 50%, 75%) as seen from the FTIR spectra. This in turn resulted in a combination of functional groups from both bagasse and eggshells in adsorbents A, B and C which were responsible for the adsorption of Pb. The optimum composition for the highest removal uptake of Pb was found to be adsorbent C constituting of 75 wt % eggshells with 25 wt% bagasse being able to treat the largest volume of water with the largest adsorption capacities.

The difference in adsorption capacities of the adsorbents can be attributed to the metal affinity towards the different surface groups of the eggshell – bagasse system. In this regard, similar

findings were reported by (Reddad et al., 2002) who also emphasized that the ionic radius and electro positive charge on Pb contributes towards the adsorption capacity.

4.5. Breakthrough curve modelling

4.5.1. Application of the Thomas model

Table 12. Breakthrough curve modelling parameters for the Thomas model

Adsorbent	*Bed Height*	$K_{th}\left(\frac{L}{mg.min}\right)$	$q_{o,th}\left(\frac{mg}{g}\right)$	$q_{exp}\left(\frac{mg}{g}\right)$	R^2	*RMSE*	*MAE*
Bagasse	4 *cm*	5.29×10^{-4}	20.48	21.05	0.962	0034	0.009
	8 *cm*	2.67×10^{-4}	20.57	22.77	0.856	0.068	0.020
	12 *cm*	1.47×10^{-4}	28.90	28.97	0.978	0.033	0.003
Adsorbent A	4 *cm*	3.55×10^{-4}	12.44	12.32	0.9087	0.029	0.004
	8 *cm*	1.85×10^{-4}	14.65	14.91	0.9155	0.039	0.001
	12 *cm*	1.35×10^{-4}	16.03	15.54	0.9486	0.037	0.010
Adsorbent B	4 *cm*	2.42×10^{-4}	14.99	16.06	0.890	0.047	0.019
	8 *cm*	1.35×10^{-4}	15.00	15.57	0.9108	0.028	0.005
	12 *cm*	5.29×10^{-4}	16.06	15.80	0.9881	0.030	0.007
Adsorbent C	4 *cm*	1.10×10^{-4}	27.79	28.05	0.9482	0.078	0.013
	8 *cm*	8.20×10^{-4}	22.16	29.95	0.884	0.080	0.036
	12 *cm*	6.0×10^{-5}	28.23	34.26	0.9265	0.048	0.017
Eggshells	4 *cm*	1.27×10^{-4}	21.48	20.33	0.9676	0.065	0.010
	8 *cm*	6.7×10^{-5}	21.11	20.69	0.9828	0.021	0.000
	12 *cm*	4.5×10^{-5}	22.08	21.51	0.9804	0.036	0.001

The experimental data was fitted to the Thomas model to determine the Thomas rate constant (K_{Th}) and the maximum solid – phase concentration ($q_{o,th}$) which were ascertained by linearising the data and calculating the parameters from this model. The maximum adsorption capacity of the adsorbents ($q_{o,th}$) were found to be in the following order: Adsorbent C > Bagasse > Eggshells > Adsorbent B > Adsorbent A.

As the bed height of the adsorbents increased, the values of the kinetic constant, $K_{Th,}$ decreased for all adsorbents concerned. In other words, a shorter contact time was required for adsorbent

– adsorbate interactions to occur since there was a greater quantity of adsorbent particles available to adsorb the solute.

Upon comparison between the experimental data ($q_{o,exp}$) and the maximum capacity from the model ($q_{o,th}$), there was a very close agreement between both values highlighting that this model was a good fit as seen from the correlation coefficients (R^2), most of which were found to be > 0.9 indicating the goodness of fit. Supporting this, the work of Malkoc et al. (2006a) showed a negligible difference between experimental and predicted values of the bed capacity suggesting that the Thomas model is valid.

From the batch studies, it was found that the removal of Pb followed pseudo – second order reaction kinetics with the equilibrium data following the Langmuir isotherm which are two assumptions of the Thomas model inferring that this model is a good fit to the experimental data. However, with this model, caution should be exercised since the adsorption process is not solely limited by chemical interaction kinetics and is often controlled by interphase mass transfer resistances as stated by (Aksu and Gönen, 2004b).

Two error metrics were used to analyse the variation in error of the experimental data against the Thomas model, namely, RMSE and MAE. It can be seen from table 12 that the values obtained were very low highlighting the good fit between the model and experimental data. In this regard, the work of (Chai and Draxler, 2014) states that RMSE is not a good indicator of average model performance which could be a misleading indicator of the average error and thus, MAE is a better metric. Considering this, the results of the MAE were < 0.02 which were much lower than the RMSE values of < 0.08.

4.5.2. Application of the Yoon – Nelson model

Table 13. Breakthrough curve modelling parameters for the Yoon-Nelson model

Adsorbent	*Bed Height*	τ_{exp} (min)	τ_{th} (min)	$K_{YN}(min^{-1})$	R^2	*RMSE*	*MAE*
Bagasse	4 *cm*	202	196	1.36×10^{-2}	0.962	0.034	0.009
	8 *cm*	284	366	2.73×10^{-2}	0.769	0.058	0.002
	12 *cm*	800	877	5.29×10^{-2}	0.979	0.027	0.006
Adsorbent A	4 *cm*	242	263	2.95×10^{-2}	0.895	0.058	0.032
	8 *cm*	585	575	1.85×10^{-2}	0.916	0.039	0.001
	12 *cm*	915	944	1.35×10^{-2}	0.949	0.037	0.010
Adsorbent B	4 *cm*	413	445	1.92×10^{-2}	0.890	0.047	0.019
	8 *cm*	925	890	1.29×10^{-2}	0.913	0.027	0.005
	12 *cm*	1408	1427	8.40×10^{-3}	0.985	0.048	0.017
Adsorbent C	4 *cm*	1188	1106	1.10×10^{-2}	0.948	0.078	0.013
	8 *cm*	2385	2246	8.20×10^{-3}	0.884	0.08	0.036
	12 *cm*	877	3374	6.00×10^{-3}	0.927	0.048	0.017
Eggshells	4 *cm*	1071	1024	1.26×10^{-2}	0.971	0.060	0.006
	8 *cm*	2106	2106	6.20×10^{-3}	0.968	0.024	0.011
	12 *cm*	3304	3262	4.20×10^{-3}	0.945	0.039	0.008

The model developed by Yoon – Nelson was used to predict the adsorption of Pb by calculating 50% of the breakthrough time required for the bed depths of the 5 adsorbents. This was done by linearising the data and calculating the desired constants, K_{YN} and τ for the model. As shown in table 13, K_{YN} decreased and τ increased as the bed height increased for all adsorbents concerned. As the mass of the adsorbents increased, there were more available adsorbent particles in the column to interact with and hence, a longer time was required to reach 50% breakthrough. In addition, by increasing the mass, a larger number of particles was available for adsorption to occur requiring a shorter contact time for adsorbent-adsorbate interactions to occur.

Upon comparison between the experimental times ($\tau_{,exp}$) and the calculated times from the Yoon-nelson model ($\tau_{,th}$), there was a relatively good agreement between both values highlighting that this model was a good fit as seen from the correlation coefficients (R^2). The work of (Zhang et al., 2011a) supported these results with the correlation coefficients R^2 being fairly close to 1 and the theoretical model matching the experimental data well.

For this study, the Yoon Nelson model was adequate in the description of the adsorption of Pb removal since the fixed bed experiments investigated a single – solute system. However, it should be noted that when dealing with multi – component systems, this model is not advised to be used. On the contrary, when estimates are required on the breakthrough times without physical information given on the adsorbent, the ease of use of this model makes it an ideal choice since it has a simple form when compared to other models as detailed data concerning the character of adsorbate – adsorbent interactions and parameters of the fixed bed are not required (Xu et al., 2013).

Two error metrics were used to analyse the variation in error of the experimental data against the Yoon Nelson model, namely, RMSE and MAE. It can be seen from table 13 that the RMSE and MAE values obtained were very low highlighting the good fit between the model and experimental data. The RMSE values calculated were < 0.06 and the MAE values < 0.03.

5. CONCLUSION AND RECOMMENDATIONS

The work done in this study looked at the adsorption process of agricultural lignocellulosic and dolomitic waste materials in the form of sugarcane bagasse and eggshells to remove metal contaminants from aqueous solutions. With circular economy and sustainability efforts taking precedence in industrial operations, this work forms a fundamental stepping stone and framework to determine if natural agricultural waste materials as biosorbents can present itself as a viable option long term.

From this research study, the following conclusions were drawn:

- From the Fourier Transform Infrared Spectroscopy (FTIR) and Energy Dispersive spectroscopy (EDX) analysis, it was found that carbon, calcium and oxygen atoms which constitute carboxylic and carbonate functional groups were present in eggshells, with carbon, hydrogen and oxygen atoms constituting hydroxyl and carbonyl groups were present in bagasse.

- Crystallographic information from the X – ray diffraction analysis (XRD) revealed a monoclinic lattice for bagasse with a rhombohedral lattice present in eggshells.

- The surface morphology of bagasse as determined from the scanning electron microscopy (SEM) micrograph was found to exhibit an irregular surface, while for eggshells, the surface was densely packed with a layered surface. Furthermore, it was found that the pore structures of both biomaterials belonged to a typical Type III isotherm which are characteristic of materials with macropores or open voids.

- Varying the particle size between the size fractions from 75 – 250 μm did not have a significant effect on the adsorption capacity and it was noted that other factors such as metal cation chemistry is important to account for in the adsorption process.

- Increasing the pH did not have a significant effect in the removal of Pb using eggshells however for bagasse, it resulted in much higher removal rates. For Cd removal, it had a comparable effect for both biosorbents.

- The adsorption of Pb reached equilibrium within 25 minutes for eggshells and 30 minutes for bagasse where the removal percentages reached 99.2% and 96.2% respectively. The removal rate of Cd required a longer equilibrium time of 60 minutes for both eggshells and bagasse with a removal rate of 71 and 73 % respectively.

- The maximum monolayer adsorption capacity of Pb and Cd removal using eggshells were found to be 277.78 and 13.62 mg/g respectively. For bagasse, the maximum capacity was found to be 31.45 mg/g for Pb and 19.49 mg/g for Cd.

- Ion exchange and complexation were the proposed mechanisms for adsorption in eggshells whereas ion exchange and complexation mechanisms were dominant in bagasse.

- Fixed bed studies showed that bed performance improved with an increase in bed depth resulting in greater mass transfer zones, breakthrough times and larger quantities of effluent treated.

- Two kinetic models (Thomas and Yoon–Nelson) were used to interpret the fixed bed breakthrough curves for the removal of Pb. The data showed good fits to both models.

- Adsorbent C was found to be most proficient in the removal of Pb with eggshells, adsorbent B, adsorbent A and bagasse following suit.

Future lines of work should look at using additional analytical techniques to complement characterisation results of the adsorbents so that meaningful results can be interpreted in addition to being used to validate characterisation studies. It is also recommended that further fixed bed experiments be conducted to investigate fundamental variables such as concentration and flowrate to assess the performance of the adsorbents to a greater extent. Time constraints

placed on the use of equipment did not allow for such experiments to occur. Moreover, it would also be beneficial to test the adsorption potential of the adsorbents using real waste effluent instead of synthesized solutions to gage whether the adsorbents can be applied at an industrial scale.

In conclusion, evidence provided in this study have shown that the re – use of natural agricultural wastes such as eggshells and bagasse show good promise to be applied as viable adsorbents for bioremediation.

6. RFERENCES

ABDEL-KHALEK, M. A., ABDEL RAHMAN, M. K. & FRANCIS, A. A. 2017a. Exploring the adsorption behavior of cationic and anionic dyes on industrial waste shells of egg. *Journal of Environmental Chemical Engineering* 5**,** 319-327.

ABDEL-KHALEK, M. A., ABDEL RAHMAN, M. K. & FRANCIS, A. A. 2017b. Exploring the adsorption behavior of cationic and anionic dyes on industrial waste shells of egg. *Journal of Environmental Chemical Engineering,* 5**,** 319-327.

ABDI, O. & KAZEMI, M. 2015. A review study of biosorption of heavy metals and comparison between different biosorbents *J. Mater. Environ. Sci. ,* 6**,** 1386-1399

ABDOLALI, A., GUO, W. S., NGO, H. H., CHEN, S. S., NGUYEN, N. C. & TUNG, K. L. 2014. Typical lignocellulosic wastes and by-products for biosorption process in water and wastewater treatment: a critical review. *Bioresource technology,* 160**,** 57-66.

ACHEAMPONG, M. A., PAKSHIRAJAN, K., ANNACHHATRE, A. P. & LENS, P. N. L. 2013. Removal of Cu(II) by biosorption onto coconut shell in fixed-bed column systems. *Journal of Industrial and Engineering Chemistry,* 19**,** 841-848.

AHMAD, M., USMAN, A.R.A., LEE, S.S., KIM, S.C., JOO, J.H., YANG, J.E. AND OK, Y.S. 2012. Eggshell and coral wastes as low cost sorbents for the removal of Pb2+, Cd2+ and Cu2+ from aqueous solutions. *JOURNAL OF INDUSTRIAL AND ENGINEERING CHEMISTRY,* 18**,** 198-204.

AHMED, S., CHUGHTAI, S. & KEANE, M. A. 1998. The removal of cadmium and lead from aqueous solution by ion exchange with Na・Y zeolite. *Separation and Purification Technology,* 13**,** 57-64.

AKCIL, A., AND KOLDAS, S. 2006. Acid Mine Drainage (AMD): Causes, treatment and case studies. *JOURNAL OF CLEANER PRODUCTION,* 14**,** 1139-1145.

AKSU, Z. 2005. Application of biosorption for the removal of organic pollutants: a review. OXFORD: Elsevier Ltd.

AKSU, Z. & GÖNEN, F. 2004a. Biosorption of phenol by immobilized activated sludge in a continuous packed bed: prediction of breakthrough curves. *Process Biochem.,* 5**,** 599–613.

AKSU, Z. & GÖNEN, F. 2004b. Biosorption of phenol by immobilized activated sludge in a continuous packed bed: prediction of breakthrough curves. *Process Biochemistry,* 39**,** 599-613.

AL-GHOUTI, M. A. & SALIH, N. R. 2018. Application of eggshell wastes for boron remediation from water. *Journal of Molecular Liquids,* 256**,** 599-610.

ALCHIN, D. & WANSBROUGH, H. 2017. *Ion Exchange Resins* [Online]. [Accessed 24/02/2018].

ALOMÁ, I., MARTÍN-LARA, M. A., RODRÍGUEZ, I. L., BLÁZQUEZ, G. & CALERO, M. 2012. Removal of nickel (II) ions from aqueous solutions by biosorption on sugarcane bagasse. *Journal of the Taiwan Institute of Chemical Engineers,* 43**,** 275-281.

AMCSD. *American Mineralogist Crystal Structure Database* [Online]. Available: http://rruff.geo.arizona.edu/AMS/amcsd.php [Accessed 02/06/2019].

ARECO, M. M., HANELA, S., DURAN, J. & DOS SANTOS AFONSO, M. 2012. Biosorption of Cu(II), Zn(II), Cd(II) and Pb(II) by dead biomasses of green alga Ulva lactuca and the development of a sustainable matrix for adsorption implementation. *Journal of Hazardous Materials,* 213-214**,** 123-132.

AYDIN, F., AYDIN, I., YASAR, F. & GUZEL, F. 2011. Determination of lead separated selectively with ion exchange method from solution onto BCW in Sirnak, East Anatolia of Turkey. *Microchemical Journal,* 98**,** 246-253.

AZHAR, S. S., LIEW, A. G., SUHARDY, D., HAFIZ, K. F. & HATIM, M. D. I. 2005. Dye removal from aqueous solution by using adsorption on treated sugarcane bagasse. *American Journal of Applied Science,* 2**,** 1499-1503.

BAI, Y. & BARTKIEWICZ, B. 2009. Removal of cadmium from wastewater using ion exchange resin *Polish Journal of Environmental Studies,* 18**,** 1191-1195.

BALÁŽ, M., ZORKOVSKÁ, A., FABIÁN, M., GIRMAN, V. & BRIANČIN, J. 2015. Eggshell biomaterial: Characterization of nanophase and polymorphs after mechanical activation. *Advanced Powder Technology,* 26**,** 1597-1608.

BANAT, F., SAMEER, A. A. & LEEMA, A. M. 2004. Utilization of raw and activated date pits for the removal of phenol from aqueous solution. *Chem. Eng. Technol,* 27**,** 80-86.

BARKA, N., ABDENNOURI, M., EL MAKHFOUK, M. & QOURZAL, S. 2013. Biosorption characteristics of cadmium and lead onto eco-friendly dried cactus (Opuntia ficus indica) cladodes. *Journal of Environmental Chemical Engineering,* 1**,** 144-149.

BASUALTO FLORES, C., POBLETE, M., MARCHESE, J., OCHOA, A., ACOSTA, A., SAPAG HAGAR, J. & VALENZUELA, F. 2006. *Extraction of cadmium from aqueous solutions by emulsion liquid membranes using a stirred transfer cell contactor*.

BECKER, M., DYANTYI, N., BROADHURST, J. L., HARRISON, S. T. L. & FRANZIDIS, J. P. 2015. A mineralogical approach to evaluating laboratory scale acid rock drainage characterisation tests. *Minerals Engineering***,** 33–36.

BELAY, K. 2015. *Removal of Methyl Orange from Aqueous Solutions Using Thermally Treated Egg Shell (Locally Available and Low Cost Biosorbent)*.

BERNARD, A. 2008. Cadmium & its adverse effects on human health. *Indian J Med Res,* 4**,** 557-564.

BHATT, M. 2015. Removal of Heavy Metals from Water (Cu and Pb) Using Household Waste as an Adsorbent. *Journal of Bioremediation & Biodegradation,* 06.

BUZZI, D. C., VIEGAS, L. S., SILVAS, F. P. C. & ESPINOSA, D. C. R. 2011. The use of Microfiltration and electrodialysis for Treatment of Acid Mine drainage. *IMWA***,** 287-292.

CAGNON, B., PY, X., GUILLOT, A., STOECKLI, F. & CHAMBAT, G. 2009. Contributions of hemicellulose, cellulose and lignin to the mass and the porous properties of chars and steam activated carbons from various lignocellulosic precursors. *Bioresource Technol***,** 292-298.

CALERO, M., HERNÁINZ, F., BLÁZQUEZ, G., TENORIO, G. & MARTÍN-LARA, M. A. 2009. Study of Cr (III) biosorption in a fixed-bed column. *Journal of Hazardous Materials,* 171**,** 886-893.

CARDOSO, S. P., AZENHA, I. S., LIN, Z., PORTUGAL, I., RODRIGUES, A. E. & SILVA, C. M. 2016. Experimental measurement and modeling of ion exchange equilibrium and kinetics of cadmium(II) solutions over microporous stannosilicate AV-6. *Chemical Engineering Journal,* 295**,** 139-151.

CARVALHO, J., RIBEIRO, A., GRAÇA, J., ARAÚJO, J., VILARINHO, C. & CASTRO, F. 2011. *ADSORPTION PROCESS ONTO AN INNOVATIVE EGGSHELL-DERIVED LOW-COST ADSORBENT IN SIMULATED EFFLUENT AND REAL INDUSTRIAL EFFLUENTS*.

CELIS, R., HERMOSIN, M. C. & CORNEJO, J. 2000. Heavy metal adsorption by functionalized clays. *ENVIRONMENTAL SCIENCE & TECHNOLOGY,* 34**,** 4593-4599.

CHAI, T. & DRAXLER, R. 2014. Root mean square error (RMSE) or mean absolute error (MAE)? *Geosci. Model Dev.,* 7.

CHAIRATA, M., SAOWANEE, R., BREMNERB, J.B. AND RATTANAPHANI, V. 2005. An adsorption and kinetic study of lac dyeing on silk. *Dyes and Pigment***,** 231–241.

CHAKRABORTY, S., DUTTA, A., SURAL, S., GUPTA, D. & SEN, S. 2013. *Ailing bones and failing kidneys: A case of chronic cadmium toxicity*.

CHANDEL, A., AF ANTUNES, F., ANJOS, V., BELL, M. J., N RODRIGUES, L., POLIKARPOV, I., DEAZEVEDO, E., BERNARDINELLI, O., A ROSA, C., PAGNOCCA, F. & DA SILVA, S. 2014. *Multi-scale structural and chemical analysis of sugarcane bagasse in the process of sequential acid–base pretreatment and ethanol production by Scheffersomyces shehatae and Saccharomyces cerevisiae*.

CHAO, H. P., CHANG, C. C. & NIEVA, A. 2014. Biosorption of heavy metals on Citrus maxima peel, passion fruit shell, and sugarcane bagasse in a fixed-bed column. *JOURNAL OF INDUSTRIAL AND ENGINEERING CHEMISTRY,* 20**,** 3408-3414.

CHIRKST, D. E., CHEREMISINA, O. V., IVANOV, M. V., . & ZHADOVSKII, I. T. 2010. Kinetics of the Ion Exchange of Lead and Sodium Cations on the Surface of Iron–Manganese Concretions. *Russian Journal of Applied Chemistry,* 83**,** 1540–1543.

CHOI , H. J. A. L., S.M. 2015. Heavy metal removal from acid mine drainage by calcined eggshell and microalgae hybrid system. *Environmental Science and Pollution Research,* 22**,** 13404-13411.

CHOJNACKA, K. 2005. Biosorption of Cr(III) ions by eggshells. *Journal of Hazardous Materials,* 121**,** 167-173.

CHOWDHURY, Z. Z., ZAIN, S. M., RASHID, A. K., RAFIQUE, R. F. & KHALID, K. 2013. Breakthrough Curve Analysis for Column Dynamics Sorption of Mn(II) Ions from Wastewater by Using Mangostana garcinia Peel-Based Granular-Activated Carbon. *Journal of Chemistry,* 2013**,** 959761.

COATES, J. 2000. Interpretation of Infrared Spectra: A Practical Approach. *Encyclopedia of Analytical Chemistry.* Chichester: John Wiley & Sons Ltd.

COBBING, J. E. 2008. Institutional Linkages and Acid Mine Drainage: The Case of the Western Basin in South Africa. *Water Resources Development,* 24**,** 451–462.

CORRALES, R. C. N. R., MENDES, F. M. T., PERRONE, C. C., SANT'ANNA, C., DE SOUZA, W., ABUD, Y., BON, E. P. D. S. & FERREIRA-LEITÃO, V. 2012. Structural evaluation of sugar cane bagasse steam pretreated in the presence of CO(2) and SO(2). *Biotechnology for Biofuels,* 5**,** 36-36.

CRUZ-OLIVARES, J., PÉREZ-ALONSO, C., BARRERA-DÍAZ, C., UREÑA-NUÑEZ, F., CHAPARRO-MERCADO, M. C. & BILYEU, B. 2013. Modeling of lead (II) biosorption by residue of allspice in a fixed-bed column. *Chemical Engineering Journal,* 228**,** 21–27.

DAS, N. 2010. Recovery of precious metals through biosorption — A review. *Hydrometallurgy,* 103**,** 180-189.

DE ANGELIS, G., MEDEGHINI, L., CONTE, A. M. & MIGNARDI, S. 2017. Recycling of eggshell waste into low-cost adsorbent for Ni removal from wastewater. *Journal of Cleaner Production,* 164**,** 1497-1506.

DONG, Y. & LIN, H. 2017. Competitive adsorption of Pb(II) and Zn(II) fromaqueous solution by modified beer lees in a fixedbed column. *Process Safety and Environmental Protection,* 111**,** 263–269.

DRIEMEIER, C., OLIVEIRA, M. M., MENDES, F. M. & GÓMEZ, E. O. 2011. Characterization of sugarcane bagasse powders. *Powder Technology,* 214**,** 111-116.

DU, Z., ZHENG, T. & WANG, P. 2018. Experimental and modelling studies on fixed bed adsorption for Cu(II) removal from aqueous solution by carboxyl modified jute fiber. *Powder Technology,* 338**,** 952-959.

ECONOMISTS, C. 2013. Overview of the Sugar Industry in South Africa: Contribution to Social and Economic Development and Contentious Issues. South Africa.

EHRAMPOUSH, M. H., GHANIZADEH, G. & GHANEIAN, M. H. 2011. EQUILIBRIUM AND KINETICS STUDY OF REACTIVE RED 123 DYE REMOVAL FROM AQUEOUS SOLUTION BY ADSORPTION ON EGGSHELL *Iran. J. Environ. Health. Sci. Eng,* 8**,** 101-108.

ELANZA, S., LEBKIRI,A.S., MARZAK, S., RIFI, E.H., LEBKIRI, M. AND SATIF, C. 2014. Removal of lead ions from aqueous solution by the sugarcane bagasse. *J. Mater. Environ. Sci.,* 5**,** 1591-1598.

ELETTA, O. A. A., AJAYI, O. A., OGUNLEYE, O. O. & AKPAN, I. C. 2016. Adsorption of cyanide from aqueous solution using calcinated eggshells: Equilibrium and optimisation studies. *Journal of Environmental Chemical Engineering,* 4**,** 1367-1375.

ELKADY, M., IBRAHIM, A. & ABD EL-LATIF, M. 2011. *Assessment of the adsorption kinetics, equilibrium and thermodynamic for the potential removal of reactive red dye using eggshell biocomposite beads*.

EPA, E. P. A. Available: www.epa.gov [Accessed 17/04/2018].

FAROOQ, U., KOZINSKI, J. A., KHAN, M. A. & ATHAR, M. 2010. Biosorption of heavy metal ions using wheat based biosorbents – A review of the recent literature. *Bioresource Technology,* 101**,** 5043-5053.

FIGUEROA-TORRES, G. M., CERTUCHA-BARRAGÁN, M. T., ACEDO-FÉLIX, E., MONGE-AMAYA, O., ALMENDARIZ-TAPIA, F. J. & GASCA-ESTEFANÍA, L. A. 2016. Kinetic studies of heavy metals biosorption by acidogenic biomass immobilized in clinoptilolite. *Journal of the Taiwan Institute of Chemical Engineers,* 61**,** 241-246.

FILHOA, N. C., VENANCIOA, E. C., BARRIQUELLOA, M. F., HECHENLEITNERB, A. A. W. & PINEDAB, E. A. G. 2007. Methylene blue adsorption onto modified lignin from sugar cane bagasse. *Ecl. Quím. São Paulo,* 32.

FLORA, G., GUPTA, D. & TIWARI, A. 2012. Toxicity of lead: a review with recent updates. *Interdiscip Toxicology,* 5**,** 47-58.

FLORES-CANO, J. V., LEYVA-RAMOS, R., MENDOZA-BARRON, J., GUERRERO-CORONADO, R. M., ARAGÓN-PIÑA, A. & LABRADA-DELGADO, G. J. 2013. Sorption mechanism of Cd(II) from water solution onto chicken eggshell. *Applied Surface Science,* 276**,** 682-690.

FONTANA, K. B., CHAVES, E. S., SANCHEZ, J. D. S., WATANABE, E. L. R., PIETROBELLI, J. M. T. A. & LENZI, G. G. 2016. Textile dye removal from aqueous solutions by malt bagasse: Isotherm, kinetic and thermodynamic studies. *Ecotoxicology and Environmental Safety***,** 329–336.

FREITAS, R., GODOY PERILLI, T. A. & LADEIRA, A. 2013. *Oxidative Precipitation of Manganese from Acid Mine Drainage by Potassium Permanganate*.

GAIKWAD, R. W., SAPKAL, V. S. S. & SAPKAL, R. S. S. 2010. Ion exchange system design for removal of heavy metals from acid mine drainage wastewater. *Acta Montanistica Slovaca***,** 298-304.

GAO, R. & WANG, J. 2007. Effects of pH and temperature on isotherm parameters of chlorophenols biosorption to anaerobic granular sludge. *Journal of Hazardous Materials,* 145**,** 398-403.

GEANKOPLIS, C. J. 2003. *Transport processes and separation process principles: includes unit operations,* Upper Saddle River, NJ, Prentice Hall Professional Technical Reference.

GERHARDSSON, L., ENGLYST, V., LUNDSTRÖM, N.-G., SANDBERG, S. & NORDBERG, G. 2002. Cadmium, copper and zinc in tissues of deceased copper smelter workers. *Journal of Trace Elements in Medicine and Biology,* 16**,** 261-266.

GUPTA, V. K., JAIN, C. K., ALI, I., SHARMA, M. & SAINI, V. K. 2003. Removal of cadmium and nickel from wastewater using bagasse fly ash—a sugar industry waste. *Water Research,* 37**,** 4038-4044.

GURGEL, L. V. A., FREITAS, R. P. D. & GIL, L. F. 2008. Adsorption of Cu(II), Cd(II), and Pb(II) from aqueous single metal solutions by sugarcane bagasse and mercerized sugarcane bagasse chemically modified with succinic anhydride. *Carbohydrate Polymers,* 74**,** 922-929.

HAMISSAA, A. M. B., LODI, A., SEFFENA, M., FINOCCHIO, E., BOTTER, R. & CONVERTI, A. 2010. Sorption of Cd(II) and Pb(II) from aqueous solutions onto Agave americana fibers. *Chemical Engineering Journal,* 159**,** 67–74.

HAN, R., WANG, Y., ZHAO, X., WANG, Y., XIE, F., CHENG, J. & TANG, M. 2009. Adsorption of methylene blue by phoenix tree leaf powder in a fixed-bed column: experiments and prediction of breakthrough curves. *Desalination,* 245**,** 284-297.

HAN, R., ZHANG, J., ZOU, W., XIAO, H., SHI, J. & LIU, H. 2006. Biosorption of copper(II) and lead(II) from aqueous solution by chaff in a fixed-bed column. *Journal of Hazardous Materials,* 133**,** 262-268.

HARPER, T. R. & KINGHAM, N. W. 1992. Removal of arsenic from wastewater using chemical precipitation methods. *Water Environment Research,* 64**,** 200-203.

HASAN, S. H., RANJAN, D. & TALAT, M. 2010. Agro-industrial waste 'wheat bran' for the biosorptive remediation of selenium through continuous up-flow fixed-bed column. *Journal of Hazardous Materials,* 181**,** 1134-1142.

HASFALINA, C. M., MARYAM, R. Z., LUQMAN, C. A. & RASHID, M. 2012. Adsorption of Copper (II) From Aqueous Medium In Fixed-Bed Column By Kenaf Fibres. *APCBEE Procedia,* 3**,** 255-263.

HAWARI, A. H. & MULLIGAN, C. N. 2006. Biosorption of lead(II), cadmium(II), copper(II) and nickel(II) by anaerobic granular biomass. *Bioresource Technology,* 97**,** 692-700.

HENSON, M. C. & CHEDRESE, P. J. 2004. Endocrine disruption by cadmium, a common environmental toxicant with paradoxical effects on reproduction. *ExpBiol Med* 383-392.

HINCKE, M. T., NYS, Y., GAUTRON, J., MANN, K. & RODRIGUEZ-NAVARRO, A. B. 2012. The eggshell: Structure, composition and mineralization. *Front. Biosci. Special Edition on Biomineralization,* 17**,** 1266–1280.

HO, Y. S. & MCKAY, G. 1999. Pseudo-second order model for sorption processes. *Process Biochemistry,* 34**,** 451-465.

HOMAGAI, P. L., GHIMIRE, K. N. & INOUE, K. 2010. Adsorption behavior of heavy metals onto chemically modified sugarcane bagasse. *Bioresource Technology,* 101**,** 2067-2069.

HUMPHRIES, B., WANG, Z. AND YANG, C. 2016. The role of microRNAs in metal carcinogen-induced cell malignant transformation and tumorigenesis. *Food Chem Toxicology***,** 58-65.

IBRAHIM, S., MEGAT HANAFIAH, M. A. K. & YAHYA, M. Z. A. 2006. Removal of Cadmium form aqueous solutions by adsorption on sugarcane bagasse. *Am. Eur. J. Agri. Environ. Sci.,* 1**,** 179-184.

IQBAL, M., SAEED, A. & ZAFAR, S. I. 2009. FTIR spectrophotometry, kinetics and adsorption isotherms modeling, ion exchange, and EDX analysis for understanding the mechanism of Cd2+ and Pb2+ removal by mango peel waste. *Journal of Hazardous Materials,* 164**,** 161-171.

IUPAC. *International Union of Pure and Applied Chemistry* [Online]. Available: https://iupac.org/ [Accessed 20/05/2019].

JAISHANKAR, M., TSETEN, T., ANBALAGAN, N., MATHEW, B. B. & BEEREGOWDA, K. N. 2014. Toxicity, mechanism and health effects of some heavy metals. *Interdisciplinary Toxicology,* 7**,** 60-72.

JAN, A. T., AZAM, M., SIDDIQUI, K., ALI, A., CHOI, I. & HAQ, Q. M. R. 2015. Heavy Metals and Human Health: Mechanistic Insight into Toxicity and Counter Defense System of Antioxidants. *International Journal of Molecular Sciences,* 16**,** 29592-29630.

JIN, Y., TENG, C., YU, S., SONG, T., DONG, L., LIANG, J., BAI, X., LIU, X., HU, X. & QU, J. 2018. Batch and fixed-bed biosorption of Cd(II) from aqueous solution using immobilized Pleurotus ostreatus spent substrate. *Chemosphere,* 191**,** 799-808.

KEFENI, K. K., MAKUDALI, T. A. M. & BHEKIE, M. 2017. *Acid mine drainage: Prevention, treatment options, and resource recovery: A review*.

KHORAMZADEH, E., NASERNEJAD, B. & HALLADJ, R. 2013. Mercury biosorption from aqueous solutions by sugarcane bagasse. *J Taiwan Inst Chem Eng,* 44**,** 266–269.

KING'ORI, A. 2011. *A Review of the uses of poultry eggshells and shell membranes*.

KOBIRAJ, R., GUPTA, N., KUSHWAHA, A. K. & CHATTOPADHYAYA, M. C. 2012. Determination of equilibrium, kinetic and thermodynamic parameters for the adsorption of Brilliant Green dye from aqueous solutions onto eggshell powder. *Indian Journal of Chemical Technology,* 19**,** 26-31.

KRISHNAN, K. A. & ANIRUDHAN, T. S. 2003. Removal of cadmium(II) from aqueous solutions by steam-activated sulphurised carbon prepared from sugar-cane bagasse pith: kinetics and equilibrium studies. *Water SA,* 29**,** 147-156.

KULKARNI, R. M., SHETTY, K. V. & SRINIKETHAN, G. 2014. Cadmium (II) and nickel (II) biosorption by Bacillus laterosporus (MTCC 1628). *Journal of the Taiwan Institute of Chemical Engineers,* 45**,** 1628-1635.

KUMAR, P. S., RAMALINGAM, S., KIRUPHA, S. D., MURUGESAN, A., VIDHYADEVI, T. & SIVANESAN, S. 2011. Adsorption behavior of nickel(II) onto cashew nut shell: Equilibrium, thermodynamics, kinetics, mechanism and process design. *Chemical Engineering Journal,* 167**,** 122-131.

LAGERGREN, S. 1898. About the theory of so-called adsorption of soluble substances. *KUNGLIGA SVENSKA VETENSKAPSAKADEMIENS HANDLINGAR,* 24**,** 1-39.

LAKHERWAL, D. 2014. Adsorption of Heavy Metals: A Review *International Journal of Environmental Research and Development,* 4**,** 41-48.

LEÃO, R. M., MILÉO, P. C., MAIA, J. M. L. L. & LUZ, S. M. 2017. Environmental and technical feasibility of cellulose nanocrystal manufacturing from sugarcane bagasse. *Carbohydrate Polymers,* 175**,** 518-529.

LIN, L., XU, X. S., PAPELIS, C., CATH, T. Y. & XU, P. 2014. Sorption of metals and metalloids from reverse osmosis concentrate on drinking water treatment solids. *SEPARATION AND PURIFICATION TECHNOLOGY,* 134**,** 37-45.

LIU, C., NGO, H. H. & GUO, W. 2015. Equilibrium and kinetic studies of various heavy metals on sugarcane bagasse. *Journal of Water Sustainability,* 5**,** 59–73.

LIU, C., NGO, H. H., GUO, W. & TUNG, K.-L. 2012. Optimal conditions for preparation of banana peels, sugarcane bagasse and watermelon rind in removing copper from water. *Bioresource Technology,* 119**,** 349-354.

LOPIČIĆ, Z., STOJANOVIĆ, M.D., MARKOVIĆ, S.B., MILOJKOVIĆ, J.V., MIHAJLOVIĆ, M.L., KALUĐEROVIĆ, R.T.S. AND KIJEVČANIN, M.L.J. 2016. Effects of different mechanical treatments on structural changes of lignocellulosic waste biomass and subsequent Cu(II) removal kinetics. *Arabian Journal of Chemistry*.

LUO, X., DENG, Z., LIN, X. & ZHANG, C. 2011a. Fixed-bed column study for Cu2+ removal from solution using expanding rice husk. *Journal of Hazardous Materials,* 187**,** 182-189.

LUO, X., LIU, F., DENG, Z. & LIN, X. 2011b. Removal of copper(II) from aqueous solution in fixed-bed column by carboxylic acid functionalized deacetylated konjac glucomannan. *Carbohydrate Polymers,* 86**,** 753-759.

LUPTAKOVA, A., UBALDINI, S., FORNARI, P. & MACINGOVA, E. 2012. Physical, chemical and biological chemical methods for treatment of Acid mine drainage. *Journal of Chemical Engineering Transactions*.

MADALA, S., NADAVALA, S. K., VUDAGANDLA, S., BODDU, V. M. & ABBURI, K. 2017. Equilibrium, kinetics and thermodynamics of Cadmium (II) biosorption on to composite chitosan biosorbent. *Arabian Journal of Chemistry,* 10**,** S1883-S1893.

MADHAV, M., SONI, S., SINGHAL, M., GAUTAM, C. K. & SHANTHI, V. 2013. Study of operational parameters and kinetics of biosorption of acid orange 7 by untreated sugarcane bagasse. *Journal of Chemical and Pharmaceutical Research,* 5**,** 523-531.

MALAKONDAIAH, K. C., KALPANA, D. A., NAIDU, D. A., KING, P. & PRASAD, V. S. R. K. 2010. Low cost biosorbent for the removal of Cu (II) from aqueous solution. *Journal of Environmental Science,* 5**,** 363-368.

MALATSE, S. & NDLOVU, M. 2015. The viability of using the Witwatersrand gold mine tailings for brickmaking *Journal of the Southern African Institute of Mining and Metallurgy*.

MALKOC, E., NUHOGLU, Y. & ABALI, Y. 2006a. Adsorption by Waste Acorn of Quercus ithaburensis in Fixed Beds: Prediction of Breakthrough Curves. *Chemical Engineering Journal,* 119**,** 61-68.

MALKOC, E., NUHOGLU, Y. & ABALI, Y. 2006b. Cr(VI) adsorption by waste acorn of Quercus ithaburensis in fixed beds: Prediction of breakthrough curves. *Chemical Engineering Journal,* 119**,** 61-68.

MAO, Y., MINGMING, S., XU, C., YANFANG, F., JINZHONG, W., KUAN, L., DA, T., MANQIANG, L., JUN, W., SCHWAB, A.P., AND XIN, J. 2017. Feasibility of sulfate-calcined eggshells for removing pathogenic bacteria and antibiotic resistance genes from landfill leachates. *Waste Management,* 63**,** 275-283.

MAREE, J. P., MUJURU, M., BOLOGO, V., DANIELS, N. & MPHOLOANE, D. 2013. Neutralisation treatment of AMD at affordable cost. *Water SA,* 39**,** 245-250.

MARISA, L., LEONARDO, D.G., CLARE, G.S.K., RACHAEL, S., OIGRES, B., MARCELO, C., CAMILA, R., CARLOS, L., DEAZEVEDO, E., NCQUEEN-MASON, S.J. AND POLIKARPOV, I. 2014. *Evaluating the Composition and Processing Potential of Novel Sources of Brazilian Biomass for Sustainable Biorenewables Production*.

MARTÍN-LARA, M. A., BLÁZQUEZ, G., CALERO, M., ALMENDROS, A. I. & RONDA, A. 2016. Binary biosorption of copper and lead onto pine cone shell in batch reactors and in fixed bed columns. *International Journal of Mineral Processing,* 148**,** 72-82.

MARTÍN-LARA, M. Á., RICO, I. L. R., VICENTE, I. D. L. C. A., GARCÍA, G. B. & DE HOCES, M. C. 2010. Modification of the sorptive characteristics of sugarcane bagasse for removing lead from aqueous solutions. *Desalination,* 256**,** 58-63.

MARTIN, S. & GRISWOLD, W. 2009. Human health effects of heavy metals. *Environmental Science and Technology Briefs for Citizens* 1-6.

MASHANGWA, T. D., TEKERE, M. AND SIBANDA, T. 2017. Determination of the Efficacy of Eggshell as a Low-Cost Adsorbent for the Treatment of Metal Laden Effluents. *Int Journal of Environ Res,* 11**,** 175-188.

MASUKUME, M., ONYANGO, M. S. & MAREE, J. P. 2014. Sea shell derived adsorbent and its potential for treating acid mine drainage. *International Journal of Mineral Processing,* 133**,** 52-59.

MATLOCK, M. M., HOWERTON, B. S. & ATWOOD, D. A. 2002. Chemical Precipitation of Lead from Lead Battery Recycling Plant Wastewater. *Industrial & Engineering Chemistry Research,* 41**,** 1579-1582.

MCCARTHY, T. S. 2011. The impact of acid mine drainage in South Africa. *S Afr J Sci.*

MEZENNER, N. Y. & BENSMAILI, A. 2009. Kinetics and thermodynamic study of phosphate adsorption on iron hydroxide-eggshell waste. *Chemical Engineering Journal,* 147**,** 87-96.

MITTAL, A., TEOTIA, M., SONI, R. K. & MITTAL, J. 2016. Applications of egg shell and egg shell membrane as adsorbents: A review. *Journal of Molecular Liquids,* 223**,** 376-387.

MOHAMAD, M., WEI, T.C., MOHAMMAD, R. AND WEI, L.J. 2017. OPTIMIZATION OF OPERATING PARAMETERS BY RESPONSESURFACE METHODOLOGY FOR MALACHITE GREEN DYE REMOVAL USING BIOCHAR PREPARED FROM EGGSHELL. *Journal of Engineering and Applied Sciences* 12**,** 3621-3633.

MOHAN, D. & SINGH, K. P. 2002. Single- and multi-component adsorption of cadmium and zinc using activated carbon derived from bagasse—an agricultural waste. *Water Research,* 36**,** 2304-2318.

MOON, R. J., MARTINI, A., NAIRN, J., SIMONSEN, J. & YOUNGBLOOD, J. 2011. Cellulose nanomaterials review: structure, properties and nanocomposites. *Chemical Society Reviews,* 40**,** 3941-3994.

MOROSANU, I., TEODOSIU, C., PADURARU, C., IBANESCU, D. & TOFAN, L. 2017. Biosorption of lead ions from aqueous effluents by rapeseed biomass. *NEW BIOTECHNOLOGY,* 39**,** 110-124.

MOUBARIK, A. 2015. Valorization of olive stone and sugar cane bagasse by-products as biosorbents for the removal of cadmium from aqueous solution. *Food research international,* v. 73**,** pp. 169-175-2015 v.73.

MUHAMAD, H., DOAN, H. & LOHI, A. 2010. Batch and continuous fixed-bed column biosorption of Cd2+ and Cu2. *CHEMICAL ENGINEERING JOURNAL,* 158**,** 369-377.

MWASISWEBE, D. 2005. *PRODUCTION OF ACTIVATED CARBON FROM SOUTH AFRICAN SUGARCANE BAGASSE.* Masters of Science in Engineering, University of KwaZulu-Natal, Durban.

NADDAFI, K., NABIZADEH, R., SAEEDI, R., MAHVI, A. H., VAEZI, F., YAGHMAEIAN, K., GHASRI, A. & NAZMARA, S. 2007. Biosorption of lead(II) and cadmium(II) by protonated Sargassum glaucescens biomass in a continuous packed bed column. *Journal of Hazardous Materials,* 147**,** 785-791.

NAICKER, K., CUKROWSKA, E. & MCCARTHY, T. S. 2003. Acid mine drainage arising from gold mining activity in Johannesburg, South Africa and environs. *Environmental Pollution***,** 29–40.

NAKANO, T., I IKAWA, N. & OZIMEK, L. 2003. *Chemical composition of chicken eggshell and shell membranes*.

NEM:WA. *National Environmental Management: Waste Act (No. 59 of 2008)* [Online]. Available: www.environment.gov.za [Accessed 28/09/2019].

NGOLE-JEME, V. M. & FANTKE, P. 2017. Ecological and human health risks associated with abandoned gold mine tailings contaminated soil. *PLOS ONE,* 12**,** e0172517.

NGUYEN, T. A. H., NGO, H. H., GUO, W. S., ZHANG, J., LIANG, S., YUE, Q. Y., LI, Q. & NGUYEN, T. V. 2013. Applicability of agricultural waste and by-products for adsorptive removal of heavy metals from wastewater. *Bioresource Technology,* 148**,** 574-585.

NWIB. *Waste Economy–2017 Market Intelligence Report* [Online]. Available: www.green-cape.co.za [Accessed 03/02/2018].

NWMS 2011. National Waste Management Strategy.

OK, Y. S., LEE, S. S., JEON, W.-T., OH, S.-E., USMAN, A. & MOON, D. H. 2011. Application of Eggshell Waste for the Immobilization of Cadmium and Lead in a Contaminated Soil. *Environ Geochem Health,* 33 Suppl 1**,** 31-9.

OKORO, I. A. & OKORO, S. O. 2011. Agricultural by products as green chemistry absorbents for the removal and recovery of metal ions from waste-water environments. *Cont J Water Air Soil Pollut,* 2**,** 15-22.

OLIVEIRA, D., BENELLI, P. & AMANTE, E. 2013. *A literature review on adding value to solid residues: Egg shells*.

PARK, H. J., JEONG, S. W., YANG, J. K., KIM, B. G. & LEE, S. M. 2007. Removal of heavy metals using waste eggshell. *Journal of Environmental Sciences,* 19**,** 1436-1441.

PARK, J., WON, S. W., MAO, J., KWAK, I. S. & YUN, Y.-S. 2010. Recovery of Pd(II) from hydrochloric solution using polyallylamine hydrochloride-modified Escherichia coli biomass. *Journal of Hazardous Materials,* 181**,** 794-800.

PILLAI, S. S., DEEPA, B., ABRAHAM, E., GIRIJA, N., GEETHA, P., JACOB, L. & KOSHY, M. 2013. Biosorption of Cd(II) from aqueous solution using xanthated nano banana cellulose: Equilibrium and kinetic studies. *Ecotoxicology and Environmental Safety,* 98**,** 352–360.

PODSTAWCZYK, D., WITEK-KROWIAK, A., CHOJNACKA, K. & SADOWSKI, Z. 2014. Biosorption of malachite green by eggshells: Mechanism identification and process optimization. *Bioresource Technology,* 160**,** 161-165.

POLETTO, M., ORNAGHI JÚNIOR, H. L. & ZATTERA, A. J. 2014. Native Cellulose: Structure, Characterization and Thermal Properties. *Materials,* 7**,** 6105-6119.

PUTRA, W. P., KANMARI, A., YUSOFF, S. N. M., ISHAK, C. F., MOHAMED, A., HASHIM, N. A. & ISA, I. M. 2014. Biosorption of Cu(II), Pb(II) and Zn(II) Ions from Aqueous Solutions Using Selected Waste Materials: Adsorption and Characterisation Studies. *Journal of Encapsulation and Adsorption Sciences,* Vol.04No.01**,** 11.

QDAIS, H. A. & MOUSSA, H. 2004. Removal of heavy metals from wastewater by membrane processes: a comparative study. *Desalination,* 164**,** 105-110.

QUINA, M. J., SOARES, M. A. R. & QUINTA-FERREIRA, R. 2017. Applications of industrial eggshell as a valuable anthropogenic resource. *Resources, Conservation and Recycling,* 123**,** 176-186.

RAJESWARI, A., JACKCINA STOBEL CHRISTY, E., GOPI, S., JAYARAJ, K. & PIUS, A. 2020. 9 - Characterization studies of polymer-based composites related to functionalized filler-matrix interface. *In:* GOH, K. L., M.K, A., DE SILVA, R. T. & THOMAS, S. (eds.) *Interfaces in Particle and Fibre Reinforced Composites.* Woodhead Publishing.

RAMLA, B. & SHERIDAN, C. 2015. The potential utilisation of indigenous South African grasses for acid mine drainage remediation. *Water SA,* 41.

RAMONTJA, T. H., COETZEE, H., HOBBS, P. J., BURGESS, J. E., THOMAS, A., KEET, M., YIBAS, B., VAN TONDER, D., NETILI, F., RUST, U., WADE, P. & MAREE, J. 2011. Mine Water Management in the Witwatersrand Gold Fields With Special Emphasis on Acid Mine Drainage Pretoria, Inter-Ministerial-Committee on Acid Mine Drainage. Report of the Team of Experts for the Inter-Ministerial Committee on Acid Mine Drainage.

RAYMUNDO, A. S., ZANAROTTO, R., BELISÁRIO, M., PEREIRA, M. D. G., RIBEIRO, J. N. & RIBEIRO, A. V. F. N. 2010. Evaluation of sugar-cane bagasse as bioadsorbent in the textile wastewater treatment contaminated with carcinogenic congo red dye. *Brazilian Archives of Biology and Technology,* 53**,** 931-938.

REDDAD, Z., GERENTE, C., ANDRES, Y. & LE CLOIREC, P. 2002. Adsorption of several metal ions onto a low-cost biosorbent: Kinetic and equilibrium studies. *Environmental Science and Technology,* 36**,** 2067-2073.

RENU, M. A., SINGH, K., UPADHYAYA, S. & DOHARE, R. K. 2017. Removal of heavy metals from wastewater using modified agricultural adsorbents. *Materials Today: Proceedings,* 4**,** 10534-10538.

REZENDE, C. A., DE LIMA, M. A., MAZIERO, P., RIBEIRO DE AZEVEDO, E., GARCIA, W. & POLIKARPOV, I. 2011. Chemical and morphological characterization of sugarcane bagasse submitted to a delignification process for enhanced enzymatic digestibility. *Biotechnol Biofuels,* 4**,** 1–18.

RÍOS-PARADA, V., JIMÉNEZ-QUERO, V. G., VALDEZ-TAMEZ, P. L. & MONTES-GARCÍA, P. 2017. Characterization and use of an untreated Mexican sugarcane bagasse ash as supplementary material for the preparation of ternary concretes. *Construction and Building Materials,* 157**,** 83-95.

ROCHA, G. J. D. M., NASCIMENTO, V. M., GONÇALVES, A. R., SILVA, V. F. N. & MARTÍN, C. 2015. Influence of mixed sugarcane bagasse samples evaluated by elemental and physical–chemical composition. *Industrial Crops and Products,* 64**,** 52-58.

ROMANOFF, A. L. & ROMANOFF, A. J. 1949. *The avian egg*, John Wiley & sons, Inc. New York, NY.

RUBCUMINTARA, T. 2015. Adsorptive Recovery of Au(III) from Aqueous Solution Using Modified Bagasse Biosorbent. *International Journal of Chemical Engineering and Applications,* 6**,** 95-100.

SAID, A. A., ALY, A. M. M., ABD EL-WAHAB, M. M. M., SOLIMAN, S. A., ABD EL-HAFEZ, A. A., HELMEY, V. & GODA, M. N. 2013. Application of modified bagasse as a biosorbent for reactive dyes removal from industrial waste water. *Journal of water resource and protection,* 5**,** 10-17.

SANS241-1:2015. *SOUTH AFRICAN NATIONAL STANDARD Drinking water Part 1: Microbiological, physical, aesthetic and chemical determinands* [Online]. Available: https://sabs.co.za [Accessed].

SAPA. 2015. *South African Poultry Association* [Online]. Available: www.sapoultry.co.za [Accessed 21/03/2018].

SARKAR, A., RAVINDRAN, G. & KRISHNAMURTHY, V. 2013. *A brief review on the effect of cadmium toxicity: from cellular to organ level*.

SARKER, T. C., AZAM, S. M. G. G. & BONANOMI, G. 2017. Recent advances in sugarcane industry solid by-products valorization. *Waste Biomass Valor,* 8**,** 241–266.

SASA. *South African Sugar Association* [Online]. Available: http://www.sasa.org.za [Accessed 02/08/2018].

SCHAAFSMA, A., PAKAN, I., HOFSTEDE, G. J. H., MUSKIET, F. A., VAN DER VEER, E. & DE VRIES, P. J. F. 2000. Mineral, amino acid, and hormonal composition of chicken eggshell powder and the evaluation of its use in human nutrition. *Poultry Science,* 79**,** 1833-1838.

SCHWANTES, D., GON, #XE7, ALVES, A. C., COELHO, G. F., CAMPAGNOLO, M. A., DRAGUNSKI, D. C., TARLEY, C., #XE9, TEIXEIRA, S. R., MIOLA, A. J., LEISMANN, E. A. V., #XF6 & LZ 2016. Chemical Modifications of Cassava Peel as Adsorbent Material for Metals Ions from Wastewater. *Journal of Chemistry,* 2016**,** 15.

SENTHIKUMAAR, S., BHARATHI, S., NITHYANANDHI, D., AND SUBBURAAM, C.V. 2000. Biosorption of toxic heavy metals from aqueous solutions *Bioresource Technology,* 75**,** 163-165.

SENTHILKUMAR, D., ETHIRAJ, A.S., VIMALA, R., RAMALINGAM, C. AND JAYANTHI, S. 2015. Biosorption of Cu (II) from aqueous solutions: Kinetics and characterization studies. *Scholars Research Library,* 7**,** 205-213.

SHANMUGAPRAKASH, M. & SIVAKUMAR, V. 2015. Batch and fixed-bed column studies for biosorption of Zn(II) ions onto pongamia oil cake (Pongamia pinnata) from biodiesel oil extraction. *Journal of Environmental Management,* 164**,** 161-170.

SIMATE, G. S. & NDLOVU, S. 2015. The removal of heavy metals in a packed bed column using immobilized cassava peel waste biomass. *Journal of Industrial and Engineering Chemistry,* 21**,** 635-643.

SINGH, V. P. 2005. *Toxic Metals and Environmental Issues* India, Sarup and Sons.

SINGHA, B. & DAS, S. K. 2012. Removal of Pb(II) ions from aqueous solution and industrial effluent using natural biosorbents. *Environ Sci Pollut Res,* 19**,** 2212–2226.

SLIMANI, R., EL OUAHABI, I., ABIDI, F., EL HADDAD, M., REGTI, A., LAAMARI, M. R., ANTRI, S. E. & LAZAR, S. 2014. Calcined eggshells as a new biosorbent to remove basic dye from aqueous solutions: Thermodynamics, kinetics, isotherms and error analysis. *Journal of the Taiwan Institute of Chemical Engineers,* 45**,** 1578-1587.

SOUNTHARARAJAH, D. P., LOGANATHAN, P., KANDASAMY, J. & VIGNESWARAN, S. 2015. Adsorptive removal of heavy metals from water using sodium titanate nanofibres loaded onto GAC in fixed-bed columns. *Journal of Hazardous Materials,* 28**,** 306–316.

STAFIEJ, A. & PYRZYNSKA, K. 2007. Adsorption of heavy metal ions with carbon nanotubes. *Separation and Purification Technology,* 58**,** 49-52.

SWATHANTHRA, P. A. 2014. Bagasse as a Potential Adsorbent of Cadmium Removal from Aqueous Solutions. *International Journal of Innovations in Engineering and Technology,* 4**,** 109-115.

TAO, H.-C., ZHANG, H.-R., LI, J.-B. & DING, W.-Y. 2015. Biomass based activated carbon obtained from sludge and sugarcane bagasse for removing lead ion from wastewater. *Bioresource Technology,* 192**,** 611-617.

TARK, Z., IBRAHIM, M. & MADHLOOM, H. 2016. *Eggshell Powder As An Adsorbent for Removal of Cu (II) and Cd (II) from Aqueous Solution: Equilibrium, Kinetic and Thermodynamic Studies*.

TCHOUNWOU, P. B., YEDJOU,C.G., PATLOLLA,A.K., AND SUTTON D.J. 2014. Heavy Metals Toxicity and the Environment *National Institute of Health* 133-164.

THOMAS, H. C. 1944. Heterogeneous Ion Exchange in a Flowing System. *Journal of the American Chemical Society,* 66**,** 1664-1666.

THOMMES, M., KANEKO, K., NEIMARK, A.V., OLIVIER,J.P., FRANCISCO, R.R., ROUQUEROL, J. AND SING, K.S.W. 2015. Physisorption of gases, with special reference to the evaluation of surface area and pore size distribution (IUPAC Technical Report). *Pure and Applied Chemistry.*

TSAI, W. T., YANG, J. M., LAI, C. W., CHENG, Y. H., LIN, C. C. & YEH, C. W. 2006. Characterization and adsorption properties of eggshells and eggshell membrane. *Bioresource Technology,* 97**,** 488-493.

ULLAH, I., NADEEM, R., IQBAL, M. & MANZOOR, Q. 2013. Biosorption of chromium onto native and immobilized sugarcane bagasse waste biomass. *Ecol Eng,* 60**,** 99–107.

VENDRUSCOLO, F., FERREIRA, G. L. D. & ANTONIOSI, N. R. 2017. Biosorption of hexavalent chromium by microorganisms. *INTERNATIONAL BIODETERIORATION & BIODEGRADATION,* 119**,** 87-95.

VIJAYARAGHAVAN, K., J, & UMID , M. 2013. Chicken Eggshells Remove Pb(II) Ions from Synthetic Wastewater. *Environmental Engineering Science,* 30**,** 67-73.

VIMALA, R. & DAS, N. 2011. Mechanism of Cd(II) adsorption by macrofungus Pleurotus platypus. *Journal of Environmental Sciences,* 23**,** 288-293.

VINODHINI, V. & DAS, N. 2009. BIOWASTE MATERIALS AS SORBENTS TO REMOVE CHROMIUM(VI) FROM AQUEOUS ENVIRONMENT- A COMPARATIVE STUDY *Journal of Agricultural and Biological Science,* 4**,** 19-23.

VOLESKY, B. & NAJA, G. 2007. Biosorption technology: starting up an enterprise. *International Journal of Technology Transfer and Commercialisation $V 6***,** 196-211.

WANG, J., AND CHEN, C. 2009. Biosorbents for heavy metals removal and their future *Biotechnology Advances,* 27**,** 195-226.

WHO. *World Health Organnisation* [Online]. Available: http://www.who.int/ [Accessed 06/01/2018].

WILLIAM, J. S. & OWEN, J. C. 1995. *Egg scienceand technology*, Food Product Press. New York.

WONG, C.-W., BARFORD, J. P., CHEN, G. & MCKAY, G. 2014. Kinetics and equilibrium studies for the removal of cadmium ions by ion exchange resin. *Journal of Environmental Chemical Engineering,* 2**,** 698-707.

WONG, S. Y., TAN, Y. P., ABDULLAH, A. H. & ONG, S. T. 2009. REMOVAL OF BASIC BLUE 3 AND REACTIVE ORANGE 16 BY ADSORPTION ONTO QUARTENIZED SUGAR CANE BAGASSE. *The Malaysian Journal of Analytical Sciences,* 13**,** 185 - 193.

XU, Z., CAI, J.-G. & PAN, B.-C. 2013. Mathematically modeling fixed-bed adsorption in aqueous systems. *Journal of Zhejiang University SCIENCE A,* 14**,** 155-176.

YEDDOU, N. & BENSMAILI, A. 2007. Equilibrium and kinetic modelling of iron adsorption by eggshells in a batch system: effect of temperature. *Desalination,* 206**,** 127-134.

YOON, Y. H. & NELSON, J. H. 1984. Application of Gas Adsorption Kinetics — II. A Theoretical Model for Respirator Cartridge Service Life and Its Practical Applications. *American Industrial Hygiene Association Journal,* 45**,** 517-524.

YU, X., TONG, S., GE, M., WU, L., ZUO, J., CAO, C. & SONG, W. 2013. Adsorption of heavy metal ions from aqueous solution by carboxylated cellulose nanocrystals. *Journal of Environmental Sciences,* 25**,** 933-943.

ZHANG, T., DONG, Z. B., QU, F., DING, F. Z., PENG, X. Y., WANG, H. Y. & GU, H. W. 2014. Removal of CdTe in acidic media by magnetic ion-exchange resin: A potential recycling methodology for cadmium telluride photovoltaic waste. *JOURNAL OF HAZARDOUS MATERIALS,* 279**,** 597-604.

ZHANG, T., TU, Z., LU, G., DUAN, X., YI, X., GUO, C. & DANG, Z. 2017. Removal of heavy metals from acid mine drainage using chicken eggshells in column mode. *Journal of Environmental Management,* 188**,** 1-8.

ZHANG, W., DONG, L., YAN, H., LI, H., JIANG, Z., KAN, X., YANG, H., LI, A. & CHENG, R. 2011a. Removal of methylene blue from aqueous solutions by straw based adsorbent in a fixed-bed column. *Chemical Engineering Journal,* 173**,** 429-436.

ZHANG, Z., M GONZALEZ, A., DAVIES, E. & LIU, Y. 2012. *Agricultural Wastes*.

ZHANG, Z., MOGHADDAM, L., O'HARA, I. M. & DOHERTY, W. O. S. 2011b. Congo Red adsorption by ball-milled sugarcane bagasse. *Chemical Engineering Journal,* 178**,** 122-128.

ZULFIKAR, M. A. & SETIYANTO, H. 2013. *Study of the adsorption kinetics and thermodynamic for the removal of Congo Red from aqueous solution using powdered eggshell*.

7. Appendices

7.1. Appendix A – Raw data for the batch studies

Table A.1. Particle size raw data

Metal	*Adsorbent*	*pH*	$C_i\ (\frac{mg}{L})$	$C_f\ (\frac{mg}{L})$	*Dosage* (g)	*Volume* (L)	*Speed* (RPM)	*Particle size* (μm)
Cd	Bagasse	5.63	100	47	1	0,1	150	250
Cd	Bagasse	5.62	100	46	1	0,1	150	150
Cd	Bagasse	5.58	100	45	1	0,1	150	75
Pb	Bagasse	5.62	100	5,1	1	0,1	150	250
Pb	Bagasse	5.60	100	4,3	1	0,1	150	150
Pb	Bagasse	5.59	100	2,9	1	0,1	150	75
Cd	Eggshell	5.57	100	77	1	0,1	150	250
Cd	Eggshell	5.69	100	73	1	0,1	150	150
Cd	Eggshell	5.68	100	45	1	0,1	150	75
Pb	Eggshell	5.62	100	0,2	1	0,1	150	250
Pb	Eggshell	5.60	100	0,7	1	0,1	150	150
Pb	Eggshell	5.59	100	0,1	1	0,1	150	75

Table A.2. pH raw data

Metal	*Adsorbent*	*pH*	$C_i\ (\frac{mg}{L})$	$C_f\ (\frac{mg}{L})$	*Dosage* (g)	*Volume* (L)	*Speed* (RPM)
Cd	Eggshell	2.19	100	64	1	0,1	150
Cd	Eggshell	3.11	100	62	1	0,1	150
Cd	Eggshell	4.22	100	59	1	0,1	150
Cd	Eggshell	5.09	100	54	1	0,1	150
Cd	Eggshell	6.25	100	57	1	0,1	150
Cd	Eggshell	7.15	100	61	1	0,1	150
Pb	Eggshell	2.19	100	6,8	1	0,1	150
Pb	Eggshell	3.07	100	0,3	1	0,1	150
Pb	Eggshell	4.30	100	0,3	1	0,1	150
Pb	Eggshell	5.22	100	0,3	1	0,1	150
Pb	Eggshell	6.01	100	0,3	1	0,1	150
Pb	Eggshell	7.14	100	0,3	1	0,1	150
Cd	Bagasse	2.27	100	84	1	0,1	150
Cd	Bagasse	3.21	100	54	1	0,1	150
Cd	Bagasse	4.08	100	46	1	0,1	150
Cd	Bagasse	5.27	100	48	1	0,1	150
Cd	Bagasse	6.04	100	48	1	0,1	150
Cd	Bagasse	7.01	100	48	1	0,1	150
Pb	Bagasse	2.25	100	4,1	1	0,1	150
Pb	Bagasse	3.18	100	6,2	1	0,1	150
Pb	Bagasse	4.01	100	2,6	1	0,1	150
Pb	Bagasse	5.18	100	3	1	0,1	150
Pb	Bagasse	6.01	100	1,8	1	0,1	150
Pb	Bagasse	7.09	100	0,5	1	0,1	150

Table A.3. Concentration Raw data

$Metal$	$Adsorbent$	pH	$C_i\ (\frac{mg}{L})$	$C_f\ (\frac{mg}{L})$	$Dosage\ (g)$	$Volume\ (L)$	$Speed\ (RPM)$
Cd	Eggshell	5.64	40	10	1	0,1	150
Cd	Eggshell	5.58	80	22	1	0,1	150
Cd	Eggshell	5.56	120	42	1	0,1	150
Cd	Eggshell	5.66	160	75	1	0,1	150
Cd	Eggshell	5.65	200	95	1	0,1	150
Cd	Eggshell	5.66	240	140	1	0,1	150
Pb	Eggshell	5.67	100	1,88	1	0,1	150
Pb	Eggshell	5.66	100	2,13	0,8	0,1	150
Pb	Eggshell	5.66	100	3,5	0,6	0,1	150
Pb	Eggshell	5.62	100	6,16	0,4	0,1	150
Pb	Eggshell	5.62	100	6,58	0,2	0,1	150
Pb	Eggshell	5.63	100	16,396	0,1	0,1	150
Cd	Bagasse	5.59	40	7,1	1	0,1	150
Cd	Bagasse	5.68	80	16,9	1	0,1	150
Cd	Bagasse	5.69	120	35	1	0,1	150
Cd	Bagasse	5.67	160	50	1	0,1	150
Cd	Bagasse	5.69	200	65	1	0,1	150
Cd	Bagasse	5.65	240	80	1	0,1	150
Pb	Bagasse	5.40	40	7	1	0,1	150
Pb	Bagasse	5.40	80	15	1	0,1	150
Pb	Bagasse	5.39	120	28	1	0,1	150
Pb	Bagasse	5.38	160	39	1	0,1	150
Pb	Bagasse	5.39	200	51	1	0,1	150
Pb	Bagasse	5.40	240	63	1	0,1	150

Table A.4. Contact time raw data

$Metal$	$Adsorbent$	pH	$C_i\ (\frac{mg}{L})$	$C_f\ (\frac{mg}{L})$	$Dosage\ (g)$	$Volume\ (L)$	$Time\ (min)$	$Speed\ (RPM)$
Cd	Eggshell	5.23	100	68	1	0,1	5	150
Cd	Eggshell	5.23	100	57,89	1	0,1	10	150
Cd	Eggshell	5.23	100	48,25	1	0,1	15	150
Cd	Eggshell	5.23	100	39,08	1	0,1	25	150
Cd	Eggshell	5.23	100	35,05	1	0,1	30	150
Cd	Eggshell	5.24	100	29	1	0,1	50	150
Cd	Eggshell	5.25	100	29	1	0,1	80	150
Pb	Eggshell	5.38	100	47,03	1	0,1	5	150
Pb	Eggshell	5.38	100	21,58	1	0,1	10	150
Pb	Eggshell	5.38	100	11,68	1	0,1	15	150
Pb	Eggshell	5.44	100	0,79	1	0,1	25	150
Pb	Eggshell	5.32	100	0,79	1	0,1	30	150
Pb	Eggshell	5.33	100	0,79	1	0,1	50	150
Pb	Eggshell	5.33	100	0,79	1	0,1	80	150
Pb	Eggshell	5.33	100	0,79	1	0,1	120	150
Cd	Bagasse	5.32	100	60,89	1	0,1	5	150

Cd	Bagasse	5.66	100	55	1	0,1	10	150
Cd	Bagasse	5.63	100	47	1	0,1	15	150
Cd	Bagasse	5.82	100	35	1	0,1	25	150
Cd	Bagasse	5.58	100	29	1	0,1	30	150
Cd	Bagasse	5.65	100	27	1	0,1	40	150
Cd	Bagasse	5.66	100	27	1	0,1	60	150
Cd	Bagasse	5.66	100	27	1	0,1	80	150
Cd	Bagasse	5.66	100	27	1	0,1	120	150
Pb	Bagasse	5.63	100	45,74	1	0,1	5	150
Pb	Bagasse	5.63	100	22,28	1	0,1	10	150
Pb	Bagasse	5.63	100	9,21	1	0,1	15	150
Pb	Bagasse	5.63	100	3,76	1	0,1	25	150
Pb	Bagasse	5.63	100	3,069	1	0,1	30	150
Pb	Bagasse	5.64	100	3,069	1	0,1	50	150
Pb	Bagasse	5.64	100	3,069	1	0,1	80	150

Table A.5. Batch Comparison test raw data

$Metal$	$Adsorbent$	$Initial\ pH$	$C_i\ (\frac{mg}{L})$	$C_f\ (\frac{mg}{L})$	$Dosage\ (g)$	$Volume\ (L)$	$Speed\ (RPM)$	$Particle\ size\ (\mu m)$
Pb	Bagasse	5.52	100	6.664	1	0,1	150	75
Pb	Adsorbent A	5.55	100	5.35	1	0,1	150	75
Pb	Adsorbent B	5.58	100	2.79	1	0,1	150	75
Pb	Adsorbent C	5.53	100	1.04	1	0,1	150	75
Pb	Eggshells	5.50	100	0.066	1	0,1	150	75
Cd	Bagasse	5.52	100	21.61	1	0,1	150	75
Cd	Adsorbent A	5.57	100	23.59	1	0,1	150	75
Cd	Adsorbent B	5.58	100	25.02	1	0,1	150	75
Cd	Adsorbent C	5.51	100	25.74	1	0,1	150	75
Cd	Eggshell	5.59	100	25.01	1	0,1	150	75

7.2. Appendix B – Raw data for the column studies

Table B.1. Raw data for bagasse

$Time$ (min)	$Ct\left(\frac{mg}{L}\right)$	$\frac{Ct}{Co}$	$Time$ (min)	$Ct\left(\frac{mg}{L}\right)$	$\frac{Ct}{Co}$	$Time$ (min)	$Ct\left(\frac{mg}{L}\right)$	$\frac{Ct}{Co}$
	4 cm			8 cm			12 cm	
0	0	0,00	0	0,00	0,00	0	0,00	0,00
30	0	0,00	30	0,00	0,00	30	0,00	0,00
60	0,01934	0,00	60	0,00	0,00	60	0,00	0,00
90	1,05	0,01	90	0,00	0,00	90	0,00	0,00
120	3,9	0,04	120	0,01	0,00	120	0,01	0,00
150	12	0,12	150	0,02	0,00	150	0,01	0,00
180	22,9	0,23	180	1,46	0,01	180	0,01	0,00
210	61,1	0,61	210	3,80	0,01	210	0,01	0,00
240	88,5	0,89	240	7,30	0,04	240	0,01	0,00
270	98,4	0,98	270	32,50	0,07	270	0,01	0,00
300	100	1,00	300	71,30	0,33	300	0,02	0,00
420	100	1,00	420	84,37	0,71	420	0,46	0,00
			540	91,50	0,92	540	3,66	0,04
			660	100,00	1,00	660	11,43	0,11
			780	100,00	1,00	780	37,25	0,37
						900	68,00	0,68
						1020	83,12	0,83
						1140	99,45	0,99
						1260	100,00	1,00

Table B.2. Raw data for adsorbent A

$Time$ (min)	$Ct\left(\frac{mg}{L}\right)$	$\frac{Ct}{Co}$	$Time$ (min)	$Ct\left(\frac{mg}{L}\right)$	$\frac{Ct}{Co}$	$Time$ (min)	$Ct\left(\frac{mg}{L}\right)$	$\frac{Ct}{Co}$
	4 cm			8 cm			12 cm	
0	0,00	0,00	0	0,00	0,00	0	0,00	0,00
30	0,00	0,00	30	0,00	0,00	30	0,00	0,00
60	0,02	0,00	60	0,00	0,00	60	0,00	0,00
90	1,05	0,01	90	0,00	0,00	90	0,00	0,00
120	3,90	0,04	120	0,00	0,00	120	0,00	0,00
150	4,00	0,04	150	0,01	0,00	150	0,00	0,00
180	12,00	0,12	180	0,04	0,00	180	0,00	0,00
210	22,90	0,23	210	0,56	0,01	210	0,00	0,00
240	48,64	0,49	240	0,65	0,01	240	0,00	0,00
270	66,90	0,67	270	1,46	0,01	270	0,00	0,00
300	80,50	0,81	300	2,80	0,03	300	0,01	0,00
420	96,40	0,96	420	12,30	0,12	420	0,22	0,00
540	100,00	1,00	540	38,50	0,39	540	1,19	0,01
			660	69,30	0,69	660	4,23	0,04
			780	94,50	0,95	780	21,10	0,21
			900	100,00	1,00	900	46,30	0,46
			1020	100,00	1,00	1020	76,64	0,77
						1140	89,41	0,89
						1260	96,06	0,96
						1380	100,00	1,00
						1500	100,00	1,00

Table B.3. Raw data for adsorbent B

$Time$ (min)	$Ct\left(\frac{mg}{L}\right)$	$\frac{Ct}{Co}$	$Time$ (min)	$Ct\left(\frac{mg}{L}\right)$	$\frac{Ct}{Co}$	$Time$ (min)	$Ct\left(\frac{mg}{L}\right)$	$\frac{Ct}{Co}$
	4 cm			8 cm			12 cm	
0	0,00	0,00	0	0,000	0,000	0	0,00	0,00
30	0,00	0,00	30	0,000	0,000	30	0,00	0,00
60	0,00	0,00	60	0,000	0,000	60	0,00	0,00
90	0,00	0,00	90	0,000	0,000	90	0,00	0,00
120	0,00	0,00	120	0,000	0,000	120	0,00	0,00
150	0,03	0,00	150	0,000	0,000	150	0,00	0,00
180	0,68	0,01	180	0,001	0,000	180	0,00	0,00
210	1,37	0,01	210	0,002	0,000	210	0,00	0,00
240	3,94	0,04	240	0,002	0,000	240	0,00	0,00
270	6,53	0,07	270	0,023	0,000	270	0,00	0,00
300	17,05	0,17	300	1,035	0,010	300	0,01	0,00
420	52,17	0,52	420	1,503	0,015	420	0,01	0,00
540	89,35	0,89	540	3,653	0,037	540	0,10	0,00
660	95,07	0,95	660	5,524	0,055	660	0,15	0,00
780	100,00	1,00	780	19,605	0,196	780	1,07	0,01
900	100,00	1,00	900	41,654	0,417	900	1,53	0,02
			1020	82,082	0,821	1020	2,56	0,03
			1140	94,222	0,942	1140	6,41	0,06
			1260	99,006	0,990	1260	24,01	0,24
			1380	100,000	1,000	1380	41,85	0,42
						1500	77,37	0,77
						1620	86,17	0,86
						1740	90,16	0,90
						1860	95,04	0,95
						1980	100,00	1,00
						2100	100,00	1,00

Table B.4. Raw data for adsorbent C

$Time$ (min)	$Ct\left(\frac{mg}{L}\right)$	$\frac{Ct}{Co}$	$Time$ (min)	$Ct\left(\frac{mg}{L}\right)$	$\frac{Ct}{Co}$	$Time$ (min)	$Ct\left(\frac{mg}{L}\right)$	$\frac{Ct}{Co}$
	4 cm			8 cm			12 cm	
0	0,00	0,00	0	0,00	0,00	0	0,00	0,00
30	0,00	0,00	60	0,00	0,00	60	0,00	0,00
60	0,00	0,00	120	0,00	0,00	120	0,00	0,00
90	0,00	0,00	180	0,00	0,00	180	0,00	0,00
120	0,00	0,00	240	0,00	0,00	240	0,00	0,00
150	0,00	0,00	300	0,00	0,00	300	0,00	0,00
180	0,00	0,00	420	0,00	0,00	420	0,00	0,00
210	0,00	0,00	540	0,00	0,00	540	0,00	0,00
240	0,00	0,00	660	0,00	0,00	660	0,00	0,00
270	0,00	0,00	780	0,00	0,00	780	0,00	0,00
300	0,01	0,00	900	0,00	0,00	900	0,00	0,00
420	0,02	0,00	1020	0,01	0,00	1020	0,00	0,00
540	1,58	0,02	1140	0,02	0,00	1140	0,00	0,00
660	5,56	0,06	1260	0,03	0,00	1260	0,00	0,00
780	9,46	0,09	1380	0,07	0,00	1380	0,00	0,00
900	18,00	0,18	1500	0,08	0,00	1500	0,00	0,00
1020	32,09	0,32	1620	0,94	0,01	1620	0,00	0,00
1140	45,66	0,46	1740	0,99	0,01	1740	0,02	0,00
1260	56,45	0,56	1860	1,03	0,01	1860	0,03	0,00
1380	81,00	0,81	1980	5,26	0,05	1980	0,05	0,00
1500	99,55	1,00	2100	9,77	0,10	2100	0,06	0,00
1620	100,00	1,00	2220	29,68	0,30	2220	0,08	0,00
			2340	41,00	0,41	2340	0,08	0,00
			2460	65,28	0,65	2460	0,09	0,00
			2580	79,41	0,79	2580	0,10	0,00
			2700	89,31	0,89	2700	1,02	0,01
			2820	100,00	1,00	2820	3,51	0,04
			2940	100,00	1,00	2940	9,33	0,09
			3060	100,00	1,00	3060	13,99	0,14
						3180	36,68	0,37
						3300	45,25	0,45
						3420	61,28	0,61
						3540	91,07	0,91
						3660	100,00	1,00

Table B.5. Raw data for eggshells

$Time$ (min)	$Ct\left(\frac{mg}{L}\right)$	$\frac{Ct}{Co}$	$Time$ (min)	$Ct\left(\frac{mg}{L}\right)$	$\frac{Ct}{Co}$	$Time$ (min)	$Ct\left(\frac{mg}{L}\right)$	$\frac{Ct}{Co}$
	4 cm			8 cm			12 cm	
0	0,00	0,00	0	0,00	0,00	0	0,00	0,00
30	0,00	0,00	30	0,00	0,00	60	0,00	0,00
60	0,00	0,00	60	0,00	0,00	120	0,00	0,00
90	0,00	0,00	90	0,00	0,00	180	0,00	0,00
120	0,00	0,00	120	0,00	0,00	240	0,00	0,00
150	0,00	0,00	150	0,00	0,00	300	0,00	0,00
180	0,00	0,00	180	0,00	0,00	420	0,00	0,00
210	0,00	0,00	210	0,00	0,00	540	0,00	0,00
240	0,00	0,00	240	0,00	0,00	660	0,00	0,00
270	0,00	0,00	270	0,00	0,00	780	0,00	0,00
300	0,01	0,00	300	0,00	0,00	900	0,00	0,00
420	0,02	0,00	420	0,00	0,00	1020	0,00	0,00
540	1,26	0,01	540	0,01	0,00	1140	0,00	0,00
660	5,21	0,05	660	0,01	0,00	1260	0,01	0,00
780	13,56	0,14	780	0,02	0,00	1380	0,02	0,00
900	24,89	0,25	900	0,02	0,00	1500	0,07	0,00
1020	44,00	0,44	1020	0,25	0,00	1620	0,09	0,00
1140	58,08	0,58	1140	0,35	0,00	1740	0,16	0,00
1260	88,25	0,88	1260	0,98	0,01	1860	0,59	0,01
1380	99,55	1,00	1380	1,08	0,01	1980	1,03	0,01
1500	100,00	1,00	1500	4,93	0,05	2100	1,17	0,01
			1620	11,45	0,11	2220	1,27	0,01
			1740	17,36	0,17	2340	1,44	0,01
			1860	23,57	0,24	2460	3,56	0,04
			1980	31,86	0,32	2580	6,34	0,06
			2100	49,24	0,49	2700	9,66	0,10
			2220	67,16	0,67	2820	11,43	0,11
			2340	84,35	0,84	2940	19,58	0,20
			2460	92,20	0,92	3060	26,00	0,26
			2580	95,53	0,96	3180	39,46	0,39
			2700	100,00	1,00	3300	49,25	0,49
						3420	77,47	0,77
						3540	85,66	0,86
						3660	100,00	1,00

7.3. Appendix C – Breakthrough curves for the 5 adsorbents

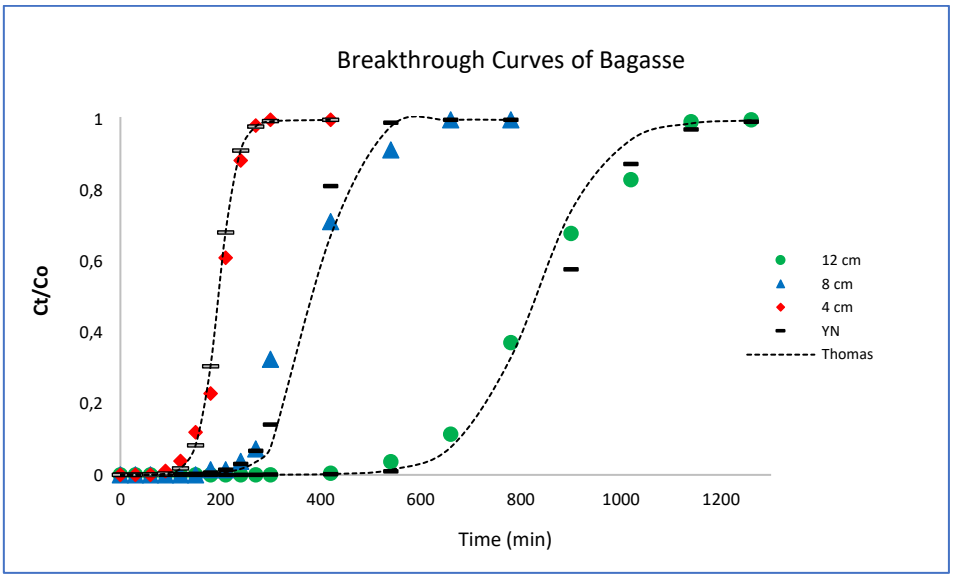

Figure C.1. Breakthrough curves for Bagasse

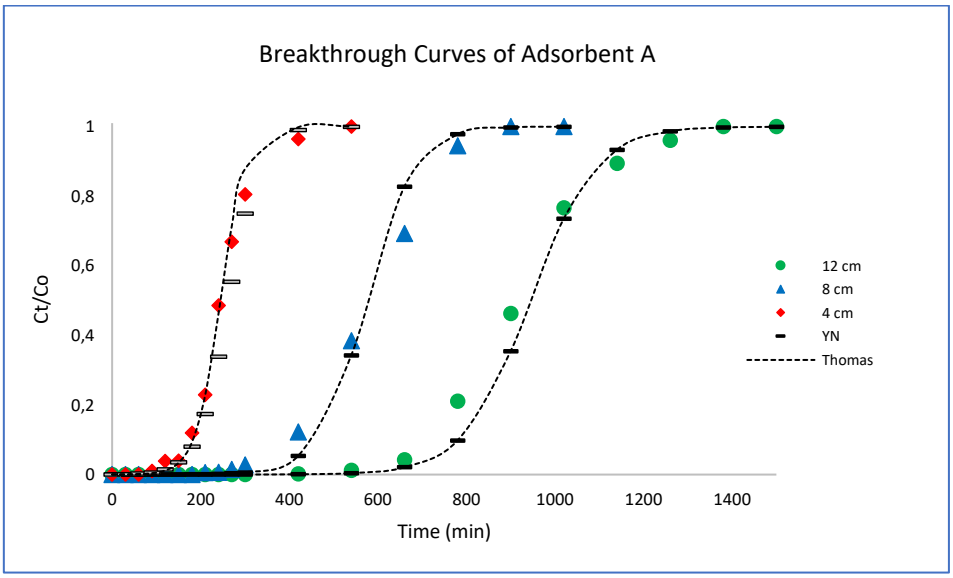

Figure C.2. Breakthrough curves for Adsorbent A

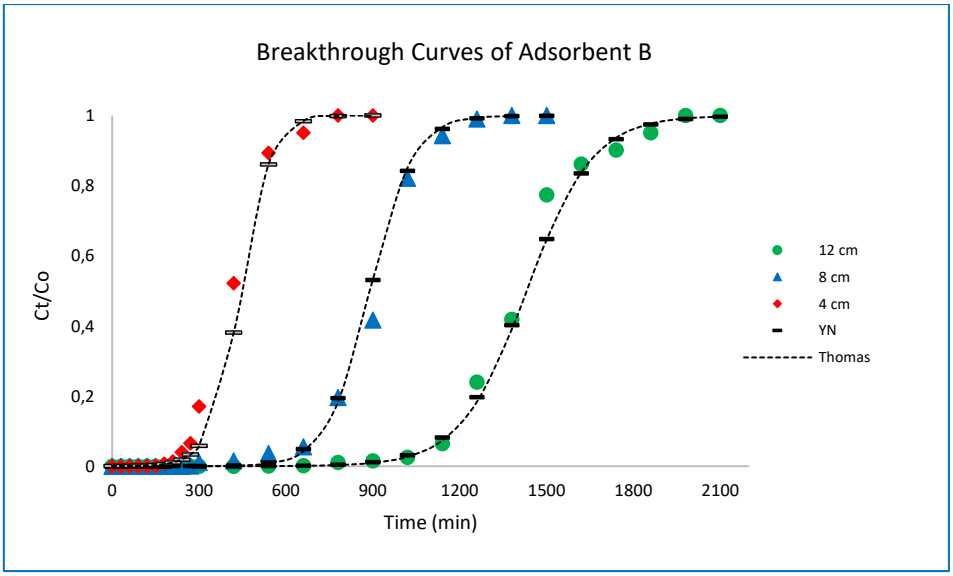

Figure C.3. Breakthrough curves for Adsorbent B

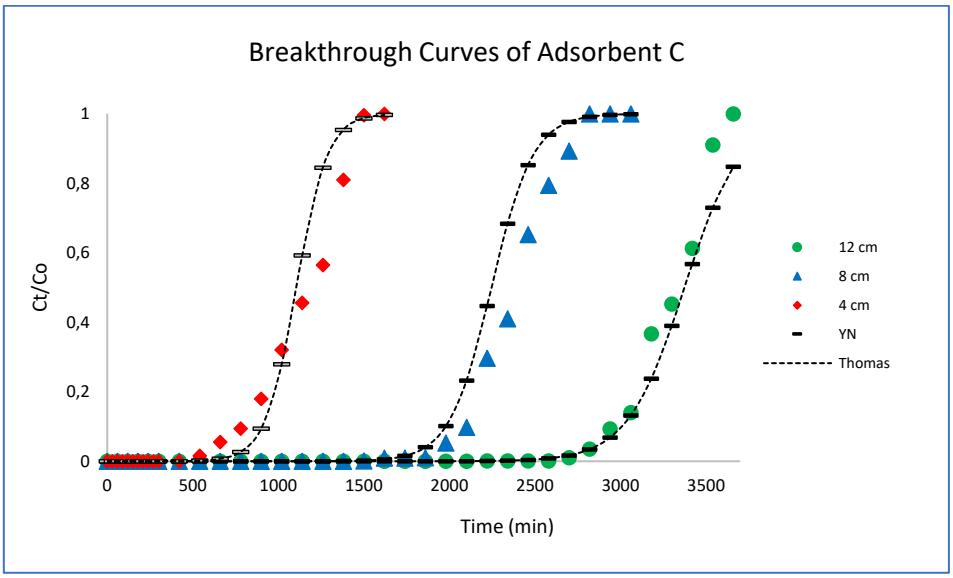

Figure C.4. Breakthrough curves for Adsorbent C

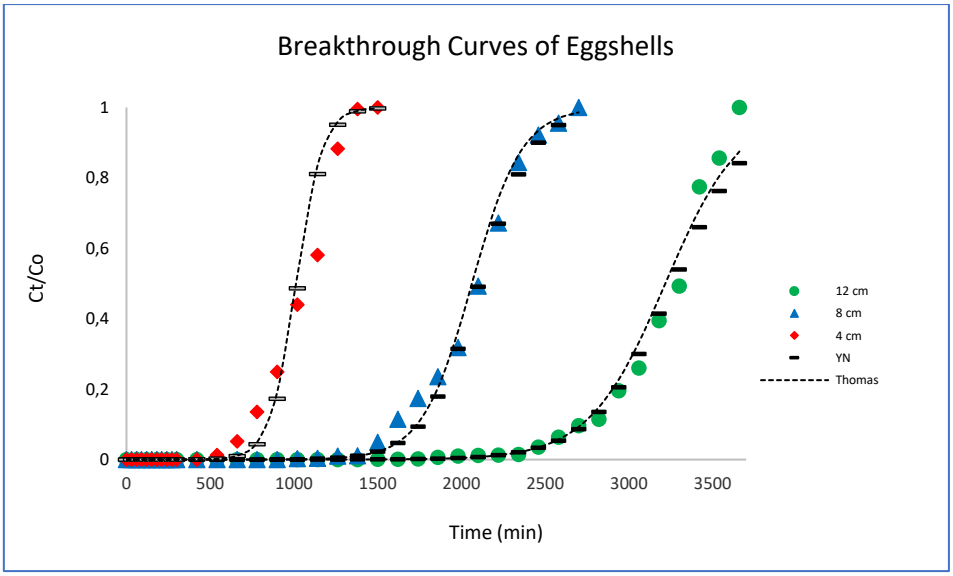

Figure C.5. Breakthrough curves for Eggshells